STATE OF NEW MEXICO
ENERGY, MINERALS AND NATURAL RESOURCES DEPARTMENT
OIL CONSERVATION DIVISION

APPLICATIONS OF GOODNIGHT MIDSTREAM PERMIAN, LLC FOR APPROVAL OF SALTWATER DISPOSAL WELLS LEA COUNTY, NEW MEXICO

CASE NOS. 23614-23617

APPLICATION OF GOODNIGHT MIDSTREAM PERMIAN LLC TO AMEND ORDER NO. R-22026/SWD-2403 TO INCREASE THE APPROVED INJECTION RATE IN ITS ANDRE DAWSON SWD #1, LEA COUNTY, NEW MEXICO.

CASE NO. 23775

APPLICATIONS OF EMPIRE NEW MEXICO LLC TO REVOKE INJECTION AUTHORITY, LEA COUNTY, NEW MEXICO

CASE NOS. 24018-24020, 24025

APPLICATION OF GOODNIGHT PERMIAN MIDSTREAM, LLC FOR APPROVAL OF A SALTWATER DISPOSAL WELL, LEA COUNTY, NEW MEXICO.

DIVISION CASE NO. 22626
ORDER NO. R-22869-A
COMMISSION CASE NO. 24123

SELF-AFFIRMED STATEMENT OF JAMES A. DAVIDSON

1. My name is James A. Davidson. I work for Netherland, Sewell & Associates, Inc. ("NSAI") as Vice President and Senior Technical Advisor. I have been with NSAI since 1998.

2. I have not previously testified before the New Mexico Oil Conservation Commission as an expert witness in petroleum engineering and petrophysics. I have attached my current curriculum vitae as **Goodnight Exhibit D-1**. It outlines my education, training, and

experience, as well as a list of my publications and presentations. I have served as a testifying and/or consulting expert on a broad variety of issues as outlined in my curriculum vitae

3. I graduated with a B.S. in petroleum engineering from Texas Tech University in 1979. I earned a M.S. in Petroleum Engineering in 1993 before obtaining my Ph.D. in Petroleum Engineering in1998 from the University of Texas at Austin. I am an active member in several professional organizations, including the Society of Professional Engineers, the Society of Professional Well Log Analysts, and the Society of Core Analysts. A list of my publications is included in my resume.

4. My work as a senior petrophysicist at NSAI involves advanced petrophysical support for reserves evaluations, major field studies, and reservoir simulation studies; consulting services and technology transfer in the areas of well log analysis, core analysis, and reservoir description; and development of comprehensive logging and core analysis programs, including detailed laboratory procedures. My projects have included petrophysical parameter distributions for probabilistic reserves evaluations and multiple-model evaluations reflecting the uncertainties in net pay and hydrocarbon pore volume resulting from uncertainties in logging measurements, formation mineralogy, shale and clay distribution, and reservoir electrical conductivity. I have performed petrophysical evaluations for wells located in most of the major petroleum provinces of the world.

5. I have particular experience working in carbonate reservoirs on the Central Basin Platform, including reservoir description and in-fill well development programs in J.L. Johnson AB Unit and North Foster Unit.

6. I believe these credentials qualify me to testify as an expert in petroleum engineering and petrophysics.

7. I have been retained by Goodnight Midstream Permian, LLC ("Goodnight Midstream") to (1) prepare a petrophysical interpretation of core and log data for the San Andres formation within the Eunice Monument South Unit ("EMSU") in these consolidated cases; (2) evaluate and assess available data and information and offer an opinion on the presence of oil and the potential for a productive residual oil zone ("ROZ") in the San Anders within the EMSU; and (3) to evaluate potential geologic barriers between the Grayburg and San Andres formations within the EMSU.

8. This statement summarizes my analysis and opinions to date. I reserve the right to amend or supplement this report, if necessary, should additional information become available to me, and to rebut any related opinions reached by experts related to these cases. All the opinions and conclusions herein are rendered to a reasonable degree of professional certainty.

Summary

9. Following are the basic conclusions derived from the petrophysical analysis of the Grayburg and San Andres Formations in the area occupied by the Eunice Monument South Unit.

- The petrophysical modeling approach employed by Empire is overly simplistic and does not accurately account for the complexities of the reservoir rock types present in the San Andres and Grayburg Formations.
- The remaining oil saturations in both the San Andres and Grayburg are significantly lower than estimated by Empire.
- A residual oil zone analogous to those where CO_2 enhanced oil recovery operations have been employed exists only in the Grayburg Formation in the Eunice Monument South Unit.

- The intervals of residual oil in the San Andres aquifer are too thin, too widely spaced, and are not likely areally continuous enough to support efficient enhanced recovery operations.
- The likely presence of long intervals of karsts and collapse breccias in the San Andres would further compromise the effectiveness of enhanced oil recovery operations.
- Given the sparse, intermittent oil saturations, the saturation profile in the San Andres aquifer is more likely representative of abandoned oil migration pathways than of a previous oil-saturated interval.
- Thick, impermeable anhydrites and anhydritic dolostones found near the top of the San Andres aquifer likely isolate the water disposal intervals in the Goodnight-operated wells from the overlying Grayburg residual oil zones.
- Given the sparse nature of the residual oil accumulations and the presence of significant karsting, Goodnight's San Andres disposal zone does not meet any reasonable definition of an ROZ.

General Petrophysical Evaluation Approach

10. The petrophysical evaluation was carried out using workflows and models specifically designed for complex carbonate reservoirs that have been developed by Jerry Lucia of the University of Texas Bureau of Economic Geology and George Asquith of the Department of Geology at Texas Tech University. From my perspective, these workflows and models are considered to be the industry standard for carbonate reservoir evaluation. I have utilized these methodologies at NSAI in one form or another for the past 25 years.

Data Available

11. I conducted an independent petrophysical evaluation for seven wells located within and nearby the Eunice Monument South Unit (EMSU). The primary dataset included open-hole well log measurements for eleven wells, mud log data for six of the eleven wells, and core dataset for three wells located within the unit. Mud log data and the results of an independent petrophysical analysis conducted by Nutech for 10 wells inside the EMSU were also provided.

12. Core analysis data from the San Andres Formation in the Enice Monument Units were very limited. The available data was limited to routine porosity, permeability, and fluid saturation measurements with very limited mineralogy descriptions. Data from analog carbonate reservoirs were used during the course of my petrophysical evaluation. The data sources are identified in the text and source publication details are included in a bibliography following the written discussion.

Porosity and Lithology

13. The porosity and lithology of the productive formations were calculated using industry standard techniques involving the gamma ray, neutron porosity, bulk density, and sonic travel time measurements from the well logs. Review of the predicted lithology results indicated the presence of a carbonate ramp environment in the San Andres. Shallow-water anhydrite intervals were present along with thick limestone intervals that would most likely be associated with deep water muds. Numerous depositional cycles appear to be present as evidenced by the appearance of several anhydrite-bearing intervals through the logged intervals. A simplified cross section showing the basic depositional model is shown in Figure 1. The relative position of each of the reservoir rock types is shown. Non-reservoir quality evaporites generally consisting of anhydrites form near the crest of the ramp where the water is shallow, and the crest is periodically

exposed to the surface. The presence of several intervals containing anhydrite shows that several depositional cycles are likely present through the drilled intervals indicating formation uplift and subsidence events occurred where the relative location of sea level changed during carbonate deposition. This is illustrated in Figure 2 which illustrates an example of a prograding ramp sequence. This shows how rock types from different parts of the ramp can be found next to one another in wells drilled through the sequence.

14. The University of Texas Bureau of Economic Geology (BEG) has performed an extensive study of a San Andres carbonate ramp in an outcrop located in the Guadalupe Mountains east of the EMSU (Kerans et al., 1994).

15. Important reservoir rock types observed in the outcrop included grainstones, moldic grainstones, grain-dominated packstones, mud-dominated packstone/wackestones, and wackestones. The following high-level observations on the San Andres can be derived from the BEG study.

- The best reservoir quality rocks tend to be those deposited in shallow-water environments where wave energy is high near the shoreline. This would correspond to the upper part of the ramp and the crest.
- In the lower energy environment associated with the deeper ramp deposits, increased content of very fine-grained carbonate mud caused a degradation of reservoir quality.
- In rocks containing little or no secondary vug porosity, the rock types associated with the lower energy portion of the carbonate ramp tended to have lower total porosities than those deposited in the higher energy environment in the upper portion of the ramp.

- It was additionally observed that increasing levels of isolated vug porosity were associated with decreasing reservoir quality primarily as the result of dissolution-reprecipitation-induced permeability impairment.
- Increasing secondary porosity was also observed to generally correspond to increases in the total porosity of the carbonate rocks. Higher total porosity did not necessarily correspond to better reservoir quality.

16. The reservoir rock types are basically characterized by grain or crystal size and the amount of very fine-grained carbonate mud found between the coarser grains. A simplified characterization of each rock type follows.

- Grainstone: relatively coarse-grained carbonate rocks with well-connected inter-granular porosity.
- Moldic grainstone: grainstones containing some level of vug porosity in addition to the inter-granular porosity.
- Grain-dominated packstones/wackestones: rocks consisting primarily of coarse to fine-grained carbonate rock fragments with minor amounts of very fine-grained carbonate mud occupying a portion of the inter-granular volume. A multimodal pore system is present consisting of pores between the coarser-grained carbonate fragments, pores between the mud-sized carbonate grains, as well as secondary vug porosity that may be present.
- Mud-dominated packstone/wackestone: rock consisting predominately of very fine-grained mud with inclusions of larger-grained carbonate rock fragments. A multimodal pore system as described above is commonly present.

- Wackestones: rocks consisting primarily of very fine-grained carbonate mud with inclusions of fine-grained rock fragments. A multimodal pore system as described above is commonly present.

17. A relatively simple means to identify shallow versus deep water deposits in a carbonate ramp environment involves the analysis of the gamma ray measurements. Uranium from sea water tends to adsorb onto very fine-grained sediments in a low-energy depositional environment (Hassan et al., 1976). Therefore, increasing gamma ray levels often indicate the presence of rock types containing some portion of carbonate mud. In a carbonate ramp environment this would correspond to the mud dominated packstones/wackestones and lime mudstones. The presence of uranium increases the gamma ray response. Rocks deposited in a high-energy environment would be expected to exhibit lower gamma ray readings. This would correspond to the grainstones and grain-dominated packstones.

18. The presence of clay minerals of clastic origin can also cause elevated gamma ray readings. However, carbonate sediments do not usually contain high levels of clay minerals. Spectral gamma ray measurements were not provided for any of the wells involved in this petrophysical evaluation, but some were provided for a few nearby wells. Clay minerals predominantly affect the thorium and potassium curves, while uranium is adsorbed onto the very fine grain carbonate materials. Notice in Figure 3, the increases in gamma ray readings deeper in the well correspond to increases in uranium while the thorium and potassium concentrations stay relatively constant. It was therefore concluded that high gamma ray readings in the San Andres are most likely the result of uranium content rather than the presence of significant volumes of clay minerals.

19. Figure 4 shows gamma ray logs from the Grayburg and San Andres interval from EMSU 746.

20. A shift in the gamma ray readings occurs near the top of the San Andres.

- The low gamma ray readings indicate that the Grayburg Formation in the EMSU is likely composed predominately of the good reservoir quality rock types associated with a shallow-water deposition (grainstones, moldic grainstones, and grain-dominated packstones).
- The higher gamma ray readings indicate the San Andres Formation is likely predominately composed of lower reservoir quality rock types that would be present in the lower energy depositional environment (mud-dominated packstones/wackestones, wackestones, lime mudstones).
- A quick review of the gamma ray measurements in the EMSU 746 indicates that roughly 55% of the Grayburg Formation consists of high energy depositional facies, while roughly 3% of the San Andres consists of high energy depositional facies.
- Additionally, the low gamma ray intervals in the Grayburg are much thicker than those in the San Andres, indicating that long periods of high energy deposition occurred during the formation of the Grayburg.

21. Rock typing procedures developed at the BEG based on core-derived porosity and permeability measurements (Lucia, 1995) tend to confirm that the Grayburg is likely dominated by shallow-water, near-shoreline sediments, while the San Andres is dominated by deeper water sediments associated with carbonate ramps. The rock types observed in the outcrop study were assumed to be present in the San Andres Formation in the area surrounding the EMSU. As a result

of the thicker high energy environment associated with the Grayburg Formation, different rock facies may exist in the Grayburg that are not present in the San Andres Formation.

Water Saturation Models

22. A version of the Simandoux model was used in Nutech's evaluation of the Grayburg and San Andres Formations in the EMSU. Robert Trentham, from the University of Texas Permian Basin, has recommended a modified Archie water saturation model for the screening of reservoirs for potential CO_2 enhanced oil recovery in residual oil zones. Both the Simandoux model and the Archie model were developed for quartz-dominated sandstone reservoirs. The Simandoux model is a modification to the Archie model designed to account for the presence of conductive clay minerals within the formation. Application of these models to carbonate reservoirs is challenging. For readers not familiar with water saturation modeling, an introduction to these models along with a brief explanation of their limitations for carbonate reservoir analysis are provided in Appendix A to this testimony that I prepared.

Core Data

23. Review of the technical literature indicates that a significant amount of core data from multiple wells is likely available for the various Eunice Monument reservoirs. Core measurements from three wells were provided to NSAI. Well log measurements were available for two of the three wells, R. R. Bell and EMSU 679. There is uncertainty concerning the coring interval for the core from R. R. Bell and due to the vintage of the resistivity measurements for this well, it is unlikely that the logs have a vertical resolution that would be sufficient for quantitative core analysis. The analysis for petrophysical model calibration relied primarily on the core data from EMSU 679. The core data from that well consisted of porosity and permeability measurement carried out at unidentified stress conditions and what appears to be Dean Stark

measurements of the oil and water saturations from the core samples. Basic core lithology descriptions were provided. Minor amounts of anhydrite and pyrite were observed in some of the samples. Vug porosity was observed in many samples.

24. An oil-wet or mixed oil-water-wet condition most likely exists in both the Grayburg and San Andres reservoirs. These conditions were found at the Seminole San Andres Unit during a formation evaluation program conducted prior to the initiation of CO_2 injection operations for the residual oil zone (ROZ) interval (Honarpour et al., 2010). The relatively high asphaltine content of the San Andres oil would tend to support the likely presence of an oil wet condition.

25. It is NSAI's understanding that no significant commercial volumes of oil have been produced from the San Andres intervals in any of the wells in the EMSU. The core from EMSU 679 was cut far below the estimated producing oil-water contact for the Grayburg reservoir (~350 ft. TVDSS). For all practical purposes it can be assumed that any oil that may exist in the limited amount of better reservoir quality San Andres rock types would be at or near residual oil saturation levels.

26. The grainstones and moldic grainstones are likely oil wet with oil coating the rock surfaces and water residing in the center of the pore networks. In a mixed wettability system, the micropores, associated with the carbonate mud component, tend to be water wet and are 100 percent water saturated. Oil and water reside in the larger pores and vugs with the oil coating the rock surfaces. At residual saturations, the oil is largely immobile as the result of the van der Waals forces that "bind" the heavier polar hydrocarbon components to the carbonate surfaces. The water likely resides in the middle of the pore network. As the core is removed from the well, dissolved gas in the oil is released as the result of decreasing pressure and displaces water from the core. Little, if any of the oil in the core would be expected to bleed out during core retrieval. That being

the case, the reported oil volumes from the Dean Stark analysis (corrected for shrinkage) should reasonably represent the residual oil condition in the reservoir. Surface water volumes would be expected to be lower than those existing at reservoir conditions as the result of flushing by gas expulsion.

27. Corrections were made to the core measurements to account for wettability, oil shrinkage, net reservoir stress, and gas expansion. The corrected oil saturation values were in reasonable agreement with residual oil saturations measured in the Seminole San Andres Unit from pressure and sponge cores obtained during a formation evaluation program carried out by Hess (Honarpour et al., 2010).

28. Intervals containing similar rock types were identified using the well log and core measurements. An averaging and cross-plotting technique developed by the BEG was used to identify the most-likely rock type for each interval (Keran et al., 1994; Lucia, 1995). The rock typing is carried out using the available core porosity and permeability measurements. Data from the San Andres outcrop study was used to guide the rock type analysis.

29. At the San Andres outcrop, vug-free carbonate samples were found to have porosities in the 10 to 15 percent range. Higher porosity was generally associated with the presence of isolated vug porosity (Kerans et al., 1994). A model to predict vug porosity in the San Andres from the neutron porosity, bulk density, and sonic travel time measurements was developed by Jerry Lucia (Lucia, 1999). Calculations with this model were performed for the wells in the evaluation that had sonic log measurements. The model indicates that high levels of vug porosity are present in both the Grayburg and the San Andres Formations within the EMSU as well as in the water disposal wells operating near the EMSU. Vugs were observed in the core plugs from EMSU 679.

30. As mentioned above, the presence of isolated vugs is generally indicative of decreasing reservoir quality. The dissolution-reprecipitation reactions associated with the development of vug porosity cause the tortuosity of the pore network to increase, increasing the electrical resistivity of the brine-filled rock. **It has been well-documented that the presence of isolated vug porosity causes the Archie cementation exponent, m, to increase to levels above the typically accepted value of 2.0 (Lucia, 1999; Asquith, 1996). Cementation exponent values exceeding 2.0 are also common when a bimodal pore size condition exists in the rocks (Asquith, 1996; Ballay, 2012).** A bimodal pore size distribution is usually present when rocks contain a mixture of intergranular porosity associated with the carbonate mud component and a separate intergranular porosity associated with the larger grains within the rock. Rock types containing some portion of carbonate mud typically exhibit elevated gamma ray readings. Bimodal pore size distributions are more common in the rock types found deeper down the carbonate ramp (grain dominated packstones/wackestones and mud dominated packstones/wackestones). **The presence of a bimodal pore system usually causes the Archie saturation exponent, n, to become variable with water saturation and to increase to levels above the traditionally utilized values of 2.0 (Suman and Knight, 1997; Fleury, 2002; Han et al., 2007)**.

31. **Another condition complicating the estimation of n is the wettability of the carbonate rocks. Oil and mixed wet rocks typically have n values much greater than 2 and often exhibit variations with increasing water saturation (Anderson, 1986).** Higher than expected n values have been routinely observed with laboratory measurements carried out on properly aged oil and mixed wet cores. Sweeney and Jennings, (1960) carried out experiments to compare the resistivity versus water saturation behavior for core samples at a water wet and an oil

wet condition. Figure 5 shows the results of the measurements. First the cores were prepared to exhibit a water wet condition (• symbols) and then the same cores were cleaned and prepared to exhibit an oil wet condition (x symbols). A highly non-linear resistivity index versus water saturation relationship is present with the oil wet samples.

32. **Nonstandard m and n behavior would be expected for each of the rock types present in the Grayburg and San Andres Formations.** In most cases, the elevated resistivity values observed in the well log measurements are likely the result of the increased tortuosity of the electrical current flow paths associated with the complex pore systems within the rocks rather than the presence of high oil saturations within the reservoirs.

33. Of the rock types present, the grainstones would be expected to have m values closest to 2.0. Pickett plot analysis carried out for the Grayburg and San Andres intervals consistently yielded estimates of m of about 2.3. This is consistent with Trentham's (2015) recommendations for ROZ screening analysis. This value is likely reasonable for the grainstones. Dziuba (1994) cautioned that 100 percent water saturated packstones and wackestones will fall to the right of the left-most leading edge of the Pickett Plot as the result of the higher m values associated with the complex pore structures of these rocks (see Figure 6). Therefore, the use of the Pickett Plot-derived m value would result in the overestimation of hydrocarbon content in those rock types.

34. Sonic travel time measurements were not available for the cored interval of EMSU 679 therefore the sonic-based m model developed for the San Andres by Lucia (1999) could not be employed. A workflow proposed by George Asquith (1996) from Texas Tech University was used to estimate m values for each of the defined rock types using correlations available in the

technical literature along with the results of laboratory measurements reported by Dziuba. Archie m values were estimated for each core plug.

35. The formation water resistivity, Rw for the cored well was estimated using standard Pickett Plot analysis. The Ro (water resistivity of a 100 percent water saturated rock) values for each plug were calculated using the Archie formation factor model $R_o = \frac{R_w}{PHI^m}$. The resistivity index (RI = Rt/Ro) was calculated for each plug assuming that the deep resistivity measurements from the well logs reasonably represented Rt.

36. Figure 7 shows a resistivity index versus water saturation crossplot constructed from the well log and core measurements. Also displayed are the constant n value trends used in the Simandoux model utilized by Nutech (Sept. 2023 Deposition) and Archie model used for the ROZ screening proposed by Trentham, et al. (2015).

37. **The core measurements consistently fall above the constant n trendlines. This would tend to verify that an oil or mixed wet condition exists and that simple, constant electrical parameter models will likely overestimate the oil saturations existing in the reservoirs (Asquith 2017)**.

38. A simple model developed by Schlumberger (Montaron, 2007, 2009) can be used to model the variable RI versus Sw behavior observed in the high-water saturation range in Figure 7. The model utilizes a single curve fit parameter denoted as the critical water saturation, Sc. Sc fits were made for each core plug and the average Sc values were computed for each rock type. Figure 8 shows a graphical representation of the Schlumberger model with the core plug measurements and the curve fits corresponding to the interpreted rock types.

39. The concave upwards behavior exhibited with the curve fits has been described with pore network and percolation models developed for oil and mixed-wet conditions at the

University of Texas (Wang and Sharma, 1988; Dunlap et al., 1991), Stanford University (Zhou et al., 1996), the University of British Columbia (Suman and Knight, 1997), Schlumberger (Montaron, 2007,2009), and the Institute of Petroleum in France (Fleury, 2003). The non-linear trend has been observed in laboratory measurements conducted with properly prepared and aged core samples from oil wet reservoirs (Sweeney and Jennings, 1960). In a water-wet system, a thin film of water remains in contact with the rock surfaces and a continuous conductive path remains in the rock allowing electrical current to flow during resistivity measurements. As the water content increases, the resistivity of the rock decreases in a predictable manner as the water film thickens making it easier for electrical current to flow. In an oil wet system, oil coats the rock grains and the water is located in the center of the pore network. As the water saturation is reduced, the water filling the larger pores becomes increasingly discontinuous as oil begins to block the pore throats, reducing the ability of the rock to conduct electricity during the resistivity measurements. For a given reduction in water saturation, the increase in resistivity for an oil wet rock is much greater than that for a water wet rock (McPhee et al., 2015).

40. The Archie water saturation model with standard m and n values tends to work well for water-wet reservoirs with simple intergranular pore systems. When a bimodal pore system is present or an oil-wet condition is present, the electrical conductivity behavior becomes more complex. Elevated resistivities can be the result of increased complexity and tortuosity of the conductive water pathways within the rock rather than simply the presence of hydrocarbons. **The use of simple Archie/Simandoux models in complex carbonate reservoirs typically results in the overestimation of the oil saturations**.

41. **The major conclusion that can be drawn based on the above discussion is that the use of the basic Archie or Simandoux water saturation model utilizing standard m and n**

values do not provide reliable water saturation estimates for the San Andres formation. A discussion of the limitations and likely biases associated with Simandoux model utilized by Nutech and the modified Archie model proposed by Trentham is provided later.

Water Saturation Estimates from Well Log Data

Wells with Sonic Measurements

42. Jerry Lucia (1995) has shown that rock types from multiple geologic facies can be simplified into four basic petrophysical facies or classes that define water saturation and flow behavior. The mapping from geologic facies into petrophysical facies for a San Andres ramp depositional environment was illustrated in the outcrop study performed by the BEG (Kerans et al., 1994). I followed the facies mapping proposed in the outcrop study to define four rock classes. The core-derived critical water saturation, Sc values were averaged to be representative of the interpreted rock class. Anhydrites and thick limestone muds were considered to be non-reservoir rocks.

43. The model developed by Jerry Lucia (1999) to predict vug porosity for the San Andres was used to estimate vug porosity for the wells where sonic measurements were available. This model was developed with core data from the Seminole San Andres Unit. Alternate calculations utilizing sonic measurements were also carried out using a model developed by George Asquith (1996). The Asquith model generally predicted higher vug porosities. In the San Andres outcrop study, it was found that the identified rock classes could be reasonably identified by defined ranges in the ratio of the vug porosity to the total porosity (VPR). Figure 9 shows the mapping of the VPR ranges defined from the outcrop study onto Lucia's four rock classes and the rock types associated with each class. I used the results of the outcrop study (Kerans et al., 1994) to define VPR ranges corresponding to each rock class.

44. Cementation exponent, m values, were calculated from the well log sonic and total porosity values using the models proposed by Lucia (1999) and Asquith (1996). VPR's were calculated and the indicated rock class was identified for each interpretation depth. Water saturation was calculated with the Schlumberger model using the log-derived m and the class-specific Sc parameter. Two water saturation estimates were calculated, one using Lucia's models and one using Asquith's models.

45. The advantage of this procedure is that it is basically "hands off", where the relative vug porosity is representative of the reservoir rock class and electrical conductivity conditions.

Wells Without Sonic Measurements, the "No Sonic" Model

46. It is inconceivable that a major oil and gas company would develop a carbonate reservoir without running sonic logs. The only sonic data provided to Goodnight was apparently synthetic sonic porosity estimates provided on Nutech's computed log results. Unfortunately, it was discovered that the sonic porosity estimates were synthetic late in my petrophysical analysis program. Data from the synthetic sonic log were found to be unreliable.

47. For the wells that did not have sonic measurements, the interpretation was more challenging. It was necessary to further simplify the rock typing. The identified rock types were divided into a shallow water rock class and deeper water (ramp) rock class. Average Sc values were computed from the core data for each class. Again, anhydrites and thick lime muds were considered to be non-reservoir rock. The rock type correlation procedure proposed by George Asquith (1996) was used to derive average m correlations for the shallow water class and the deeper water class.

48. To distinguish the shallow water class from the deep-water class from the well log measurements, procedures recommended by Lucia and Asquith were employed. Asquith (1996,

2004) proposes the use of a resistivity-derived porosity estimate to help distinguish rock with a primarily single modal intergranular porosity from rocks with bimodal porosity distributions. The resistivity porosity is calculated from the shallowest Rxo resistivity measurements and the mud filtrate resistivity. When the resistivity porosity is near the log-derived total porosity, an intergranular (shallow water) rock type is indicated. When the resistivity porosity is much smaller than the total porosity, a vugular or bimodal pore system (deeper water) is indicated. As mentioned above, gamma ray measurements can be used to distinguish shallow versus deep-water depositional environments (Hassan et al. 1976). Shallow-water deposits tend to have lower gamma ray readings while rocks having a higher mud component (deeper water environment) tend to have higher gamma ray readings. Thresholds were defined using the resistivity porosity and gamma ray criteria to select the appropriate rock class (shallow water versus deeper water ramp) for each interpretation interval. Numerous depositional cycles of shallow water and deeper water deposition appear to be present within the Grayburg and San Andres intervals. The gamma ray and resistivity porosity thresholds were adjusted to bring the log-derived water saturation estimates into the best possible agreement with the corrected core measurements. During the model-to-core calibration operations, it was observed that the critical water saturation, Sc values derived from the core measurements correlated with porosity. The best quality rock tended to have the lowest Sc values. This is consistent with the findings from the outcrop study discussed above. It was possible to model the transition from grainstone to moldic grainstone using the observed Sc versus porosity correlation. The log-to-core water saturation match was further refined by incorporating information from the mud filtrate invasion profiles derived from the shallow and deep resistivity measurements.

Permeability

49. Rock type class-specific permeability versus porosity transforms based on lab measurements were reported in the BEG outcrop study (Kerans et al., 1994). These transforms were used as the basis for my permeability estimates.

50. Low-porosity limestones and anhydrites and anhydritic dolostones were assumed to be virtually impermeable and were assigned a permeability of 0.01 mD. Intervals containing significant volumes of anhydrite were identified through the mineralogy analysis carried out during the porosity modeling. Anhydrite was mentioned in several of the core plug descriptions provided for EMSU 679. The small amounts of anhydrite found in the core plugs are below the resolution of the density-neutron crossplot mineralogy analysis. It is important to recognize the presence of anhydrite when evaluating the core-derived porosity and permeability measurements. Anhydrite is very unstable and can suffer structural damage and dissolution with changes in water salinity and temperature, both of which occur during core fluid extraction and cleaning operations. Specific cold solvent extraction procedures must be employed to prevent structural alterations and dissolution and even then, damage can occur that can compromise the porosity and permeability measurements. In most cases, anhydrite damage results in artificially increasing the porosity and permeability of the core plug. These special extraction procedures are usually performed only in the research facilities operated by major oil companies and few commercial core analysis laboratories offer them. For this reason, I chose to exclude the core measurements from intervals with enough anhydrite to show up in the log mineralogy analysis.

51. Plugs containing minor amounts of anhydrite were included in the modeling operations discussed above. The permeability estimates derived from the permeability versus porosity transforms discussed above may be optimistic in intervals containing anhydrite. In fact,

formation damage resulting from dissolution/reprecipitation reactions in anhydrite-bearing intervals has been identified as a source of areal flow barriers in the Grayburg waterflood operated within the J.L. Johnson Unit (Prentice, 1984).

Match to Core Data

52. The porosity and oil saturation match between the "no sonic" model and the corrected core measurements is shown in Figure 10. My permeability estimates are also displayed. Since Nutech did not evaluate the cored well, I did not have their solutions for comparison. Instead, water saturations were estimated using their described Simandoux model and these results along with the water saturation estimates predicted by the procedure proposed by Trentham et al. (2015) are also shown. For Trentham's model, a permeability versus porosity transform derived from core data reported in the Seminole San Andres formation evaluation study was used to predict permeability from my porosity estimates. **Both the Nutech and Trentham models overestimate the corrected oil saturations from the core measurements**.

53. A reasonable water saturation match was obtained with the simplified "no sonic" model. The model appears to overestimate the oil saturation in the poorer quality rock near the base of the core. The water saturation estimates were in general agreement when compared to the interpretation results from the wells where sonic measurements were available. The m correlations used in the "no sonic" model are based solely on interpreted rock type and total porosity. Variations in vug porosity are only approximately accounted for. The oil saturation results from the "no sonic" model were found to agree with the fluorescence and cut observations recorded on the available mud logs. The right-most track in Figure 10 shows the raw core oil and water saturation measurements. The separation between the measurements is indicative of water loss from the cores. The reservoirs are oil or mixed wet so significant oil losses from the core would

not be expected. Water was likely flushed from the cores during core retrieval due to the expansion of dissolved gas released from the oil as the result of decreasing pressure. Note that little water loss is apparent in the interpreted wackestone interval near the bottom of the display. This could be a result of the relatively low oil saturation, but it could also be the result of the presence of immature organic matter in the cores.

54. Preserved organic matter has been identified in several areas of the San Andres Formation in the Northern Shelf region in West Texas. It is possible that it could be found in the Northwest shelf region of New Mexico as well. Analysis of the likely thermal history indicates that the organic matter did not mature into the oil window and therefore the San Andres did not self-source. Organic matter has a high asphaltine content. Asphaltines are polar and will be attracted to and wet the surfaces of the host rock. Total organic carbon values ranging from 0.26 to 3.1 percent have been reported with an average vitrinite reflectance value of about 0.42 percent (immature) in the Northern Shelf region of the San Andres. **Therefore, any organic matter present in the San Andres in the EMSU is likely very immature**.

55. Organic matter is usually preserved in an anoxic environment. This usually occurs in very fine-grained sediments deeper in the depositional environment. In the San Andres this would likely be in the more mud-dominated packstones, wackestones, and lime mudstones. Organic matter could exist in the micropores associated with the mud components of the rocks further restricting the flow of electrical current. **The high resistivities recorded in regions of the San Andres containing mud-dominated packstones, wackestones, and lime muds are more likely the result of the presence of organic matter rather than the presence of oil**.

56. Immature organic matter has a density similar to oil and it fluoresces. It is possible that some of the fluorescence that has been observed in the mud logs from the San Andres

Formation, in intervals where the apparent gas content (C1) is very low, may be from organic matter rather than oil (see Figure 11). Another problem is that organic matter is soluble in the solvents used to extract oil from the core samples. During the Dean Stark extraction and fluid saturation experiments, organic matter can be mis-identified as oil.

57. The descriptions for the plugs taken near the base of the core mention the presence of solid black hydrocarbons. This is likely immature organic matter.

58. **The Nutech model and the Trentham screening model overestimate the oil saturations in the cored well**. The resistivity-based model employed by Nutech does not properly account for the reservoir wettability conditions commonly present in the Grayburg and San Andres Formations nor the complex conductivity conditions of the carbonate rock types present. The model proposed by Trentham for ROZ screening does approximately account for the expected rock wettability conditions (through an elevated n value of 3.4) but cannot handle the non-linear conductivity behavior associated with the rock types present in this part of the Northwest Shelf. The Trentham model may yield reasonable estimates of residual oil saturations for reservoirs associated with the Central Basin Platform where the San Andres reservoirs may be more dominated with shallow-water sediments. **I am of the opinion that both the Simandoux model utilized by Nutech and the modified Archie model proposed by Trentham overestimate the oil saturations in the San Andres Formation and much of the Grayburg Formation**.

59. An argument could be made that the core water saturations are too high, and the oil saturations are too low as the result of mud filtrate invasion during drilling. If that were the case, the core data would indicate the presence of mobile oil in this well with oil saturations in the Grayburg up to 80 percent. At these oil saturation levels, the water saturation would be near irreducible levels, which is inconsistent with the observed production performance from this well.

The perforated Grayburg interval produced at a water cut exceeding 94 percent for this well shortly after it was drilled in 1990.

60. My analysis took into account the complexity of the pore structures of the rock types interpreted to be present in the San Andres and Grayburg Formations as well as the variability of the electrical conductivity parameters necessary to accurately estimate the water and oil saturations present in the reservoir.

Oil Saturation Profiles

ROZ Profile

61. In the ROZ scenario proposed by Trentham and Melzer, the original (paleo) oil water contact is translated upward as the result of structural displacement resulting from faulting, a trap breach, or by changing hydrodynamic conditions below the main accumulation. Oil is displaced and a shallower oil-water contact is established. The interval between the paleo oil-water contact and the current oil-water contact is occupied by residual oil and is defined as the residual oil zone (ROZ). In this model, an interval originally containing relatively high oil saturations is swept by an upward-moving oil-water contact leaving residual oil behind in the swept zone. Movement of meteoric water through the ROZ interval has been proposed as an additional factor contributing to the residual oil saturation condition. The residual oil saturation profile expected behind an upward-moving oil-water contact is shown in Figure 12 and shows the oil saturation within the ROZ is 20% or higher. (Trentham, 2016).

62. A residual oil zone consistent with the model proposed by Trentham and Melzer has been identified at the Seminole San Andres Unit (Honarpour et al., 2010). Core flood experiments have been carried out with core samples from the Seminole San Andres Unit by the BEG (Wang et al., 1998). These experiments showed that residual oil saturations would likely

range from about 20 to 45 percent with the highest residual saturations existing in the poorer quality reservoir rocks with the highest isolated vug contents (see Figure 13). These results are consistent with the observations from the outcrop study discussed above. Oil saturations from pressure and sponge core recovered from the ROZ interval in the Seminole San Andres Unit consistently ranged from 20 to 40 percent, regardless of the permeability for intervals with permeabilities greater than 0.1 mD. The important point is that the residual oil saturations were somewhat independent of rock quality as expressed through permeability.

63. To test the validity of my model, calculations were performed for SSAU 4113 R which was drilled in 2017 as a part of the ROZ enhanced recovery program. The results of the model calculations are shown in Figure 14 along with the interpretation results for EMSU 746.

64. Review of the spectral gamma ray measurements from SSAU 4113 R indicate that the clay mineral content of the San Andres is relatively low and that the elevated gamma ray readings are primarily the result of the presence of uranium. This indicates that the San Andres interval in this well is most likely in a carbonate ramp environment which is very similar to that present in the EMSU. Note that the gamma ray readings from SSAU 4113 R are very similar to those in EMSU 746.

65. The estimated oil saturations in SSAU 4113 R derived from the "no sonic" model are in the range (20 to 40 percent) observed in the pressure and sponge core measurements reported in the reservoir characterization study from the Seminole Field (Honarpour et al. 2010). Unlike in the SSAU 4113 R, a continuous interval of residual oil saturations exceeding 20 percent is not present in the San Andres interval in EMSU 746.

66. The estimated oil saturations in EMSU 746 are generally much lower and the intervals with saturations in the 20 to 40 percent range are short and spread out over long distances

through the San Andres. Long intervals with oil saturation values of less than 10 percent are present. Many of these may consist of organic matter rather than live oil.

67. **Given the sparse, intermittent oil saturations, the saturation profile in the San Andres is more likely representative of abandoned oil migration pathways than of a previously oil-saturated interval. This saturation profile shows that the San Andres aquifer does not meet any reasonable definition of an ROZ.**

68. The interpreted logs indicate that the Grayburg Formation within the confines of the EMSU exhibits an oil saturation profile consistent with the characteristics of a residual oil zone (ROZ) as defined by Trentham and Melzer with relatively continuous interval of residual oil saturations exceeding 20 percent.

Oil Migration Pathways

69. Oil in the San Andres formation most likely originated in the deeper Wolfcamp formation and migrated upwards through major faults. Fault lineaments penetrating the San Andres and Wolfcamp formations have been identified in Southeast New Mexico (Ramondetta, 1982). During migration, oil finds the path of least resistance as it moves upward due to the buoyancy force resulting from the density difference between oil and water. During migration, oil resides in the center of the pore network and is completely surrounded by a film of water which is in contact with the pore surfaces. Migration typically occurs through the portions of the formation with the highest permeability. In the San Andres, this would likely correspond to the grainstone and grain-dominated packstone intervals (Kerans et al., 1994). Oil moves when a continuous pathway through the pore throats is established (Schowalter, 1979). Mercury injection capillary pressure curves from San Andres grainstone and fine-grained dolostone core samples indicate that continuous flow paths can be established when the oil saturation reaches from 10 to 40 percent of

the pore volume (Ghosh and Friedman, 1989). As long as the oil is moving, it remains in the center of the pores with the thin film of water residing between the oil and the pore surfaces. During migration of the oil between the faults and the shallower portions of the formation where the oil is trapped, the oil tends to move through narrow and irregular pathways through the higher permeability portions of the rock. Pathway heterogeneity is caused by macroscopic heterogeneity of the petrophysical properties of the formation through which migration is occurring. Modeling has shown that migration typically occurs only through a small fraction of the volume of the formation (Luo, 2011). For example, Figure 15 shows a simulation of the behavior of migration paths migrating upstructure from a major fault from an overhead or map view. In this example the migration paths only covered around ~17% of the area. Outcrop studies have shown that there is extreme permeability heterogeneity in the San Andres formation (Kerans et al., 1994). Once migration ends and water begins to move through the formation, the remaining oil in the migration paths becomes trapped in the center of the pores as the moving water displaces the oil from the pore throats. The trapped oil saturation **within the meandering migration pathways** would therefore be expected to be somewhere between 10 percent to at most 40 percent of the pore volume of the higher permeability rock. Once the trapped oil becomes static, the weak electro-static van der Waals forces at the carbonate grain surfaces can begin to act on the oil. Van der Waals forces are the forces that hold water droplets on the surfaces of a shower wall. Polar components (compounds composed of molecules with positive and negative ends) within the oil are attracted by the electro-static forces at the pore surfaces and the oil slowly begins to coat the carbonate grains. Eventually, the oil completely coats the grain surfaces and the water moves to the center of the pores. The rock becomes oil-wet. Micropores within the rock can remain water wet as the result of the strong capillary forces binding the water to the pore surfaces. The larger

mesopores and macropores usually become oil wet as the result of contact with the residual oil. When both wettability conditions exist, the rock is said to have mixed wettability.

70. **The primary feature that distinguishes a migration path from a swept residual oil zone is that the swept ROZ was once occupied by relatively high oil saturations and swept to residual oil saturations while a migration path was never occupied by oil saturations greater than residual levels.** In the migration path scenario, poor quality rock would be expected to have little oil present because high oil saturations were never present to begin with. Interpretation of the available sonic measurements indicates that significant levels of vug porosity are present in both the Grayburg and San Andres in the vicinity of the EMSU. Vugs have also been identified in the core samples. **Based on the results of the core flood experiments carried out by the BEG (discussed above), the residual oil saturations in the San Andres would be expected to be higher (in the 20 to 40 percent range) if those intervals had been saturated to higher levels in the past.**

71. **The San Andres Formation, both inside the EMSU and in the areas outside the EMSU where Goodnight operates salt-water disposal wells, has an oil saturation profile that appears to be more representative of paleo oil migration pathways**. **Thick, continuous intervals of oil saturation exceeding 20 percent are not present in the San Andres within the EMSU.** Long intervals containing no hydrocarbons at all are present in most of the interpreted wells below 875 ft. TVDSS. It is likely that much of the interpreted hydrocarbons in the intervals with elevated gamma ray readings consist largely of immature organic matter rather than live oil. Low methane (C1) values on the available mud logs are consistent with the possible presence of immature organic matter. **Narrow, meandering migration paths would not likely be mappable between wells either areally or vertically.**

72. In the reservoir characterization study for the Seminole San Andres Unit (Honapour et al., 2010) it was reported that the residual oil saturation in core samples flooded with CO_2 were reduced to about 12 percent. Returning to Figure 14, the log-derived oil saturations in the main pay zone (MPZ) typically never fell below about 20 percent. The MPZ has undergone CO_2 and water flooding for over 40 years. This suggests that 20 percent rather than 12 percent may be a more representative estimate of the residual oil saturation achievable by long-term CO_2 injection. The ROZ enhanced oil recovery target for the Eunice Monument South Unit in the Grayburg likely consists of intervals with residual oil saturations greater than 20 percent.

73. Flags identifying intervals with oil saturations exceeding 20 percent are displayed on the interpreted log displays that I have prepared and are included in Appendix B. Comments addressing each well analyzed are included in Appendix C.

74. **Thick, mappable intervals of oil exceeding 20 percent oil saturation do not appear to be present in the San Andres in the well logs analyzed**. However, mappable ROZ intervals are present in the Grayburg.

Vertical Flow Barriers, Loss Circulation, and Karsts

75. A vertical to horizontal permeability correlation was built from core measurements reported for the Seminole San Andres Unit in the paper outlining Hess's formation evaluation program carried out prior to their ROZ CO_2 flood (Honarpour et al., 2010). Vertical permeabilities were estimated from my horizontal permeability estimates and a barrier flag was posted on the interpreted log displays when the vertical permeability fell below 0.01 mD.

76. **Thick, impermeable anhydrites and anhydritic dolostones found near the top of the San Andres Formation likely isolate the water disposal intervals in the Goodnight-operated wells from the overlying Grayburg residual oil zones.** Evidence of this zonal isolation

has been found in the loss circulation behavior observed during drilling operations. Flags identifying the top of the lost circulation intervals are displayed on the interpreted log plots. The stark contrast in the computed water saturation profiles between the Grayburg and San Andres provides further evidence of the zonal isolation. **The fact that the San Andres and Grayburg Formations appear to be isolated from one another suggest that a continuous oil column did not exist between these formations. This would also prevent water migrating from the San Andres upwards into the Grayburg, and thus the San Andres would not meet Trentham's definition of an ROZ. Water disposal operations in the San Andres aquifer are unlikely to impact a Grayburg ROZ CO_2 enhanced recovery project.**

77. Major uplift of the San Andres Formation has occurred resulting in the outcrop of the formation west of the Eunice Monument Units. Vance, et al. (2011) have mapped several likely water migration fairways that move meteoric water from outcrops of the San Andres in New Mexico eastward toward Texas. Calculations have indicated that on the order of 20 pore volumes of water may have passed through these fairways (Trentham and Melzer, 2016). Likely fairways have been mapped in the San Andres in the area occupied by the various Eunice Monument Units and the area where Goodnight's water disposal operations are occurring. The potentially high volumes of water throughput help to explain the high levels of vug porosity that the models developed by the BEG and George Asquith predict to be present in both the Grayburg and San Andres. With sufficient throughput of reactive waters, connected vug networks can form which increase the permeability of the host rocks. Dissolution reactions resulting from the long-term mixing of formation water with fresher meteoric water can further enlarge the vug networks creating karsts and collapse breccias within the formation (Lucia, 1999). **Loss circulation problems consistently experienced during drilling operations through the San Andres**

aquifer and the fact that high volumes of water can be injected on a vacuum in the Goodnight disposal wells, indicate that large karsted intervals are likely present. Flags identifying potentially karsted intervals are provided on the interpreted log displays. In many cases, the karst flags are considerably deeper than the top loss circulation flags indicating that karsting may be more prevalent in the San Andres than my model predicts. The levels of matrix permeability exhibited in the core measurements suggest that sufficient matrix permeability would not likely exist in the San Andres aquifer to account for the high volumes of water that are being injected, indicating the presence and importance of karsting in the San Andres. Potentially karsted intervals have also been identified in the Grayburg. The thicker karsts appear to be limited to the San Andres. **The presence of large karsted intervals would make it challenging to perform efficient CO_2 enhanced oil recovery (EOR) operations in the EMSU**.

Injection Flag

78. Flags are posted on the interpreted log displays identifying areas where CO_2 could invade the formation. These flags correspond to intervals with estimated horizontal permeabilities greater than 0.1 mD. A permeability versus porosity crossplot was prepared from the corrected core measurements. Based on the regression shown in Figure 16, a porosity cutoff of 7 percent was selected to define reservoir vs non-reservoir rock. The far right track on the log images displays the injection flag based on the magnitude of permeability (the larger the flag the higher the permeability with blue being lowest values to red being highest). It is reasonable to expect that CO_2 would preferentially sweep the intervals with the highest permeabilities (red flags). The log-derived permeability estimates do not take the potential presence of karsts and collapse breccias into account. Karsted and brecciated intervals will have permeabilities that are likely several

orders of magnitude higher than the log-derived permeability estimates and thus the injected CO_2 would be more likely to fill these intervals instead.

Issues with the Water Saturation Approach Used by Nutech and Trentham

79. The major issue with the Simandoux water saturation model used by Nutech and the Archie model proposed by Trentham is not necessarily the models themselves, but the fact that Nutech and Trentham proposed using these models with single values of m and n. It has been well established that a variety of carbonate rock types exist in both the Grayburg and San Andres Formations. Each rock type has distinct electrical conductivity behavior. Variations in both m and n are certainly present. **Unfortunately, the single parameter values chosen by Nutech and by Trentham result in the significant overestimation of the oil saturations in the San Andres Formation and much of the Grayburg Formation.** More reasonable oil saturation estimates could have been obtained with either of these models had the variability of m and n with rock type and reservoir wettability been taken into account. In almost all cases, the m and n values for the rock types present would be greater than the single values adopted by Nutech and Trentham. Increases in m and n result in increases in the estimated water saturations.

80. The Simandoux model used by Nutech includes shale volume and shale resistivity terms that are intended to account for conductive clay minerals in the host rocks which attenuate the measured resistivities. Shale volume is typically computed based on the gamma ray measurements. In the deeper water sediments, elevated gamma ray readings can occur as the result of the adsorption of uranium from sea water onto fine-grained sediments. The actual shale volumes can be much lower than indicated by the gamma ray measurements. Estimates from nearby wells completed in the San Andres logged with spectral gamma ray tools indicates that actual shale volumes are typically less than one-third of that predicted from the raw gamma ray

measurements. It is therefore likely that shale volume estimates derived solely from gamma ray measurements will be overstated. This situation likely contributed to the overestimation of oil saturations in the San Andres.

81. The oil saturations predicted by these models do not accurately reflect the oil saturations from the available core measurements and do not conform to observed well performance.

82. To illustrate the issues with the Simandoux and Archie models, calculations were performed for SSAU 4113 R. For the Simandoux model, m and n were set to 2.0 as proposed by Nutech. For the Archie model m was set to 2.3 and n was set to 3.4 as proposed by Trentham (2015). Formation water salinity was taken from data presented for the Seminole San Andres Unit by Honarpour et al. (2010). The estimated formation water resistivity derived using this salinity was found to be consistent with an Rw value derived from Pickett Plot analysis. Shale volume estimates for the Simandoux model were derived from the raw gamma ray measurements and a nearby shale above the San Andres was used to estimate the shale resistivity. The results of these calculations are displayed in Figure 17. SSAU 4113 R is roughly located in the center of the Seminole San Andres Unit (Figure 18). Enhanced oil recovery operations involving CO_2 and water injection in the main production zone (MPZ) have been underway for over 40 years. CO_2 injection in the residual oil zone (ROZ) began sometime after 2010. The Simandoux model predicts oil saturation ranging from 70 to 90 percent through the MPZ. The Archie model predicts oil saturation ranging from 40 to 70 percent through the MPZ. Neither of these is plausible. The oil saturation estimates from NSAI's "no sonic" model range from 20 to 40 percent through the MPZ and ROZ. These oil saturation values are in general agreement with the oil saturations observed from the pressure and sponge core measurements reported from the Seminole San Andres Unit

reported by Honarpour et al. (2010). These calculations further confirm the validity of our petrophysical model.

Well-Level Oil in Place Calculations

83. Oil in place calculations in terms of MMbbls/section have been prepared for each well discussed in Empire's testimony from September 2023. Based on the well log interpretation of SSAU 4113 R, the residual oil saturation to long-term CO_2 and water flooding appears to be about 20 percent. I flagged intervals with oil saturations greater than 20 percent as potential targets for EOR operations. For the purposes of the oil in place calculations, only the hydrocarbon pore volume in intervals containing oil saturations of 20 percent or greater were included. The results are summarized below.

	OIP (MMBO/sec)	
Well	Nutech	NSAI
EMSU 628	89.4	6.8
EMSU 658	60.9	0.0
EMSU 660	98.1	2.7
EMSU 673	61.1	3.1
EMSU 713	13.6	0.0
EMSU 746	174.5	13.3
Ryno 1	91.5	6.9
Total	589.1	32.8

84. **Based on these calculations, the effective oil in place in the San Andres is only about 6 percent of the value reported by Empire in the September 2023 deposition**. However, these calculations assume 100 percent areal coverage. If the oil in the San Andres is indeed contained in paleo migration pathways, the areal coverage would only be a small fraction of a section. This is illustrated conceptually in Figure 15.

85. **Given the sparse nature of the residual oil accumulations and the presence of significant karsting, it is my opinion based on my experience and the data and information I**

reviewed to date that Goodnight's San Andres disposal zone does not meet any reasonable definition of an ROZ.

86. These intervals of sparse oil accumulations in the San Andres aquifer that do not meet the definition of an ROZ are too thin, widely spaced, and are not likely areally continuous enough to support enhanced recovery operations.

87. I affirm under penalty of perjury under the laws of the State of New Mexico that the foregoing statements are true and correct. I understand that this self-affirmed statement will be used as written testimony in this case. This statement is made on the date next to my signature below.

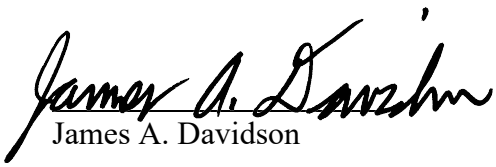

James A. Davidson

August 16, 2024
Date

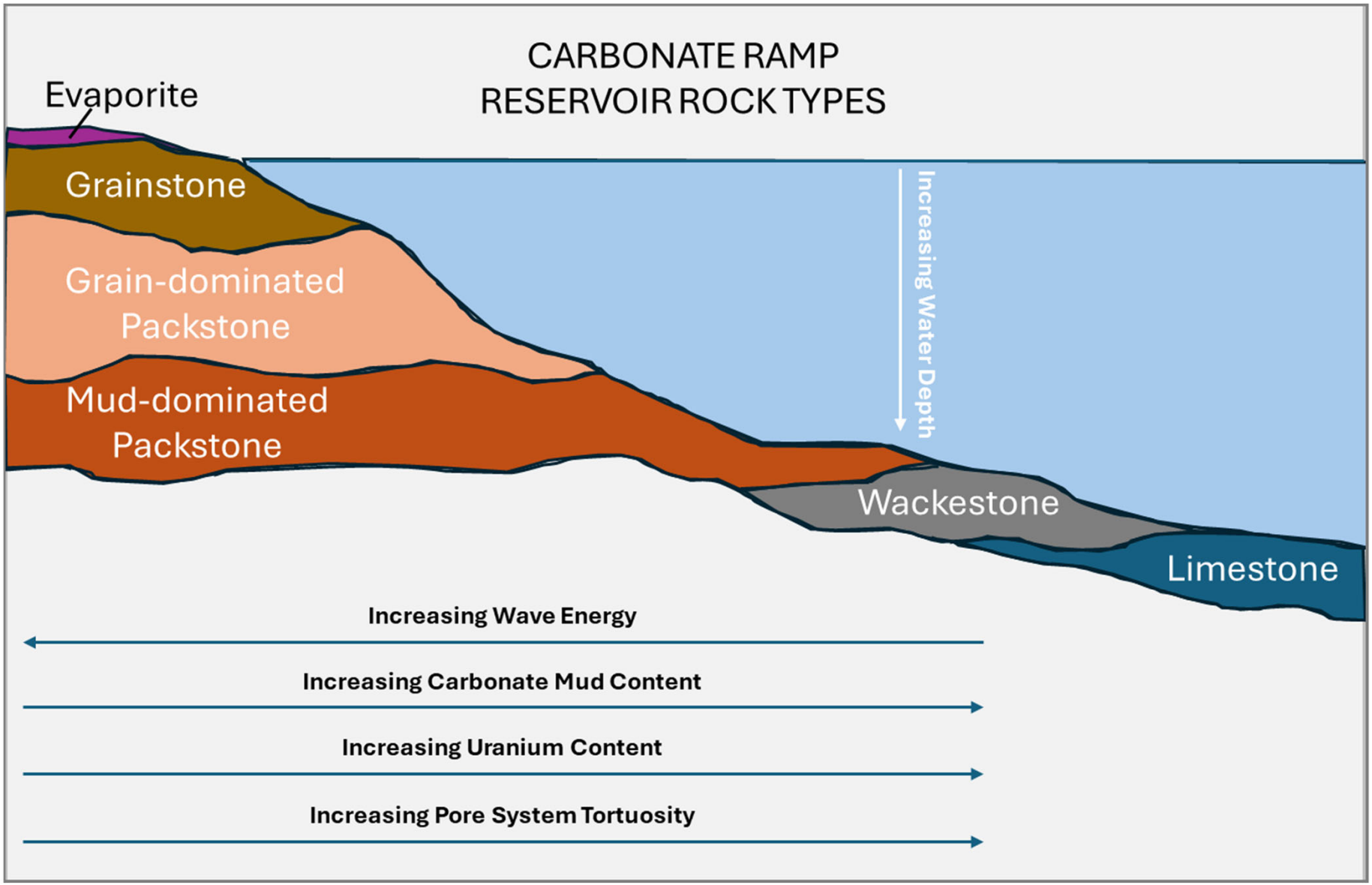

Figure 1

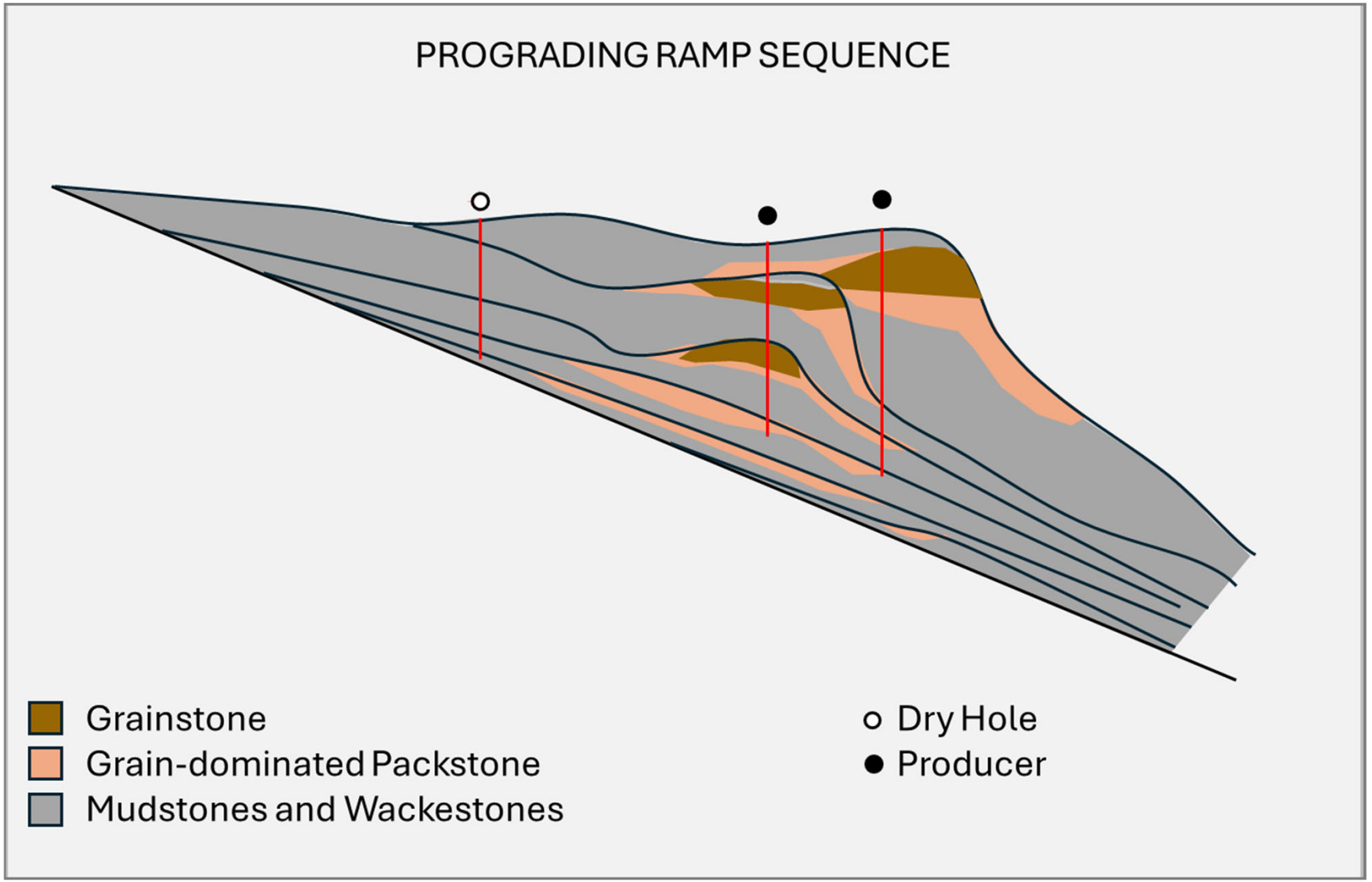

Figure 2

NETHERLAND, SEWELL & ASSOCIATES, INC.

SEMU BTD 123

30-025-31178

Central Drinkard Unit #441

30-025-39805

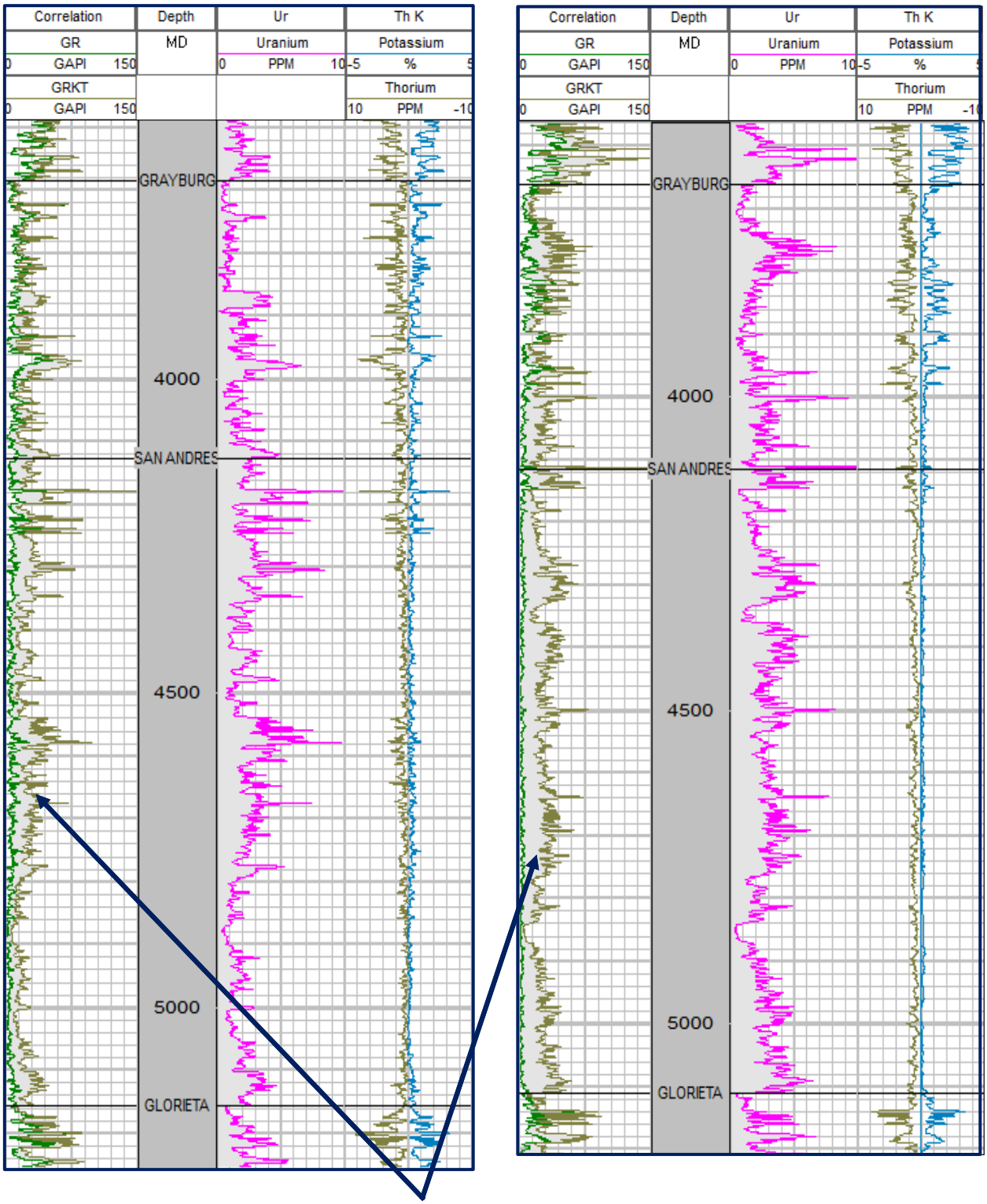

Uranium concentrations shaded in light gray. As you move deeper, uranium becomes more dominant features of gamma ray signal.

Figure 3

NETHERLAND, SEWELL & ASSOCIATES, INC.

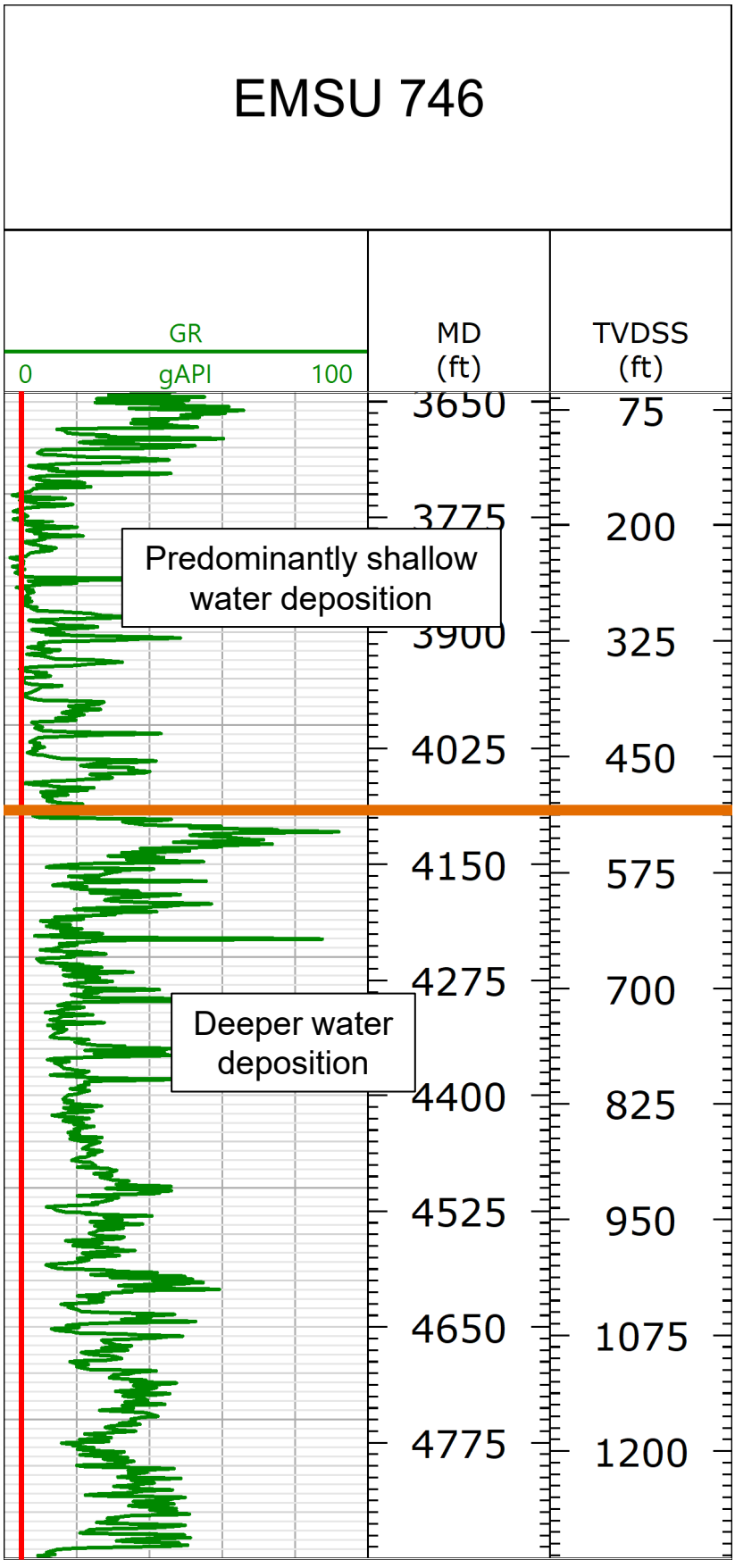

All estimates and exhibits herein are part of this NSAI report and are subject to its parameters and conditions.

Figure 4

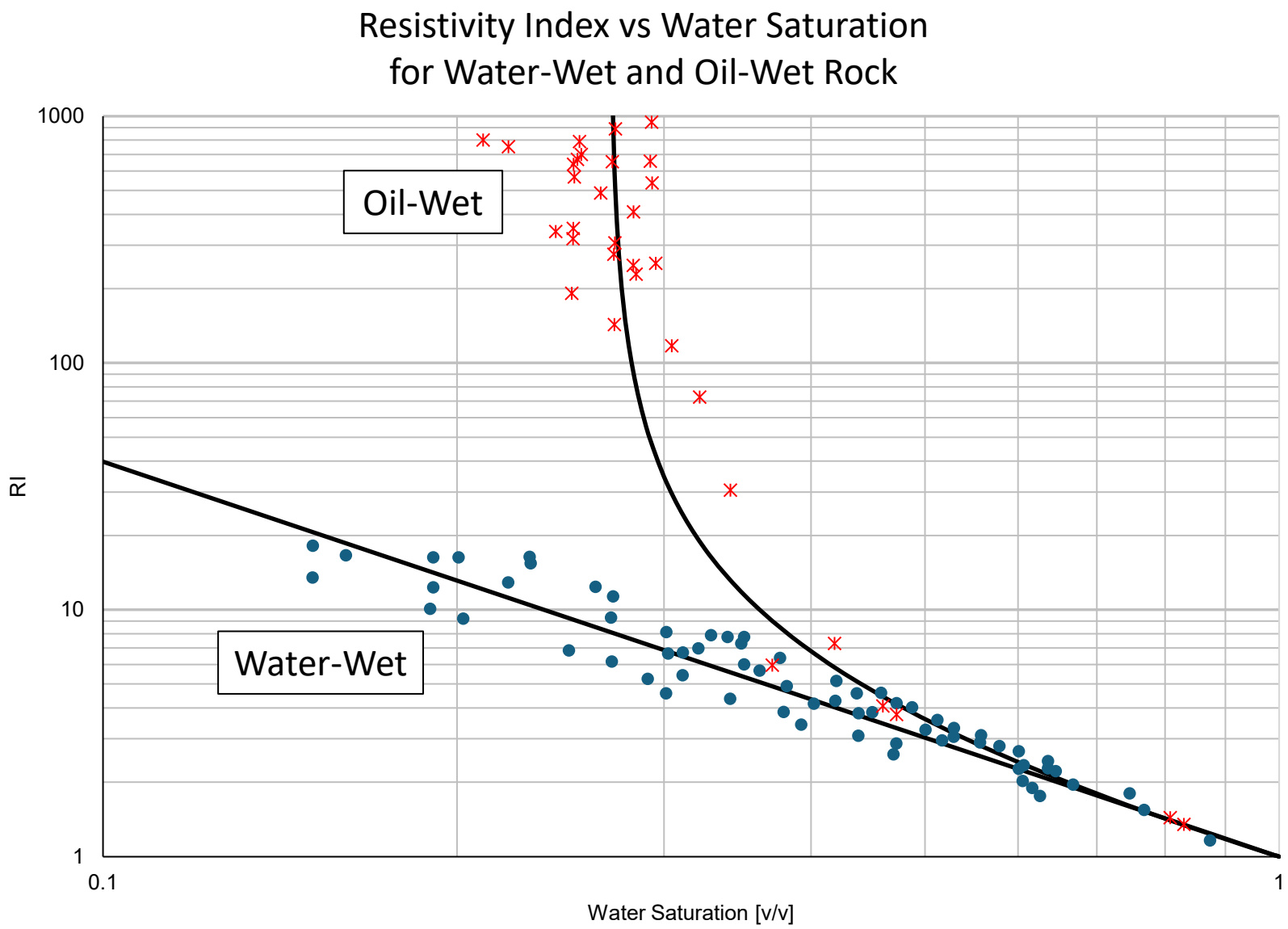

Figure 5 Data from Sweeney and Jennings, 1960.

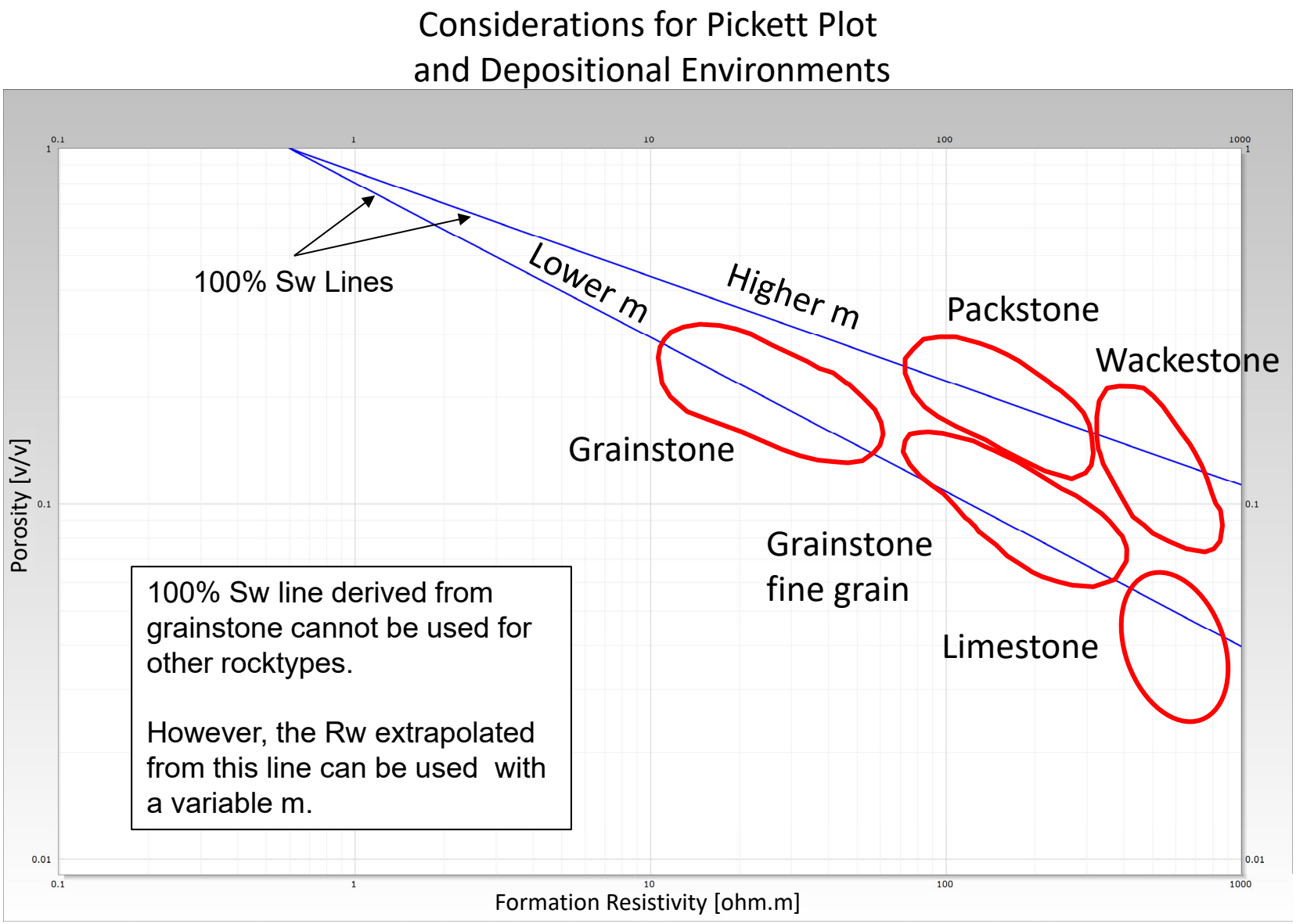

Figure adapted from Dziuba, 1994.

Figure 6

EMSU 679
Core RI vs Water Saturation

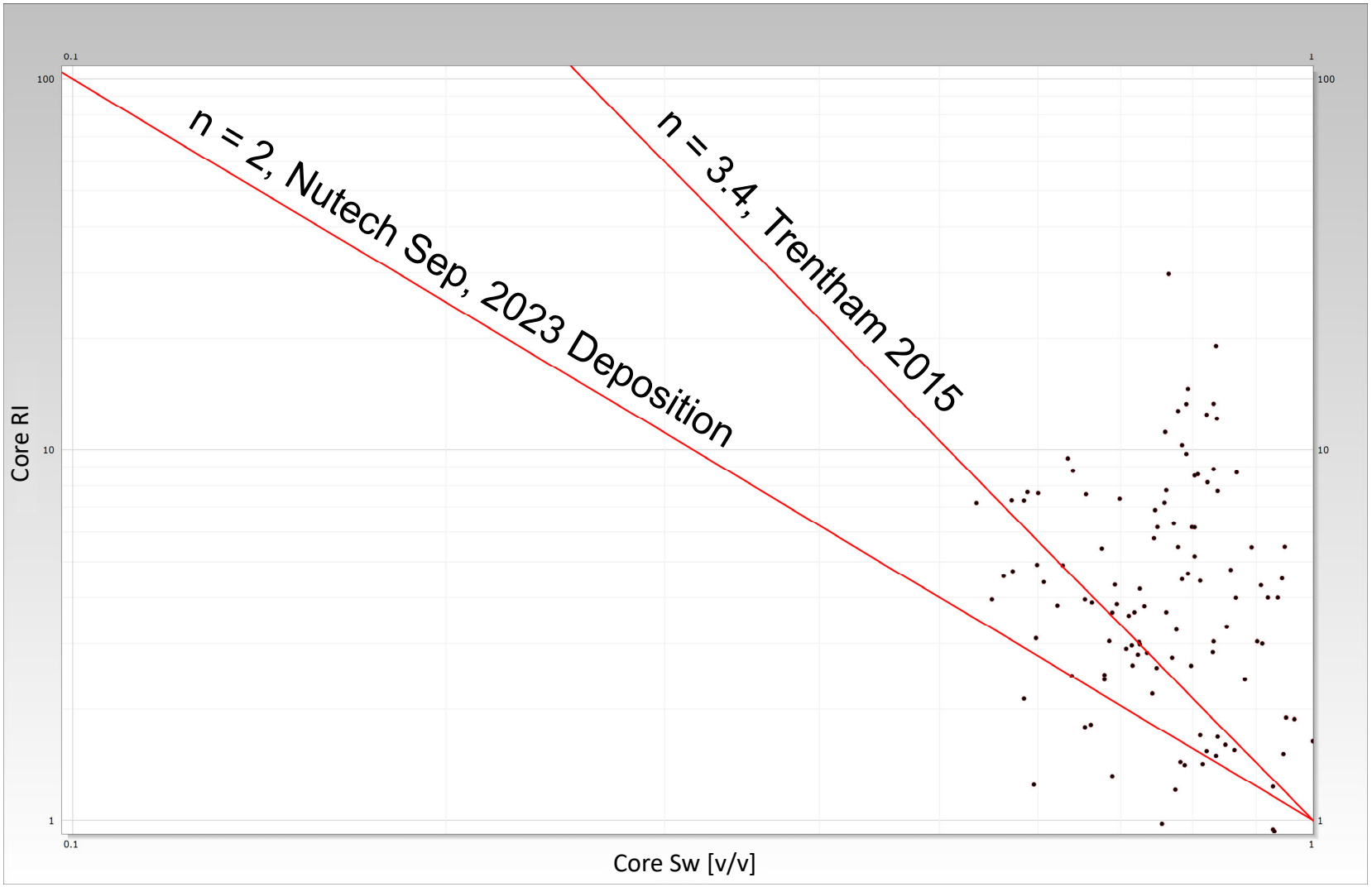

Figure 7

EMSU 679
Core RI vs Sw with Sc Curves

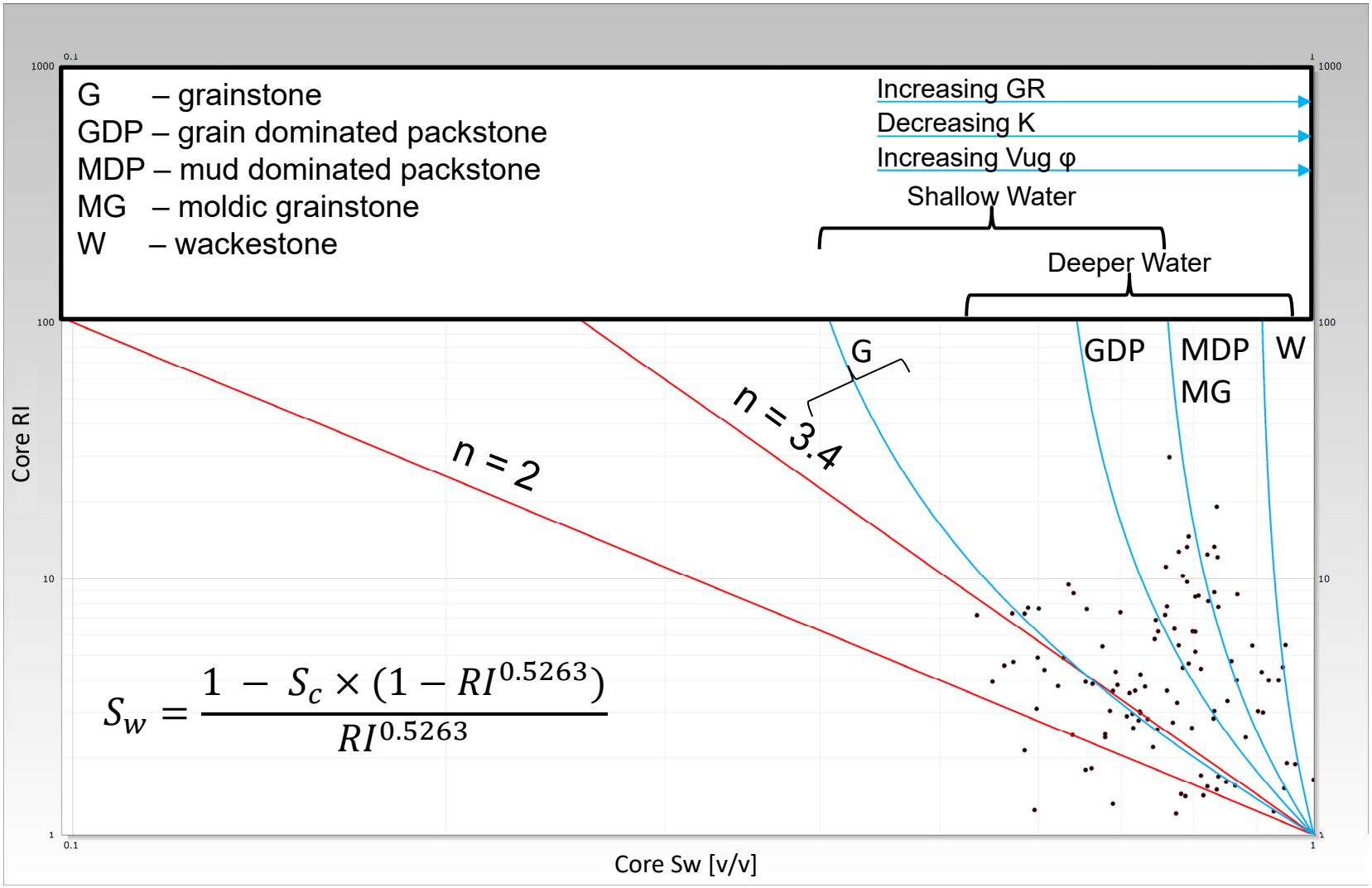

Figure 8

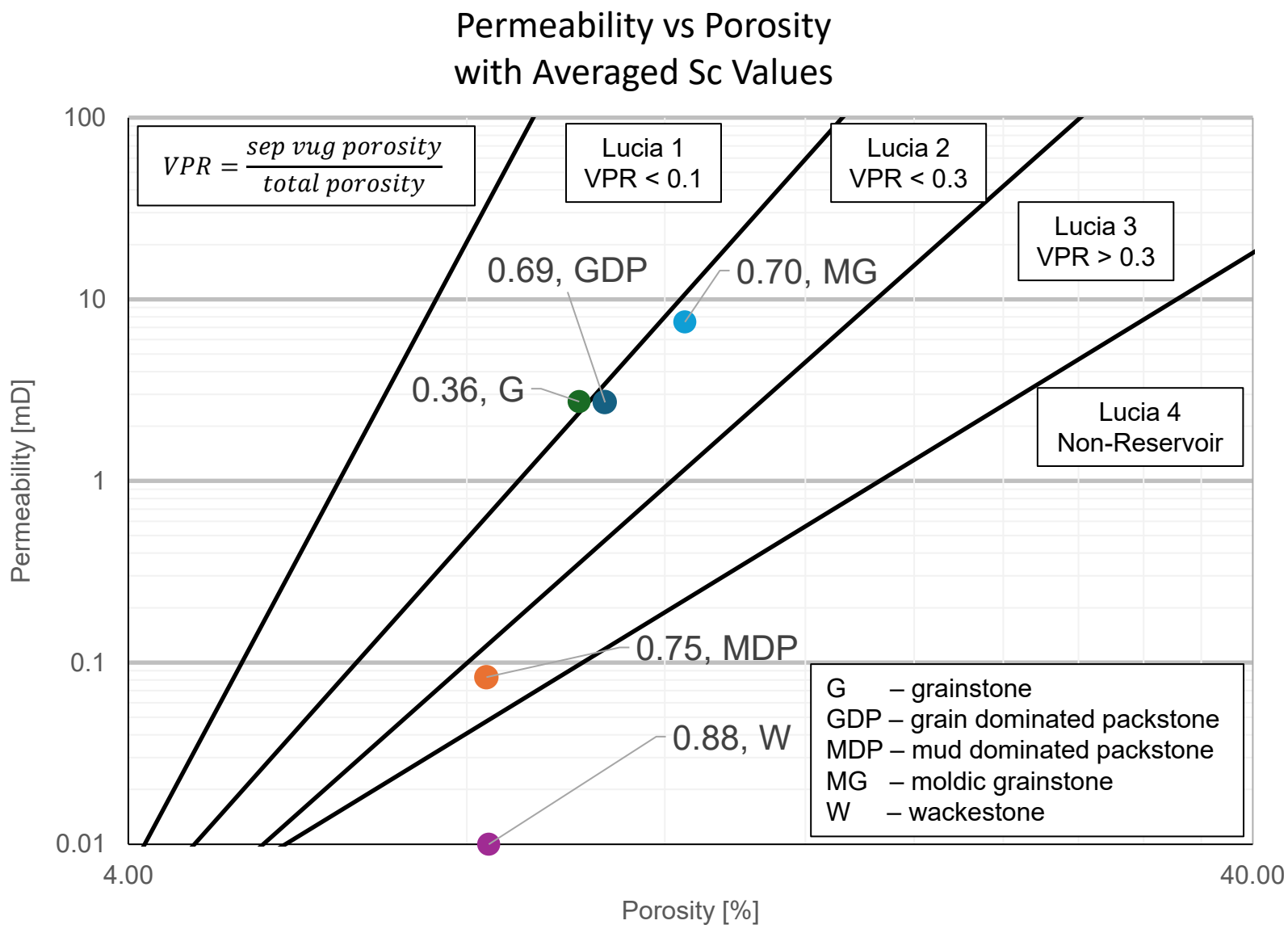

Figure 9

NETHERLAND, SEWELL & ASSOCIATES, INC.

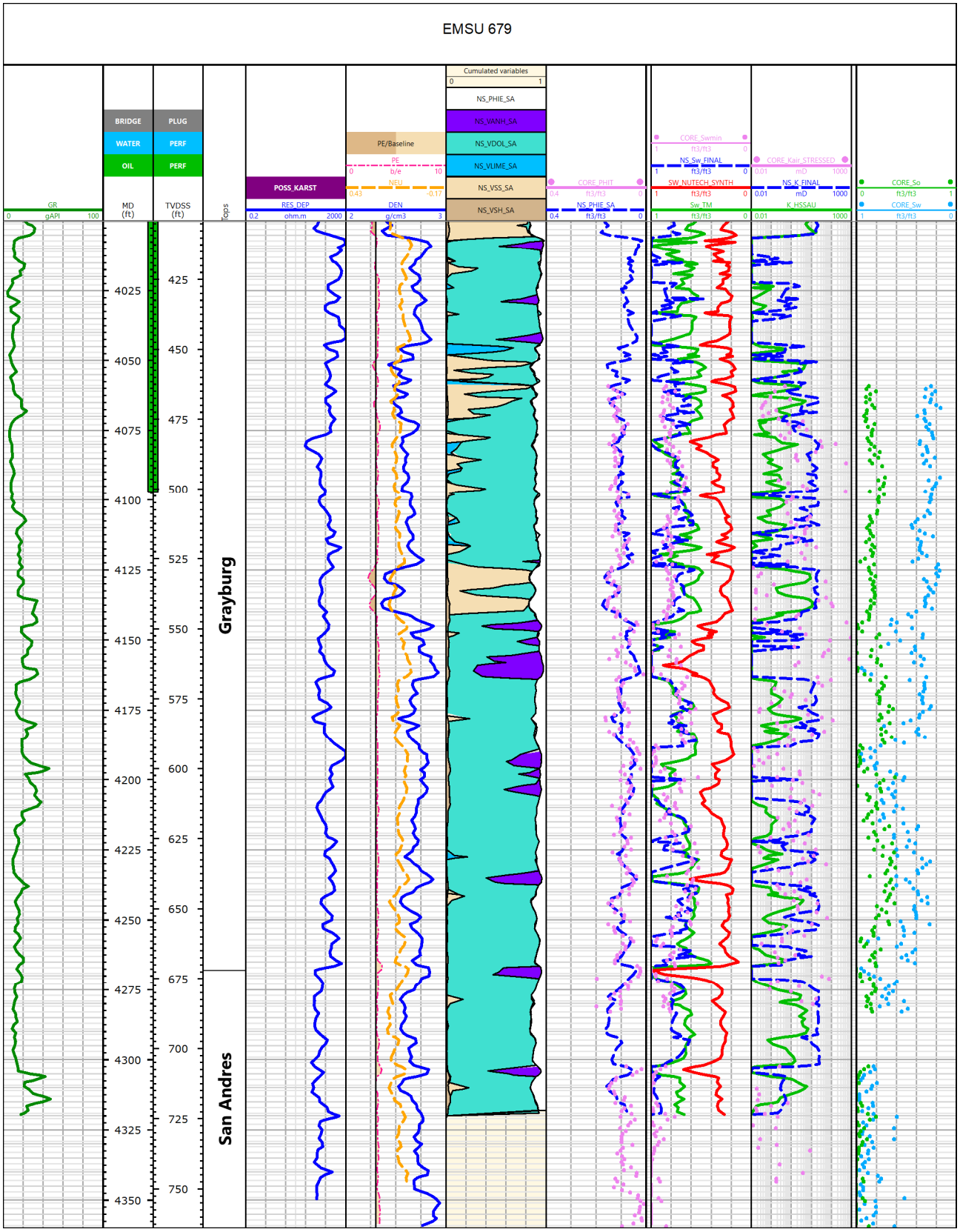

All estimates and exhibits herein are part of this NSAI report and are subject to its parameters and conditions.

Figure 10

NETHERLAND, SEWELL & ASSOCIATES, INC.

EMSU 660 MUDLOG
POSSIBLE EVIDENCE OF ORGANIC MATTER

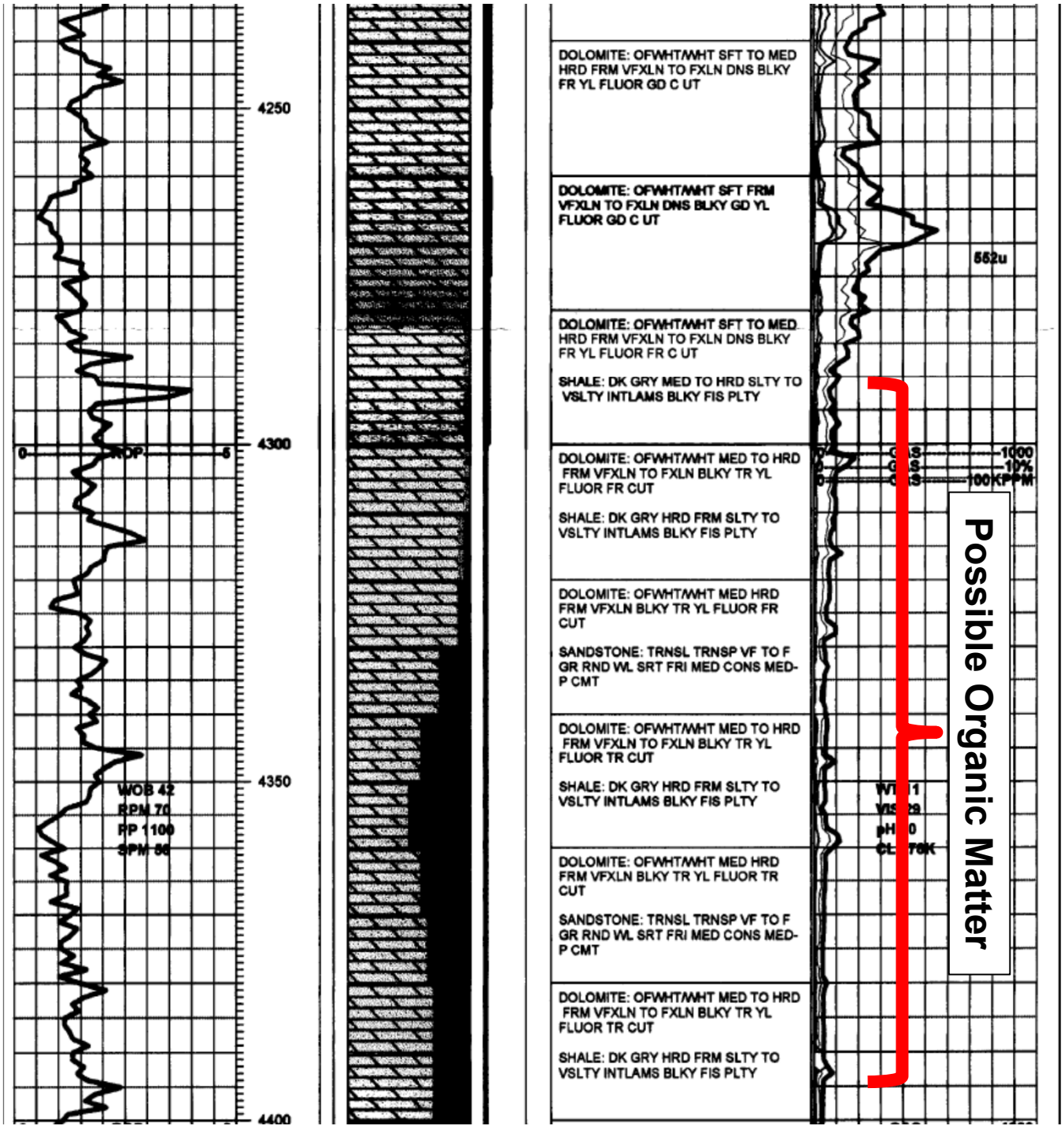

Description indicates fluorescence for intervals with both high and low methane (C1)

NETHERLAND, SEWELL & ASSOCIATES, INC.

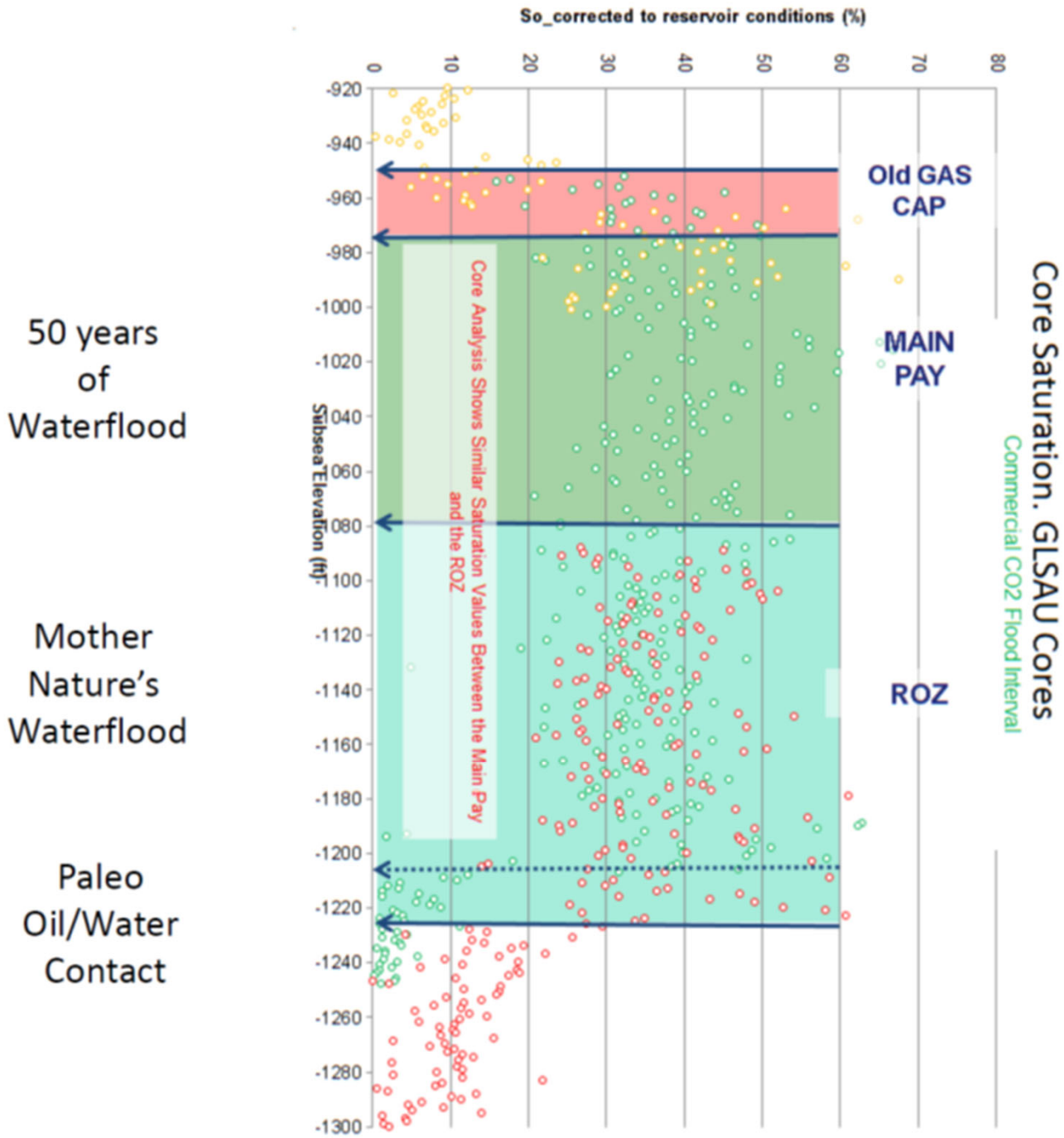

Figure adapted from Trentham, R. and Melzer, S., 2016.

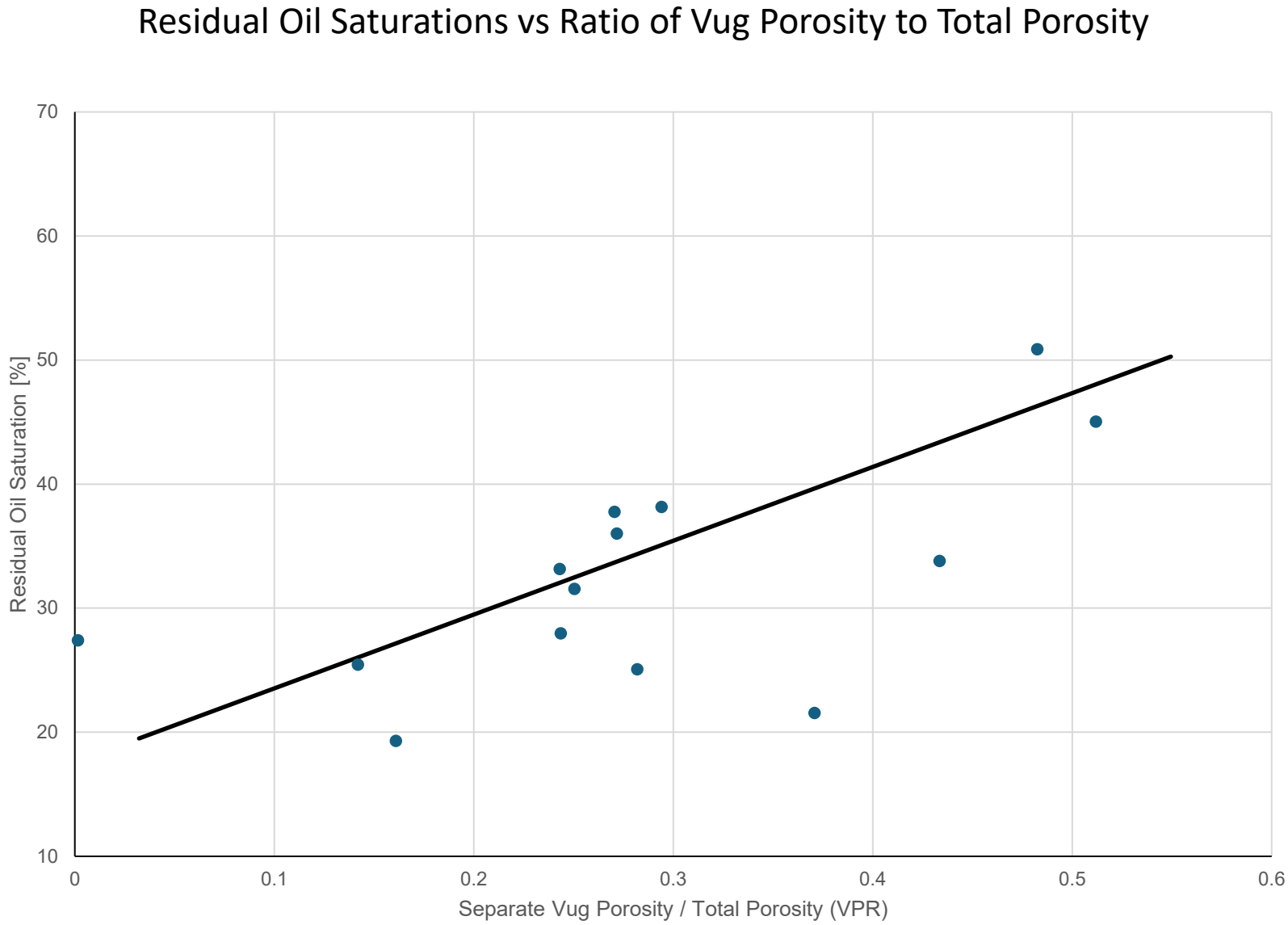

Figure 13

Data from Seminole San Andres Unit from Wang, 1998.

NETHERLAND, SEWELL & ASSOCIATES, INC.

EMSU and SSAU ROZ Comparison

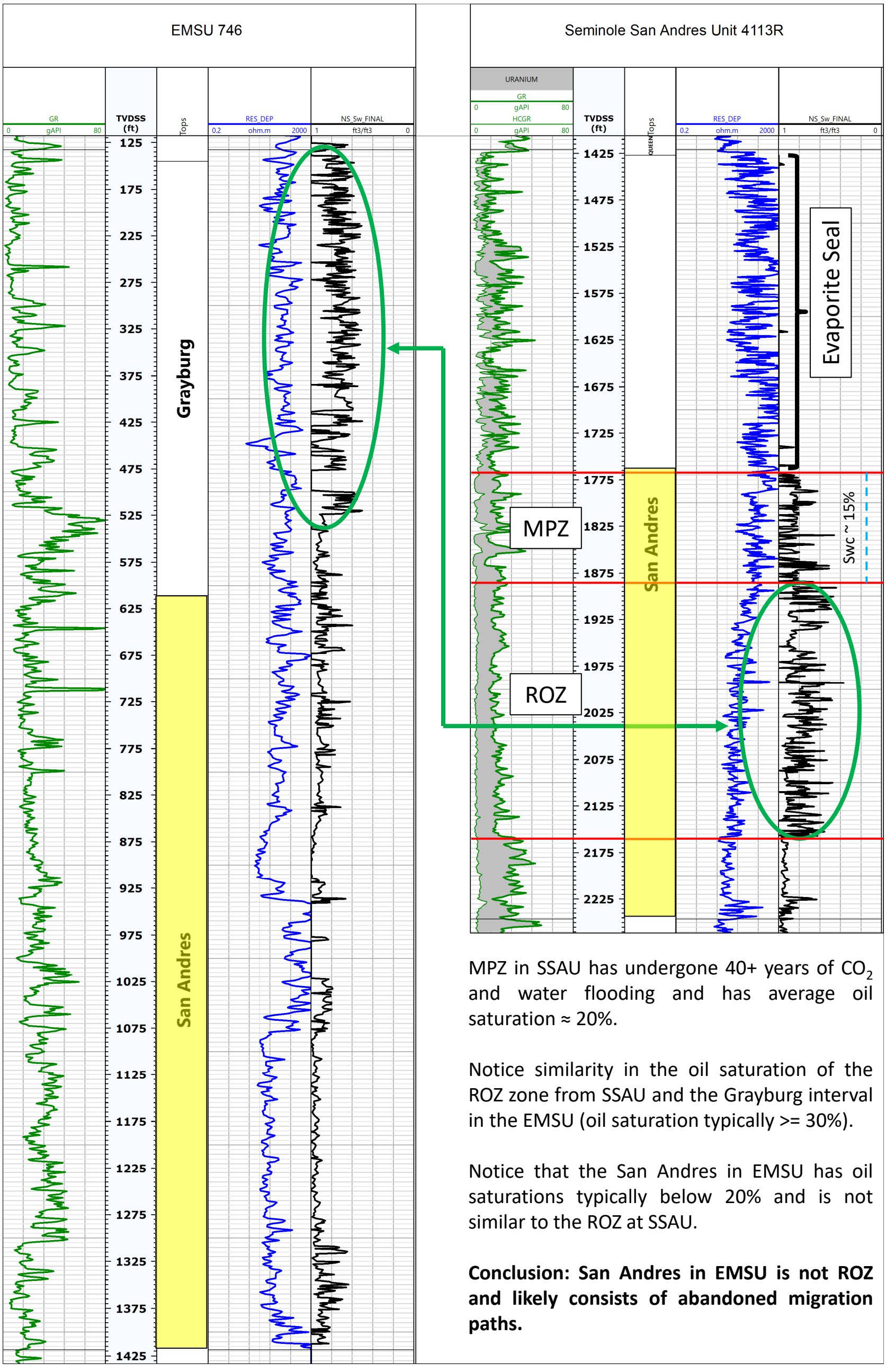

MPZ in SSAU has undergone 40+ years of CO_2 and water flooding and has average oil saturation ≈ 20%.

Notice similarity in the oil saturation of the ROZ zone from SSAU and the Grayburg interval in the EMSU (oil saturation typically >= 30%).

Notice that the San Andres in EMSU has oil saturations typically below 20% and is not similar to the ROZ at SSAU.

Conclusion: San Andres in EMSU is not ROZ and likely consists of abandoned migration paths.

Figure 14

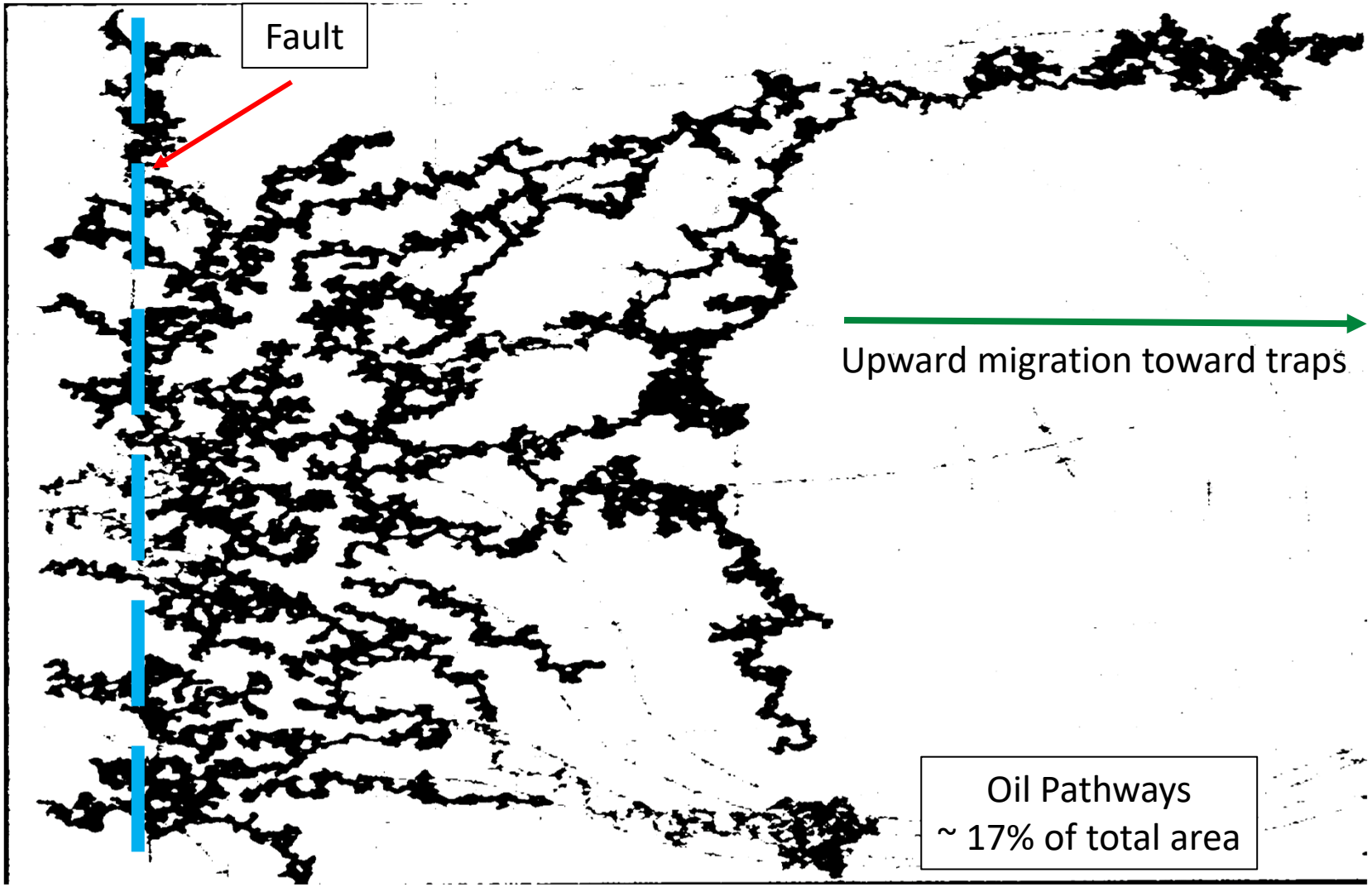

Figure modified from Luo, X., 2011.

Figure 15

EMSU 679
Stress Corrected Core K-PHI

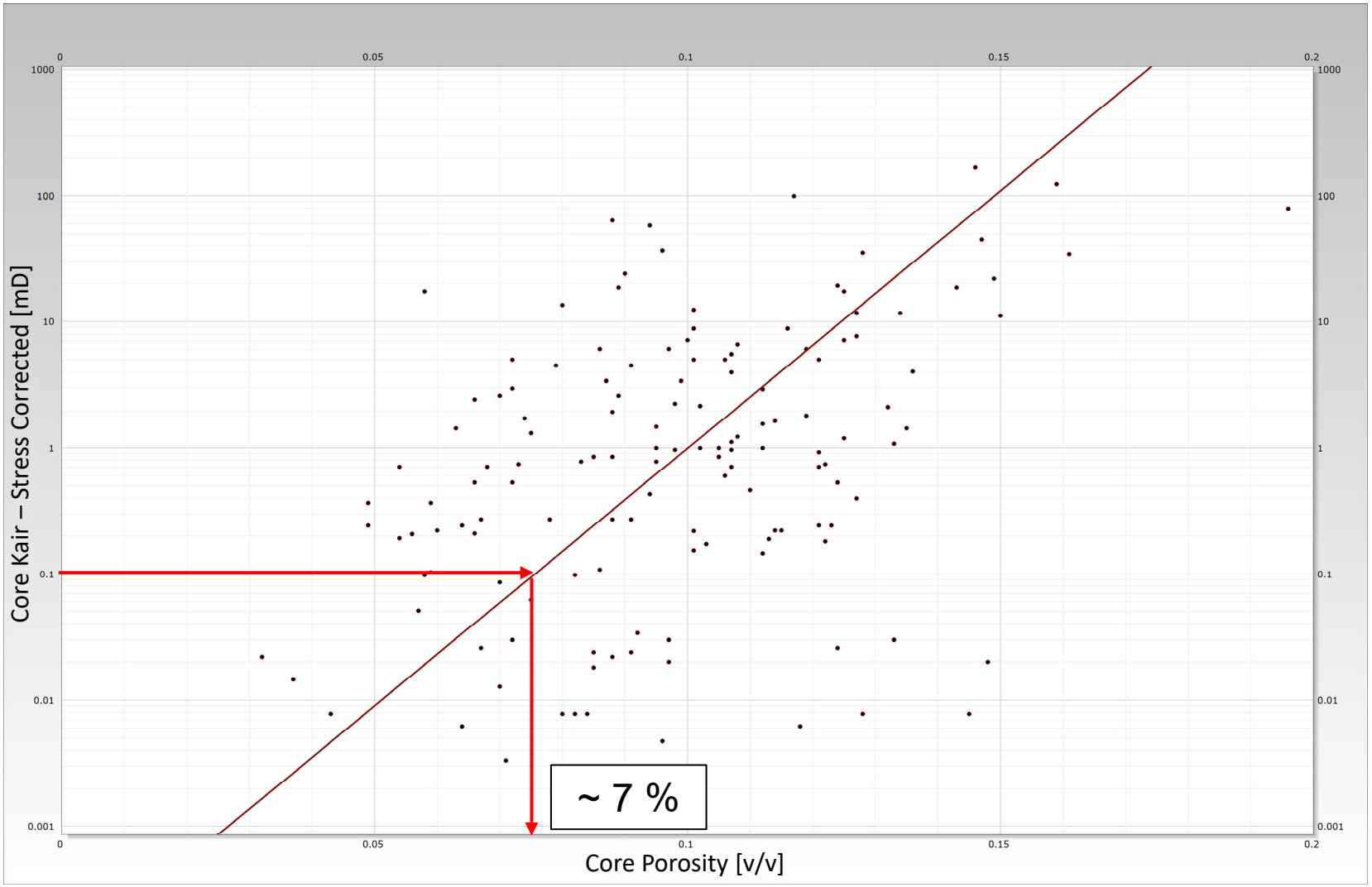

Figure 16

NETHERLAND, SEWELL & ASSOCIATES, INC.

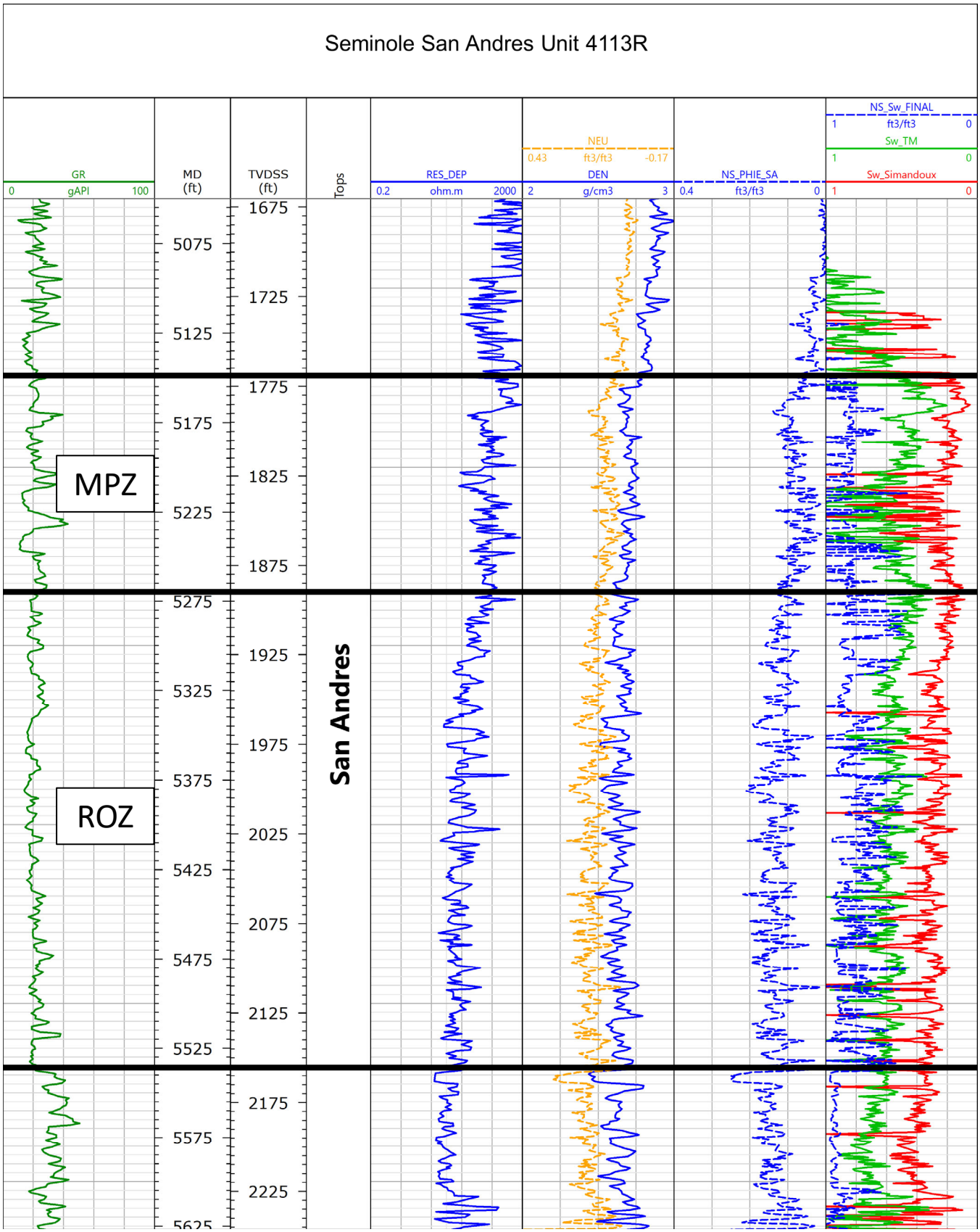

All estimates and exhibits herein are part of this NSAI report and are subject to its parameters and conditions.

Figure 17

NETHERLAND, SEWELL & ASSOCIATES, INC.

SSAU 4113R Well Location in Seminole Field San Andres Unit

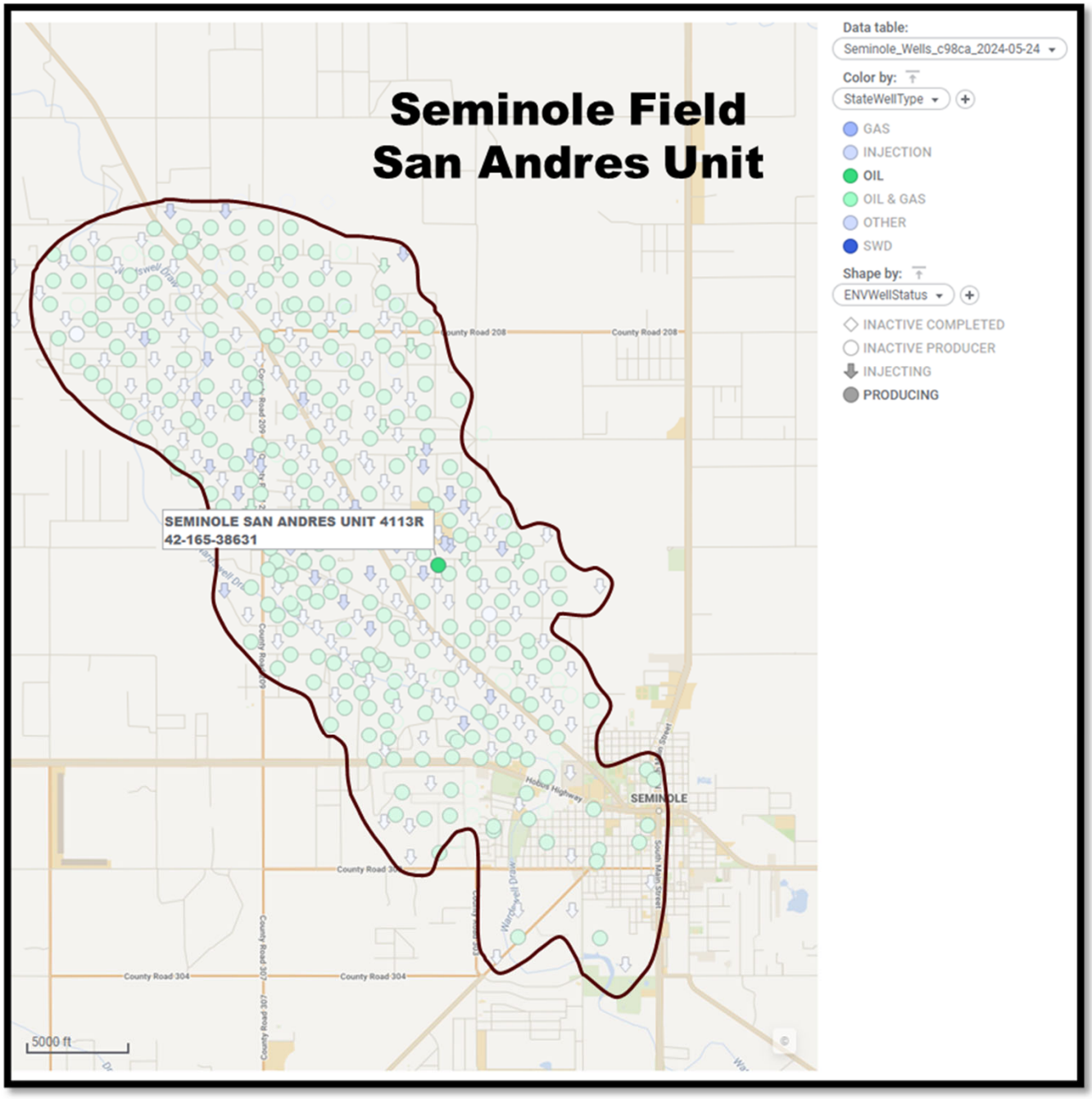

APPENDIX A: WATER SATURATION MODELS

Wettability

1. In most reservoir rocks, water coats the surfaces of the rock grains, and oil or gas occupy the center of the pores. This is known as a water wet condition. An oil wet condition exists when an oil film wets the surfaces of the rock grains, and the water resides in the middle of the pores. In a neutral wet condition both oil and water are in contact with the rock grain surfaces. A mixed wettability can exist in rocks containing two or more pore sizes. The smallest pores typically are water wet and are 100 percent water saturated. The larger pores can have an oil or neutral wettability. Rock wettability has a large impact on the way electrical current flows through the rock when formation resistivity measurements are being conducted during well logging operations. Wettability also affects the values of the electrical parameters needed for water saturation modeling.

Archie Model

2. The Archie water saturation model was developed for water wet quartz sandstone reservoirs where the rock grain and inter-granular pore sizes are reasonably uniform. Reservoir brine will conduct electrical current during resistivity log measurements in a wellbore. The resistivity of the rock when 100 percent saturated with brine, Ro, is established either through measurements of wet sands or by measurements in the laboratory with core samples. Oil is not conductive. The presence of oil in the pores increases the resistivity of the rock because it interferes with the flow of current by reducing the volume of water capable of conducting electricity and increases the tortuosity of the current path. The electrical current must flow through the thin water film existing between the hydrocarbons in the center of the pores and rock grain surfaces. Laboratory measurements are typically made to define the relationship between the measured resistivity and the water saturation within the core sample.

3. Gus Archie (1941) found that the resistivity of a brine saturated rock, Ro could be modeled relatively simply based on the porosity of the rock and the resistivity of the brine saturating the rock, Rw.

$$R_o = \frac{R_w}{\varphi^m}$$

4. The term m is known as the cementation exponent and accounts for the size and tortuosity of the pore network within the rock. It has been found that the value of m is about 2.0 in most water wet clastic rocks. The value of m is generally determined with laboratory measurements with core samples. If the porosity and brine resistivity of the rock are known, m can be determined from resistivity measurements in wet sandstone intervals.

5. Using a similar line of thinking, Archie was able to develop a relatively simple relationship between the measured resistivity of an oil-bearing rock, Rt and the resistivity of the rock at a 100 percent brine saturated condition, Ro.

$$S_w{}^n = \frac{R_o}{R_t} = \frac{R_w}{\varphi^m \times R_t}$$

6. The term n is known as the saturation exponent and accounts for the tortuosity of the current path through the thin water film between the hydrocarbons and the rock surfaces. The value of n is usually about 2.0 for most clastic rocks. Laboratory measurements have shown that n is usually relatively constant over the range of water saturations typically present in water wet clastic reservoirs.

7. A graphical representation of the Archie water saturation model is shown in Figure A1. The resistivity index, RI is simply the ration of the measured resistivity of the rock, Rt divided by the resistivity of the rock when 100 percent brine saturated, Ro.

8. The following conditions can cause the Archie m and n values to deviate from the standards values or to become variable with porosity and/or water saturation.

- The presence of fine and coarser grained sediments intermixed within the rock with distinct pore sizes.
- The presence of voids or vugs within the rock.
- The presence of an oil or mixed wettability condition within the rock.
- The presence of conductive minerals within the rocks (shale, clay minerals, pyrite, etc.).
- The presence of minerals precipitated from pore waters that coat the pore surfaces and occlude pore throats increasing the tortuosity of the pore network.
- The presence of fractures or dissolution channels within the rock.

9. The Archie model can be applied in carbonate reservoirs using standard m and n values when a uniform grain or crystal size is present, and the pore network is well connected. Complex pore systems are more typically present in carbonates and carbonates are more likely to have mixed or oil wet wettability conditions. In many cases it is necessary to use nonstandard m and n values to obtain representative water saturation estimates from the Archie model.

Simandoux Model

10. The Simandoux water saturation model is an empirical modification to the Archie model designed to account for the presence of conductive shale or clay mineral inclusions within the host rock (Simandoux, 1963). This model utilizes the Archie m and n values discussed above along with a shale volume parameter, Vsh and a shale resistivity parameter, Rsh to account for the effect of the conductive shale inclusions on the resistivity of the rock. A version of the Simandoux model was employed by Nutech in its evaluation of well log measurements from the EMSU.

$$S_w \cong \left\{\left(\frac{R_w}{\varphi^m}\right)\left(\frac{1}{R_t} - \frac{V_{sh}}{R_{sh}} S_{w\,guess}\right)\right\}^{1/n}$$

11. The shale volume and shale resistivity values are typically derived from gamma ray log measurements and from resistivity measurements in shale formations adjacent to the reservoir. Sw appears on both sides of the equation, therefore an iterative algorithm is used to find an Sw solution.

12. When shale or clay is not present, the Simandoux model reduces to the Archie Model.

Issues with Carbonates

13. Carbonate sediments are typically composed of grains and fragments consisting of a wide range of sizes. Wave energy helps to sort the grains into narrower size ranges near the shoreline, but sediments in the deeper water tend to be composed of grains with large size variations. Small grains often fill the voids between the larger grains, reducing the porosity of the sediments. Chemical reactions resulting from acidic pore waters create dissolution-reprecipitation reactions which typically increase the tortuosity of the pore network. Dissolution of shell fragments can create vugs within the rocks. All these diagenetic changes typically result in an increase in the m values. In many cases, increased porosity is associated primarily with increasing vug content.

14. Core measurements with samples of the important rock types have shown distinct trends in the value of m with increasing porosity. Figure A2 shows how Archie's m values increase with porosity for three different carbonate rock types.

15. Grainstones are deposited in the near shore environment and typically are composed of larger grains with a relatively narrow range in grain sizes. Grainstones are more likely to behave like clastic sandstones and have m values nearer to the traditional value of 2.0.

Packstones are deposited in a relatively deeper water environment farther from the shoreline. They are composed of larger grains with minor amounts of very fine grain sediments filling the voids between the larger grains. Overall, they have greater grain and pore size variations than grainstones and have higher m values as the result of the higher tortuosity of the pore networks. Wackestones are deposited in the deep water where wave energy is low. They are composed primarily of fine-grained sediments with some coarser grained sediments (usually shell fragments). The pores are small, not well connected, and the pore networks are highly tortuous.

16. Figure A3 shows how m increases for a given carbonate rock type as the relative vug content increases. The Archie n values increase with increased pore network tortuosity and vug content as well.

17. Reservoir wettability has a major impact on the behavior of n. The value of n is generally determined using a resistivity index versus water saturation crossplot derived from laboratory measurements. An example for a core sample originally prepared to exhibit a water wet condition and then a neutral wet condition and finally an oil wet condition is shown in Figure A4.

18. In the water wet condition, a relatively continuous water film exists along the pore surfaces allowing electrical current to flow at all water saturations levels, as shown in Figure A5. A linear slope is present on the RI versus Sw crossplot. In this situation the n value for the core sample is constant.

19. In the neutral wet condition, both oil and water can wet the pore surfaces. The current path is more tortuous as the result of the presence of oil coating a portion of the pore surfaces. The slope of the RI versus Sw plot is higher, reflecting the increased tortuosity, but a linear trend is still present.

20. In an oil wet rock, the water resides in the center of the pores with a film of oil setting between the water and the pore surfaces. At high water saturations, the water in the pores is well connected from one pore to another, as shown in Figure A6. As the oil saturation increases, oil begins to fill the pore throats, isolating water in the center of the larger pores. This is shown in Figure A7. Examples of thin sections for oil wet rocks from carbonates in Mexico are shown in Figures A8 and A9. Note the thin film of oil in direct contact with the pore surfaces. The isolated water can no longer conduct electrical current during the resistivity measurements. As the oil saturation increases, more and more of the water becomes isolated. This condition creates the concave upward shape on the resistivity index versus water saturation crossplot. Basically, Archie's n becomes variable with water saturation. Values of n much larger than the traditional value of 2.0 develop very rapidly.

21. The accurate evaluation of water saturation in carbonate reservoir requires a knowledge of the rock types present and the wettability of the reservoir.

22. Another issue associated with carbonates is the presence of adsorbed uranium on very fine-grained sediments that have been deposited in a low energy, deeper water environment. The source of the uranium is typically sea water. Uranium elevates the gamma ray log readings. High gamma ray readings are typically associated with the presence of clastic clay minerals. It is therefore possible to mistake elevated gamma ray readings as indications of the presence of conductive clay minerals. This is important when a model such as the Simandoux model is being used. The actual clay volume may be much lower than indicated by the raw gamma ray measurements.

Why is the Impact of Oil Wettability Not Widely Recognized in the Oil Industry?

23. The standard procedure in most commercial core analysis laboratories is to perform the measurements designed to determine m and n with water and air. The cores are cleaned and

dried and then fully saturated with a synthetic formation brine. Resistivity measurements are made and then the water saturation is decreased (typically with a centrifuge) and resistivity measurements are periodically repeated as a function of decreasing water content. The experiments are relatively cheap and can be conducted in a short period of time. The problem is that the results are valid only for water wet reservoir conditions.

24. On many cases, operators are simply unaware of the actual wettability condition present in the reservoir and do not request the proper laboratory measurements to determine the most likely wettability conditions and then perform the m and n measurements to deliver the most applicable results.

Schlumberger Model

25. The nonlinear, concave upward character of the RI versus Sw plot for the oil wet reservoir condition illustrated above creates a complication in the water saturation calculations. If Archie's n parameter is used, it is necessary to derive an equation to predict n as a function of RI and Sw. The problem is that the water saturation is what you are trying to calculate. A trial and error or iterative algorithm would be necessary to complete the water saturation calculations. A simple model developed by Schlumberger can be used to overcome this problem.

26. Montaron (2007) developed a simple curve-fit model utilizing basic core measurements to define a parameter he called the critical water saturation, Sc. Sc curve fits can be made for each core sample and then average Sc values can be calculated for each rock type. As an added benefit, he showed how the Sc values could be used to estimate the wettability of the reservoir rock.

27. Once rock-type specific Sc values are available, the following equation can be used to compute the water saturation from the well log measurements.

$$RI = \frac{R_t}{R_o}$$

$$S_w = \frac{1 - S_c\left(1 - RI^{(1/\mu)}\right)}{RI^{(1/\mu)}}$$

28. Schlumberger recommends that the μ parameter be set to 1.9 as an initial estimate. This parameter controls the curvature of the Sc curve. An RI versus Sw plot illustrating Sc curves for common carbonate rock types is shown in Figure A10.

29. Archie's m values are still employed in the Schlumberger model through the calculation of the resistivity index via Ro.

30. Inspection of Figure A10 indicates that several different water saturation estimates are possible for a given value of the resistivity index. It is therefore necessary to devise means to identify the various carbonate rock types from the well log measurements.

Identifying Carbonate Rock Types

31. The carbonate rock types present are identified using cores recovered from the reservoir. To determine the most likely rock types present in wells that do not have core measurements, it is necessary to estimate the rock types present from available well log measurements. The basic process involves identifying characteristic well log responses associated with each of the rock types identified from the cores. Methods to predict rock types from well log measurements for the Grayburg and San Andres Formations have been developed by Jerry Lucia from the University of Texas Bureau of Economic Geology and by George Asquith from the Department of Geology of Texas Tech University. Rock type determination involves the integrated analysis of the following well log measurements.

- Shallow and deep resistivity measurements
- Gamma ray measurements

- Bulk density measurements
- Neutron porosity measurements
- Sonic travel time measurements

32. For example, porosity and lithology (sandstone, dolomite, limestone, anhydrite, etc.) can be estimated using standard cross-plotting procedures involving the bulk density and neutron porosity measurements. At a high level, shallow versus deep water rock types can be differentiated using the relative magnitudes of the gamma ray measurements through the well. It is possible to identify rock types with bimodal pore size distributions by comparing porosity estimates derived from the resistivity measurements to those derived from the bulk density and neutron porosity measurements. Vug porosity can be derived from the sonic travel time measurements.

Basic Water Saturation Workflow

33. The following steps are required to derive reasonably accurate water saturation estimates from well log measurements.

- Define rock types from available core samples.
- Correct core-derived porosity, permeability, and fluid saturation measurements to reservoir conditions.
- Define the Archie cementation exponent, m for each sample either through laboratory measurements or based on core-derived correlations of m with porosity and/or permeability for the identified rock type.
- Calculate Ro for each sample.

- Determine the most-likely reservoir wettability conditions based on laboratory testing or by resistivity analysis (RI vs. Sw) of the available core saturation measurements.
- Determine water saturation exponent, n or the critical water saturation, Sc for each core plug either by laboratory testing or through resistivity analysis (RI vs. Sw).
- Define average n and/or Sc values for each rock type.
- Using the available well log measurements, develop a rock type identification algorithm which brings the well-log-derived water saturation estimates into the best agreement with the core measurements.
- Evaluate the water saturations for each well and review the calculation results for reasonableness. Identify erroneous rock type identification issues and adjust the model to eliminate interpretation artifacts.
- Once a consistent rock type identification procedure and saturation calculation procedure has been developed, prepare water saturation estimates for each well.

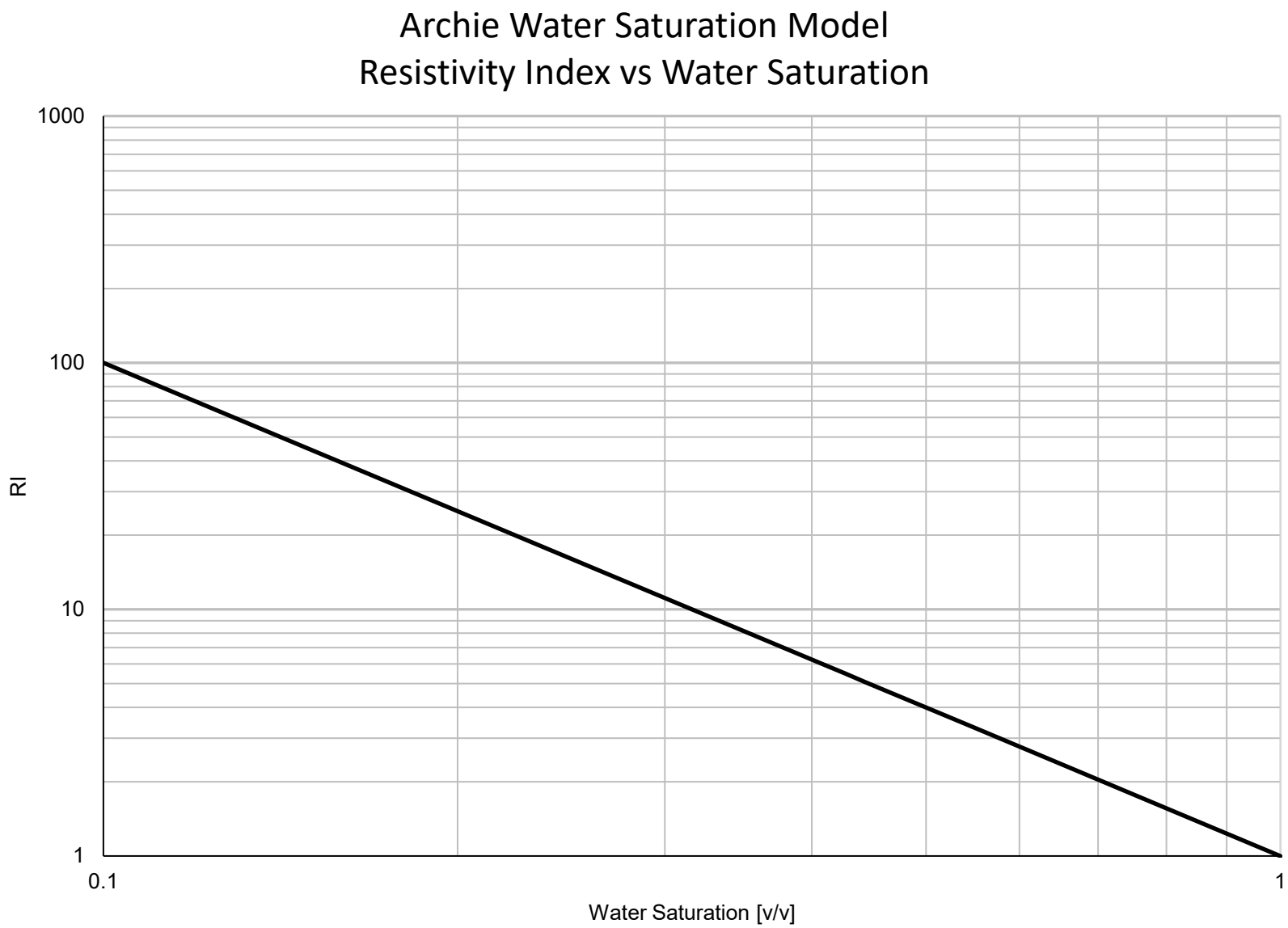

Figure A1

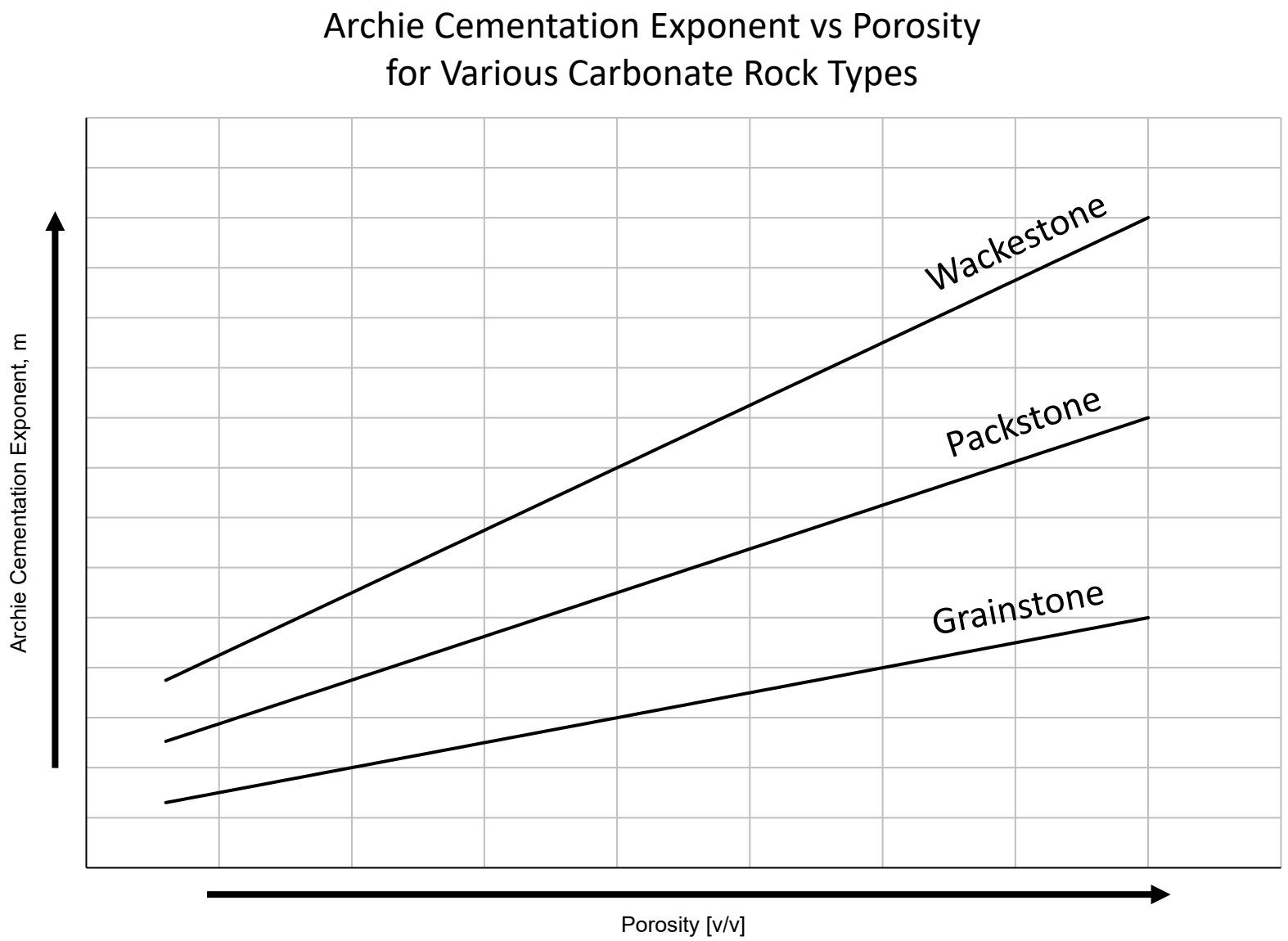

Figure A2

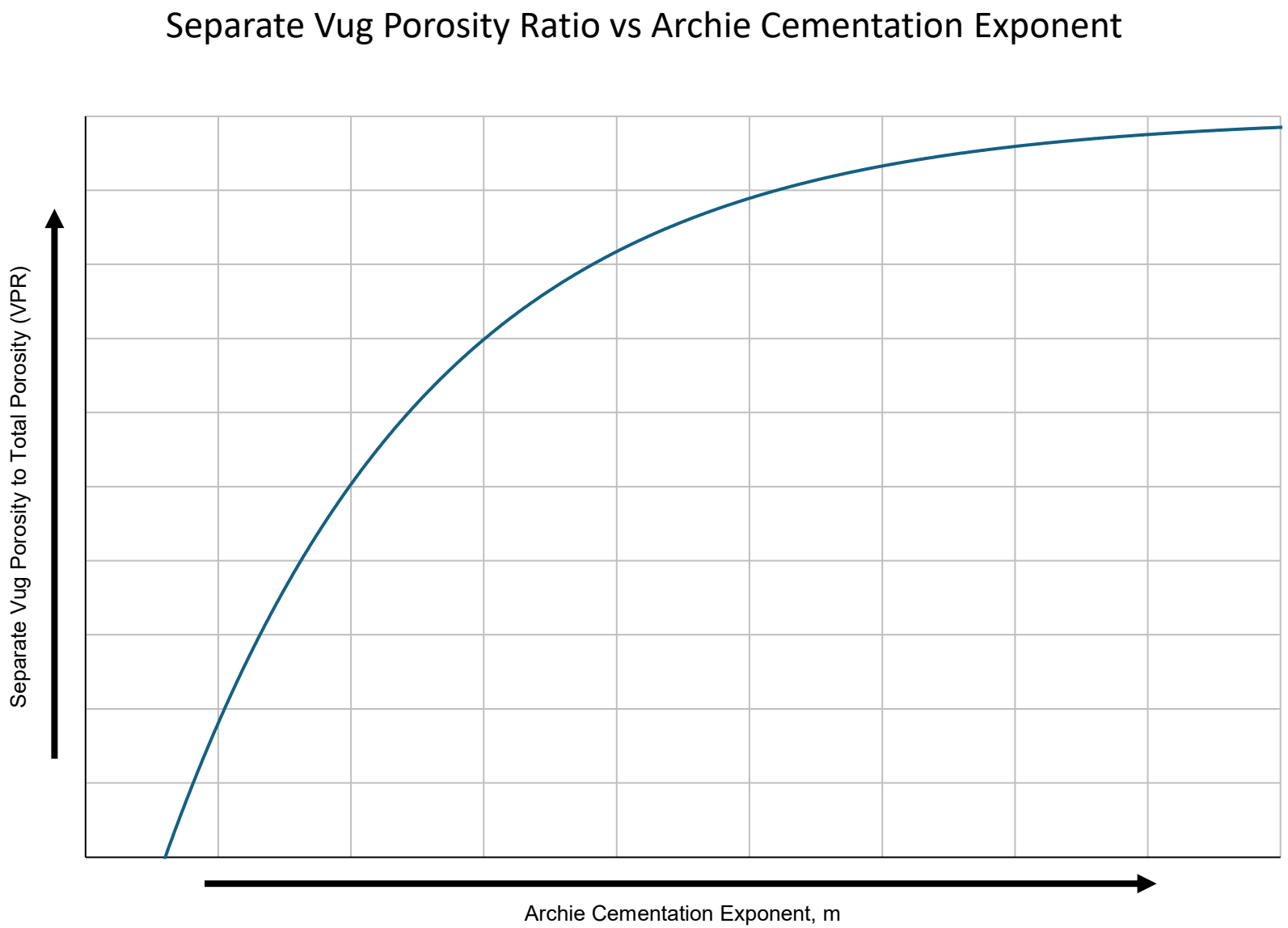

Figure A3

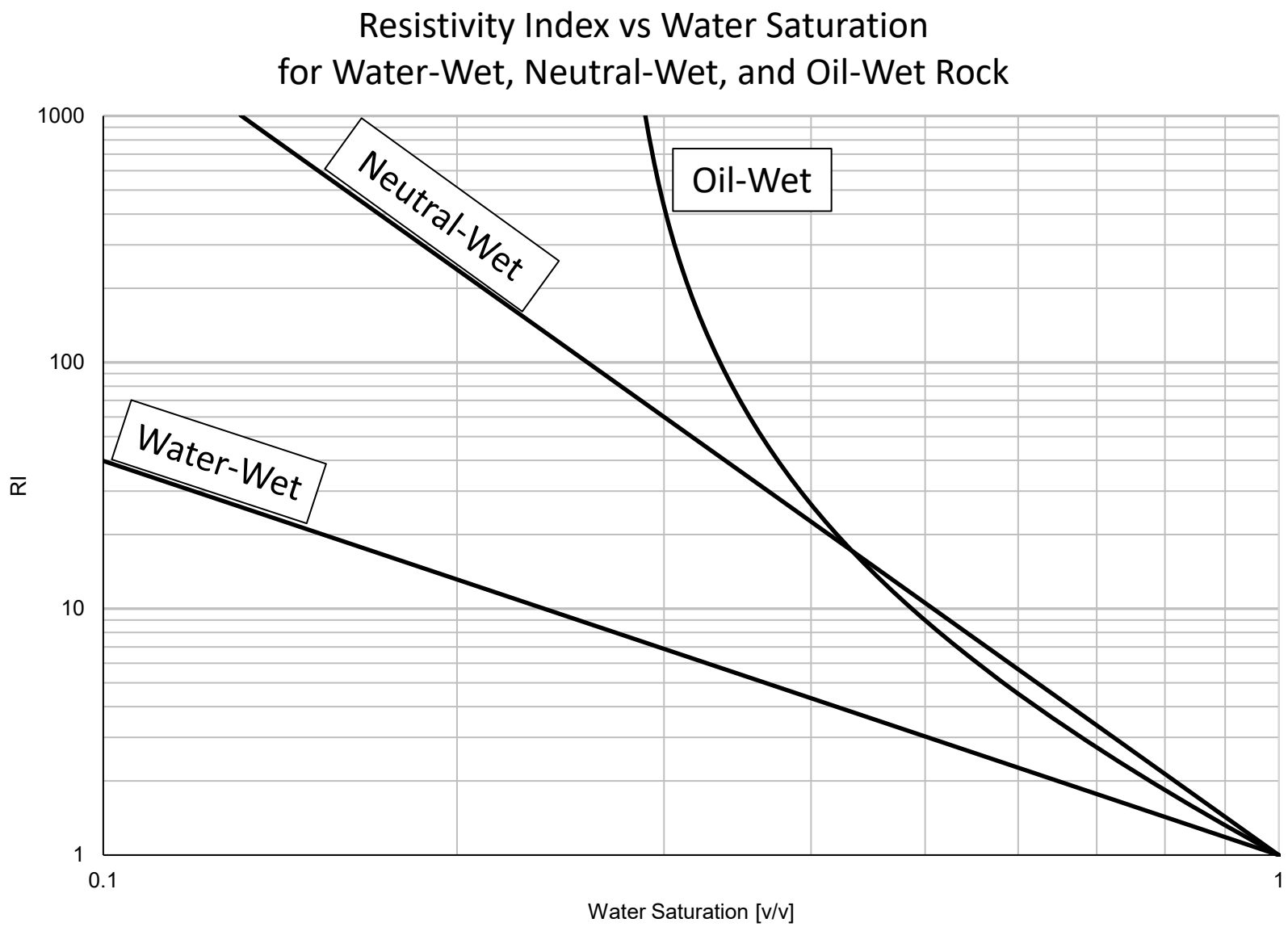

Figure A4

Water Wet Pore System
With Continuous Conductivity Path

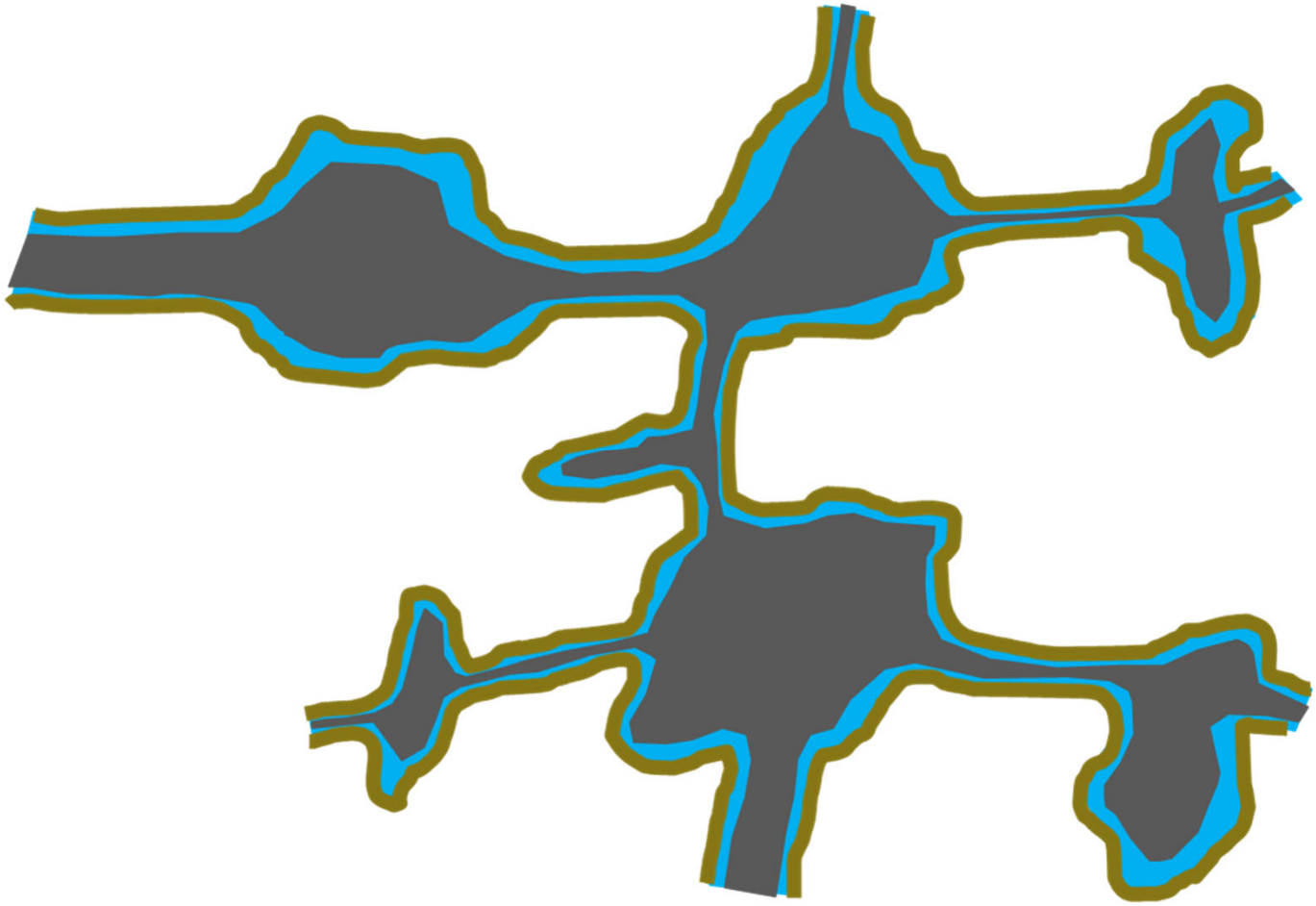

Figure A5

Oil Wet Pore System
With Continuous Conductivity Path

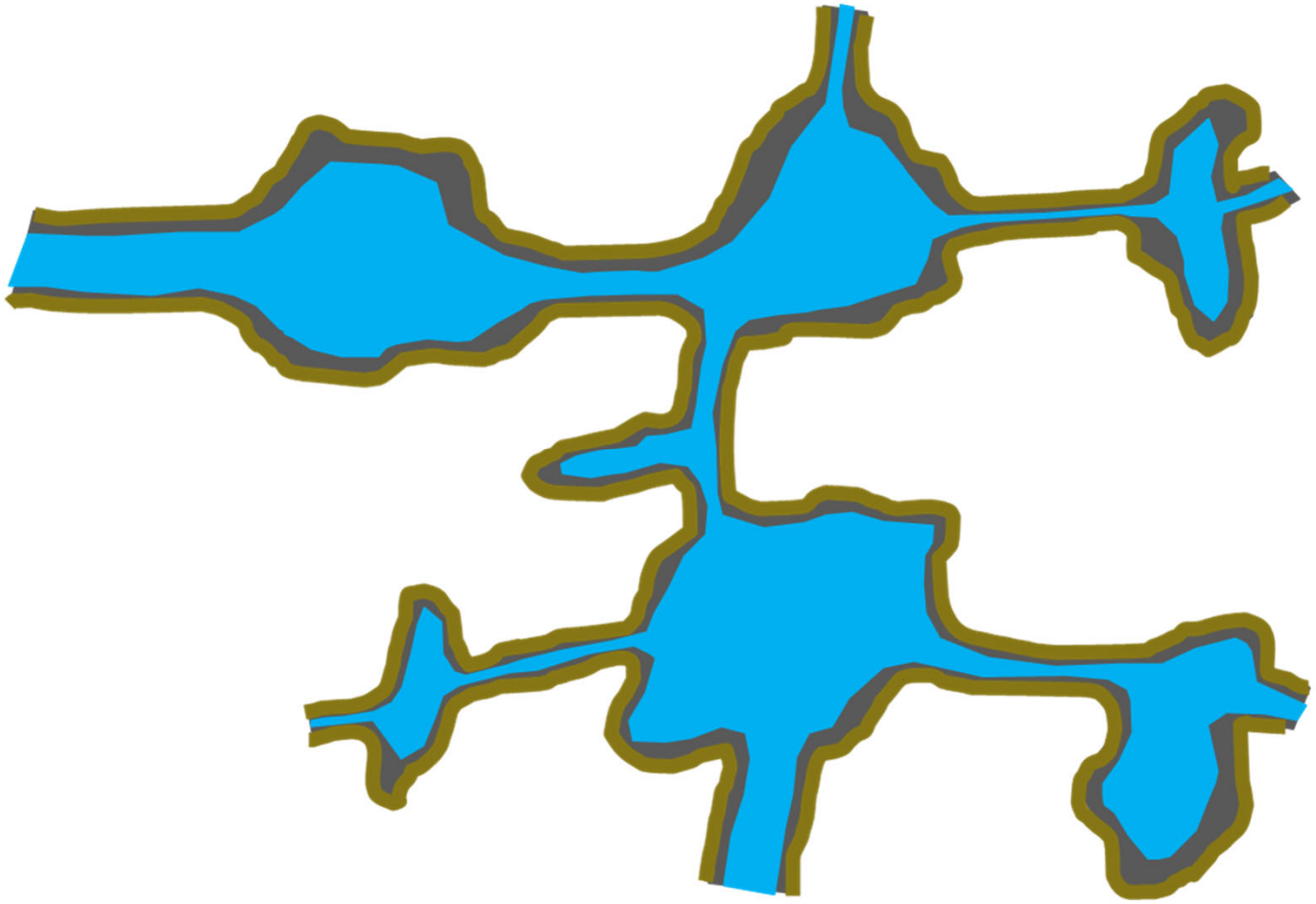

Figure A6

Oil Wet Pore System
Without Continuous Conductivity Path

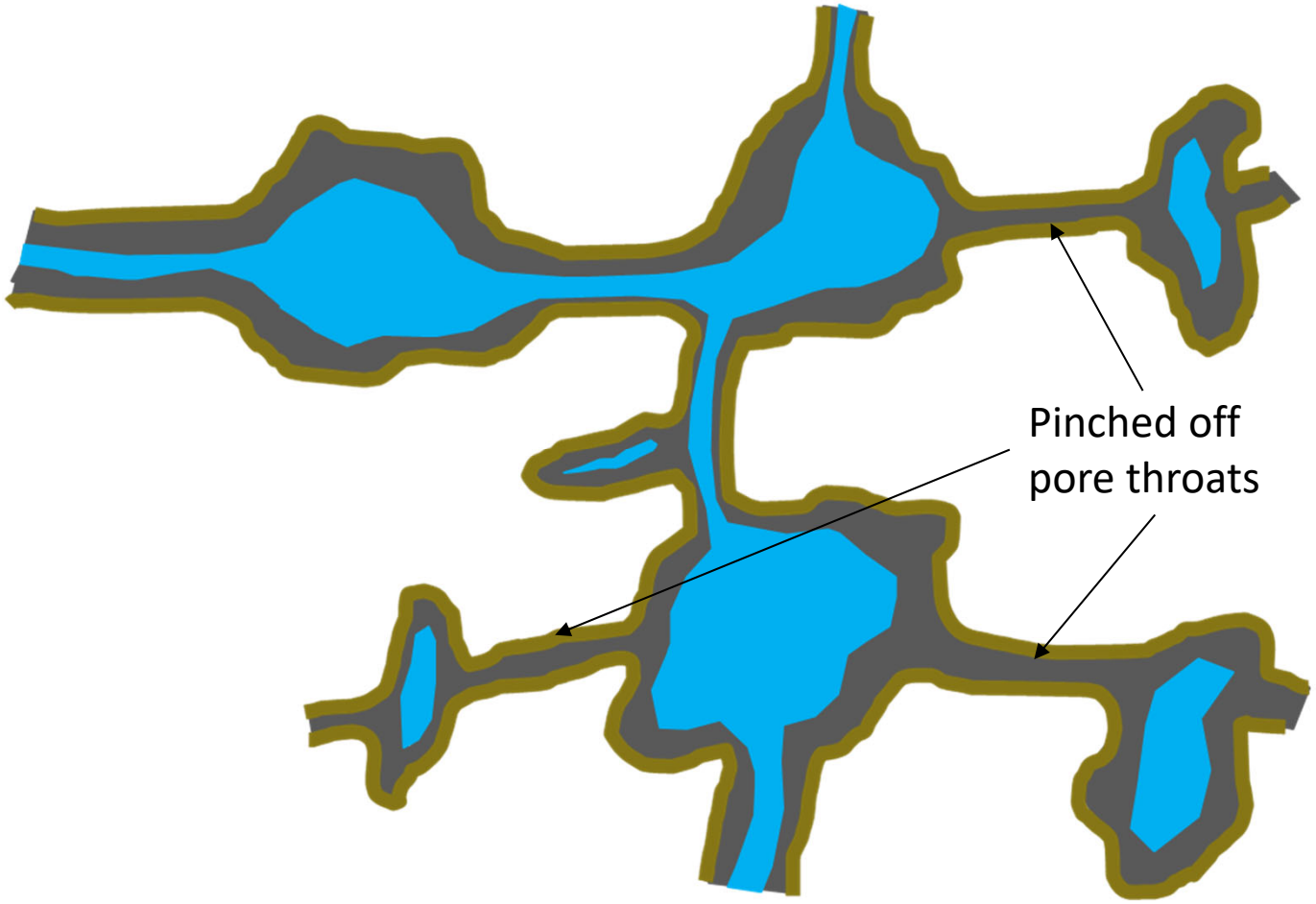

Figure A7

Example Thin Section 1
Oil Wet Carbonate Rock

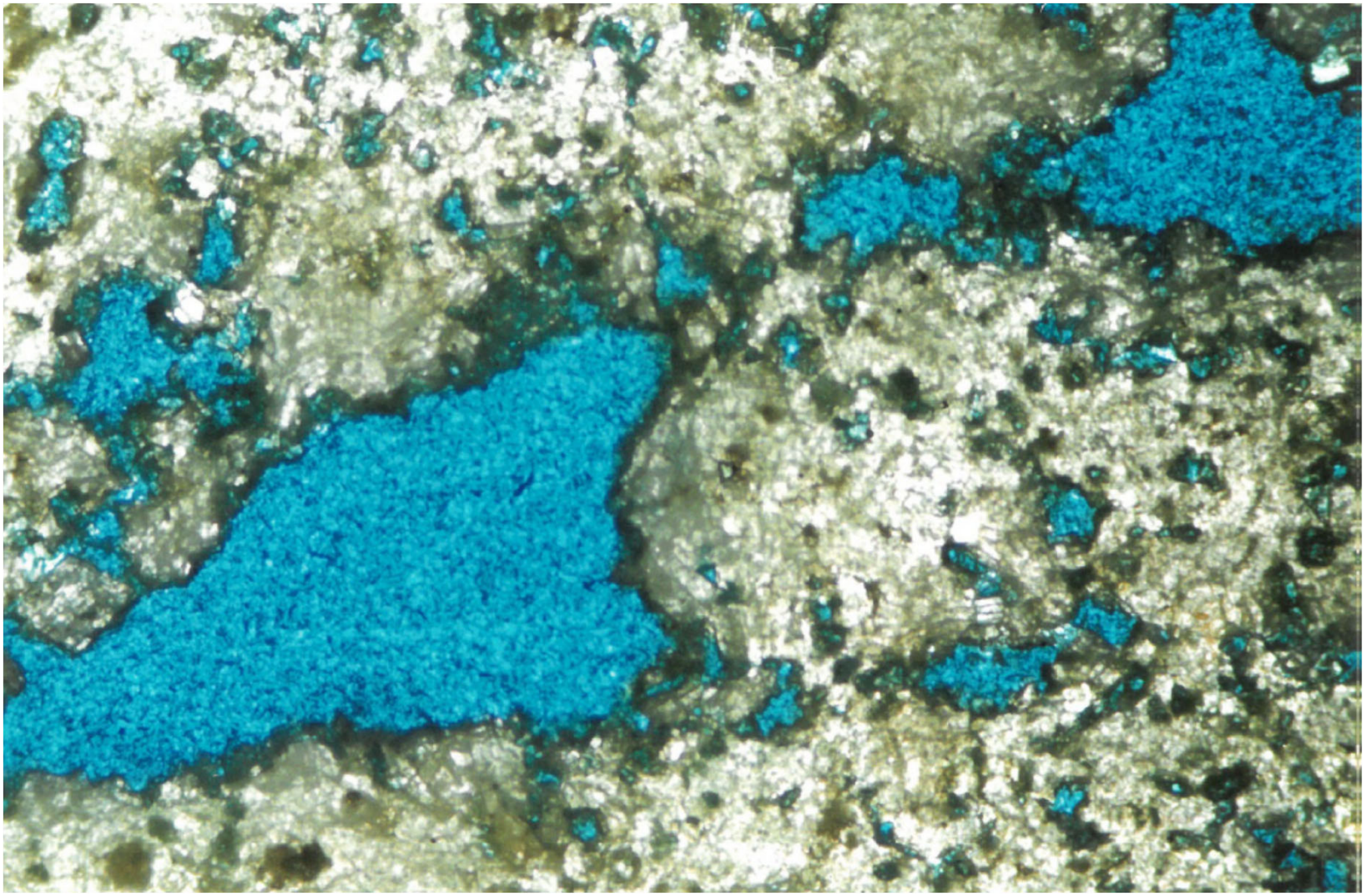

Figure A8

Example Thin Section 2
Oil Wet Carbonate Rock

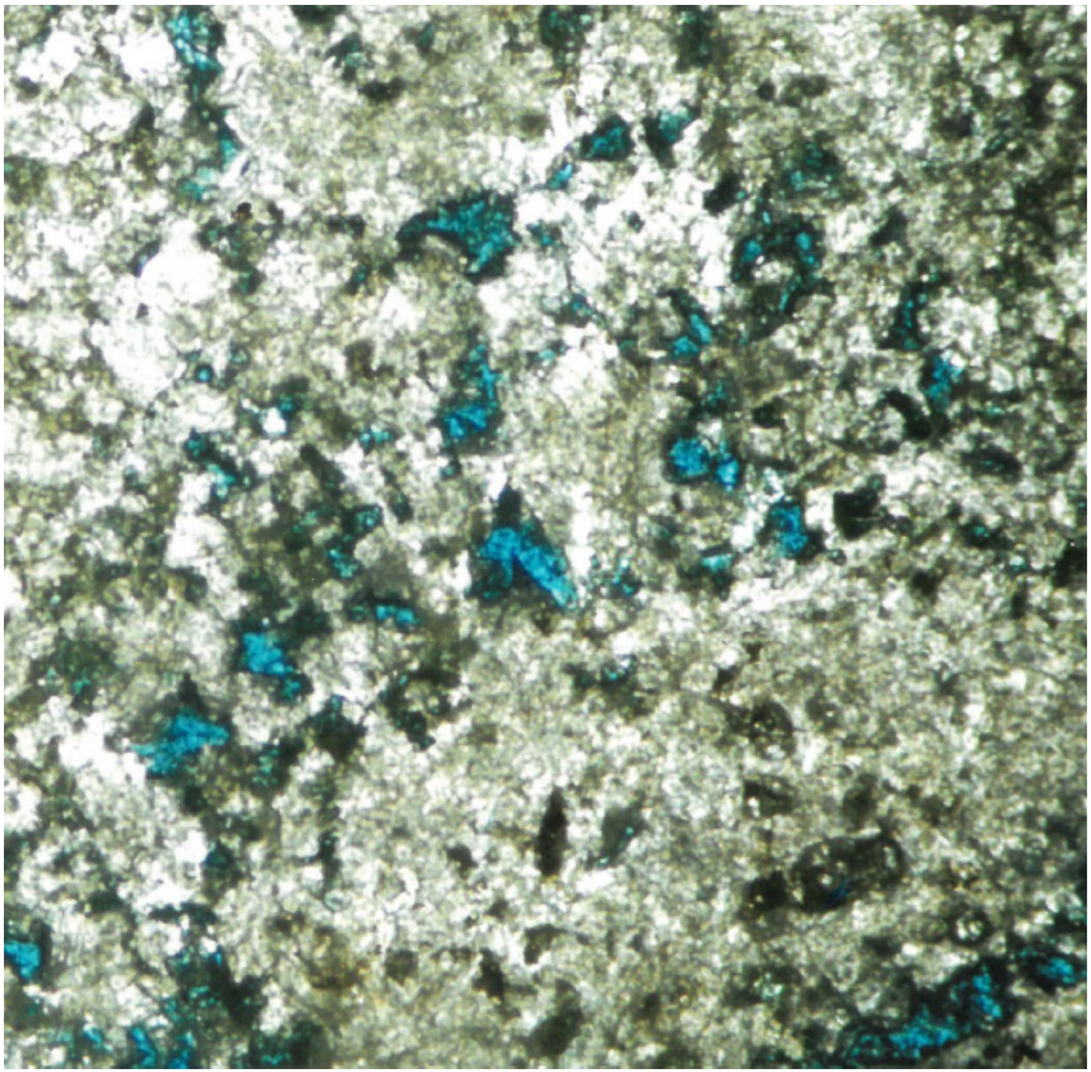

Figure A9

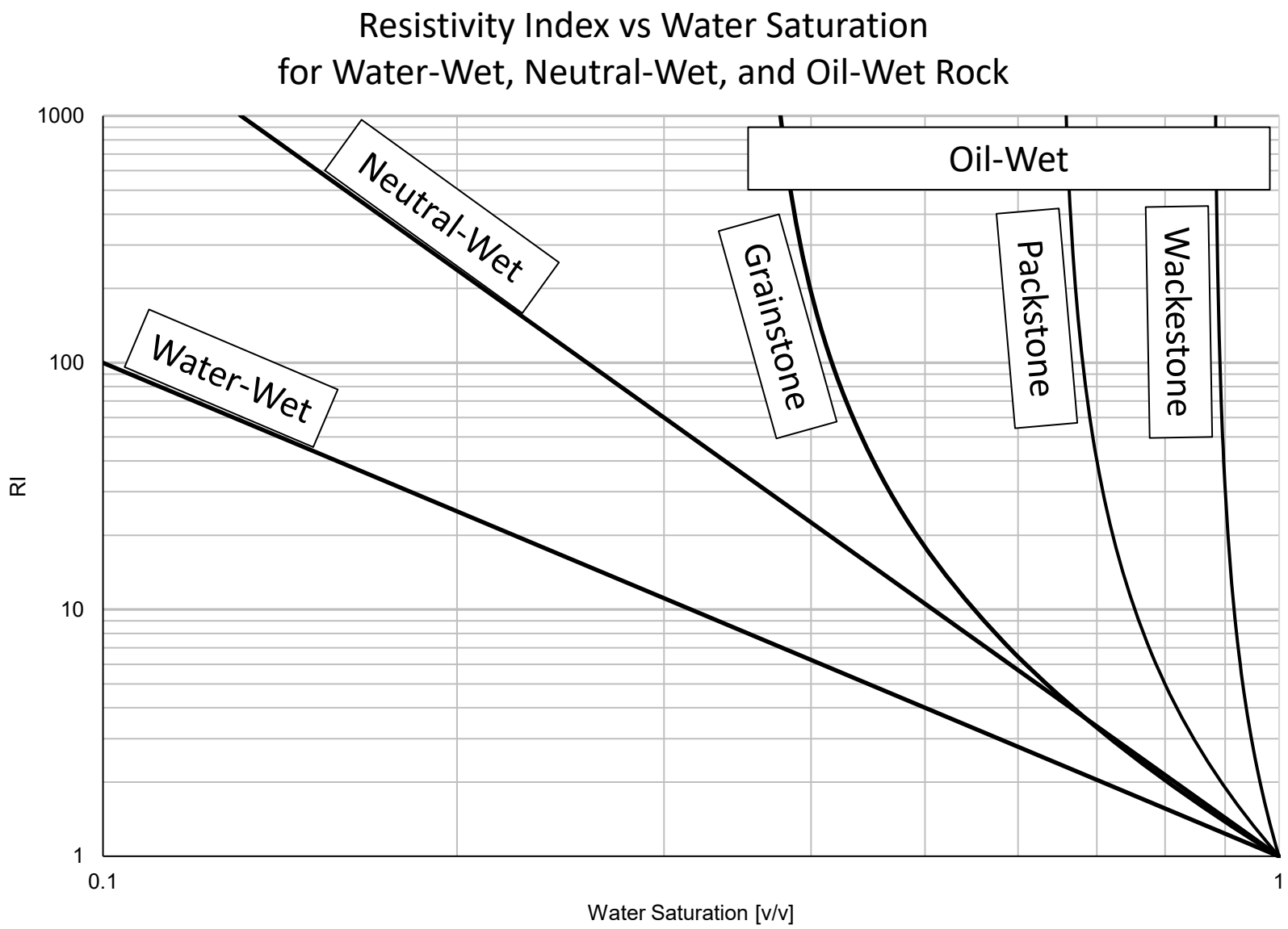

Figure A10

NSAI NETHERLAND, SEWELL & ASSOCIATES, INC.

APPENDIX B: WELL LOGS

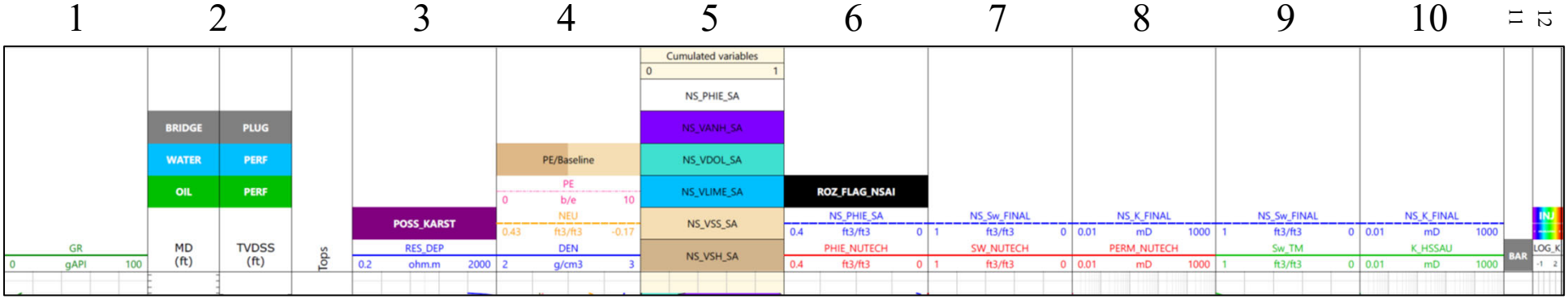

Track 1: Raw Gamma Ray – Gamma ray curve
Track 2: Depth & Miscellaneous – Depth track presented in measured depth and true vertical depth subsea. Track contains flags for perforations (green produced oil, blue produced water only), bridge plugs (grey), and fluid circulation loss (dark blue across track) in some wells.
Track 3: Raw Resistivity & Possible Karst Flag – Deep resistivity curve and flag that highlights possible karsted intervals.
Track 4: Raw Porosity & PE – Density, neutron, and PE curves
Track 5: Lithology – PHIE along with volumetric carbonates (VANH, VDOL, VLIME), clastic (VSS), and shale (VSH)
Track 6: Porosity & ROZ Flag – Comparison between Nutech and NSAI solutions, along with ROZ flag based on NSAI solutions. Nutech solutions shown in this track when available. Core data also shown in this track when available.
Track 7: Water Saturation – Comparison between Nutech and NSAI solutions. Nutech solutions shown in this track when available. Core data also shown in this track when available.
Track 8: Permeability – Comparison between Nutech and NSAI solutions. Nutech solutions shown in this track when available. Core data also shown in this track when available.
Track 9: Water Saturation – Comparison between Trentham & Melzer model and NSAI solution.
Track 10: Permeability – Comparison between SSAU correlation and NSAI solution.
Track 11: Potential Barrier – Flag to identify vertical barrier zones.
Track 12: Potential CO_2 Entry – Flag that shows intervals where CO_2 may enter. Blue is least likely, red is most.

Note: For Snyder SWD #1 (now called Ryno), track 7 and 8 contain only NSAI solutions using two different models for vuggy porosity based on sonic data. There is no track 9 or 10 for this well.

EMSU 628

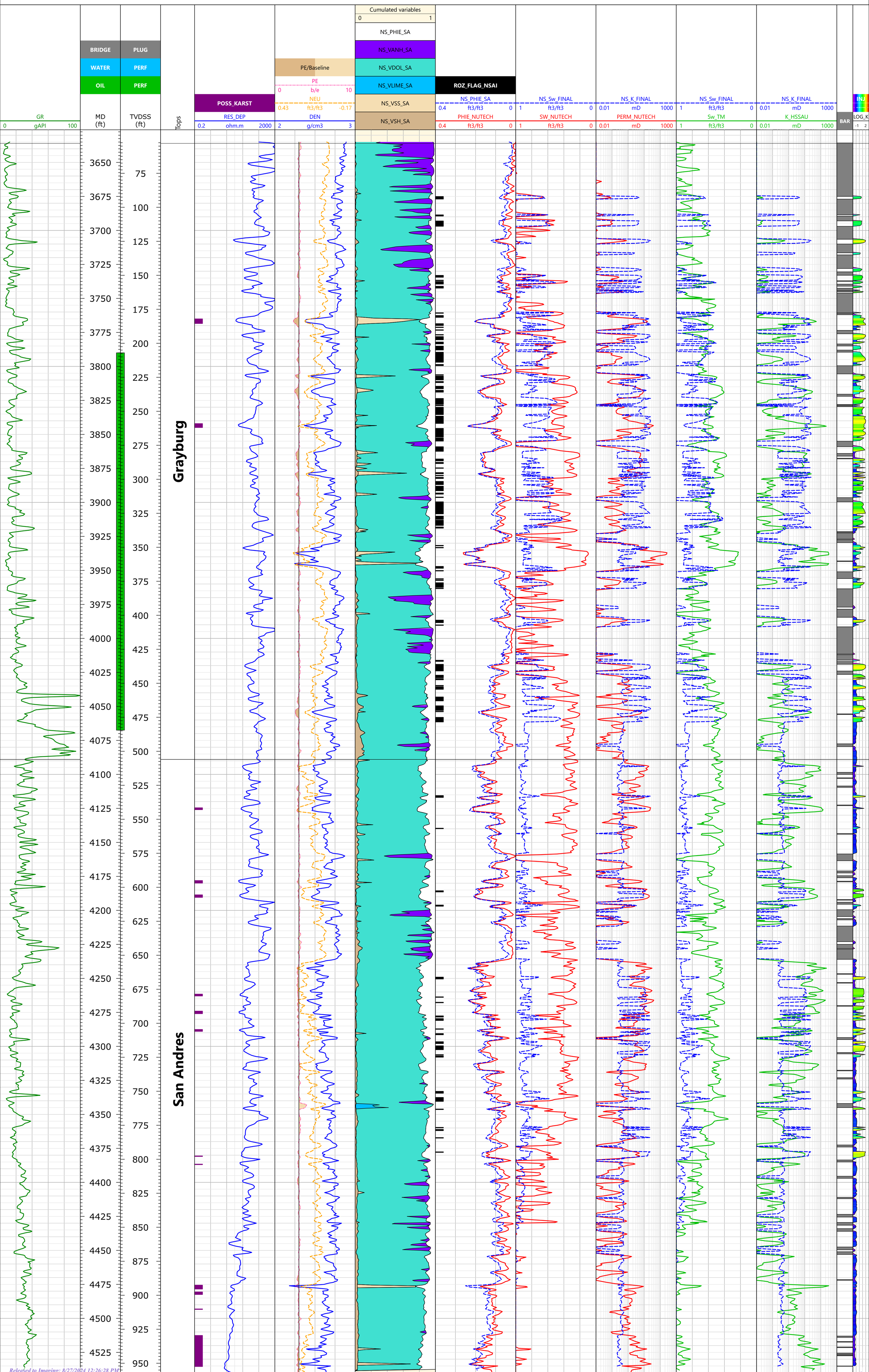
BRIDGE
WATER
OIL
PLUG
PERF
PERF
GR
0 gAPI 100
MD (ft)
TVDSS (ft)
Tops
Grayburg
San Andres
POSS_KARST
RES_DEP
0.2 ohm.m 2000
PE/Baseline
PE
0 b/e 10
NEU
0.43 ft3/ft3 -0.17
DEN
2 g/cm3 3
Cumulated variables
0 1
NS_PHIE_SA
NS_VANH_SA
NS_VDOL_SA
NS_VLIME_SA
NS_VSS_SA
NS_VSH_SA
ROZ_FLAG_NSAI
NS_PHIE_SA
0.4 ft3/ft3 0
PHIE_NUTECH
0.4 ft3/ft3 0
NS_Sw_FINAL
1 ft3/ft3 0
SW_NUTECH
1 ft3/ft3 0
NS_K_FINAL
0.01 mD 1000
PERM_NUTECH
0.01 mD 1000
NS_Sw_FINAL
1 ft3/ft3 0
Sw_TM
1 ft3/ft3 0
NS_K_FINAL
0.01 mD 1000
K_HSSAU
0.01 mD 1000
BAR
INJ
LOG_K
-1 2
3650
3675
3700
3725
3750
3775
3800
3825
3850
3875
3900
3925
3950
3975
4000
4025
4050
4075
4100
4125
4150
4175
4200
4225
4250
4275
4300
4325
4350
4375
4400
4425
4450
4475
4500
4525
75
100
125
150
175
200
225
250
275
300
325
350
375
400
425
450
475
500
525
550
575
600
625
650
675
700
725
750
775
800
825
850
875
900
925
950

EMSU 658

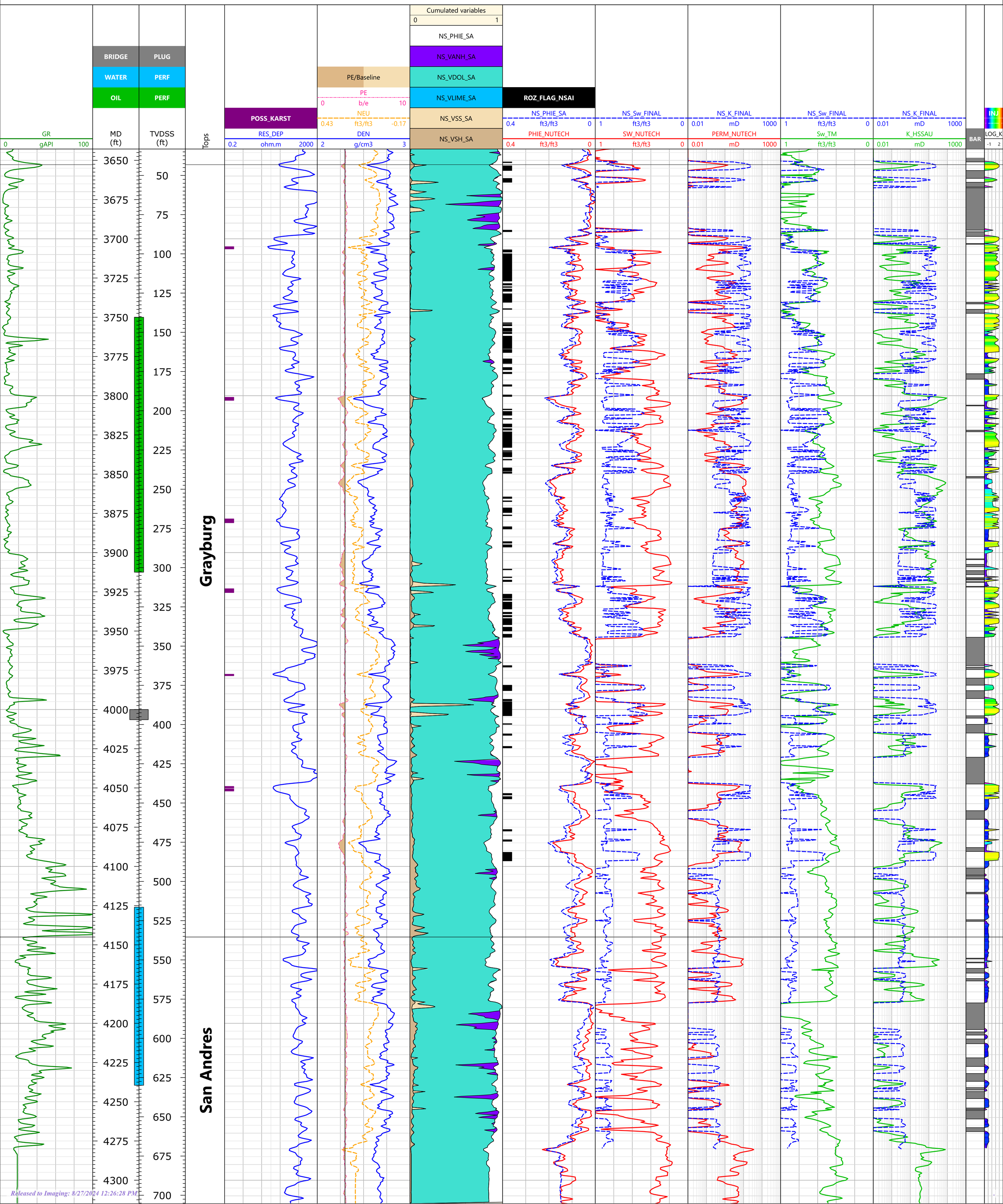
Cumulated variables
0
1
NS_PHIE_SA
NS_VANH_SA
NS_VDOL_SA
NS_VLIME_SA
NS_VSS_SA
NS_VSH_SA
BRIDGE
WATER
OIL
PLUG
PERF
PERF
PE/Baseline
PE
0
b/e
10
NEU
0.43
ft3/ft3
-0.17
POSS_KARST
ROZ_FLAG_NSAI
GR
0
gAPI
100
MD
(ft)
TVDSS
(ft)
Tops
RES_DEP
0.2
ohm.m
2000
DEN
2
g/cm3
3
NS_PHIE_SA
0.4
ft3/ft3
0
PHIE_NUTECH
0.4
ft3/ft3
0
NS_Sw_FINAL
1
ft3/ft3
0
SW_NUTECH
1
ft3/ft3
0
NS_K_FINAL
0.01
mD
1000
PERM_NUTECH
0.01
mD
1000
NS_Sw_FINAL
1
ft3/ft3
0
Sw_TM
1
ft3/ft3
0
NS_K_FINAL
0.01
mD
1000
K_HSSAU
0.01
mD
1000
BAR
INJ
LOG_K
-1
2
3650
3675
3700
3725
3750
3775
3800
3825
3850
3875
3900
3925
3950
3975
4000
4025
4050
4075
4100
4125
4150
4175
4200
4225
4250
4275
4300
50
75
100
125
150
175
200
225
250
275
300
325
350
375
400
425
450
475
500
525
550
575
600
625
650
675
700
Grayburg
San Andres

EMSU 660

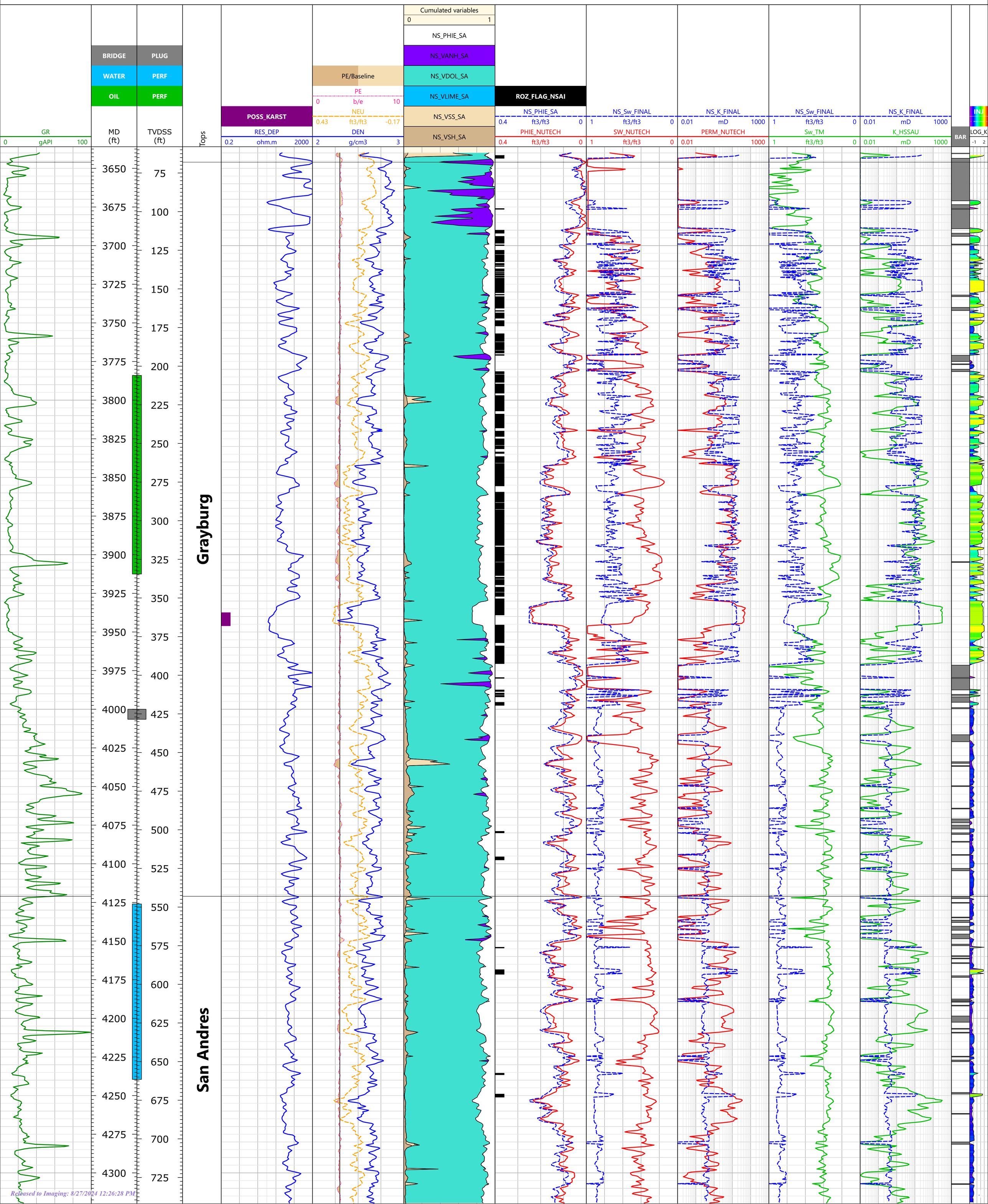

EMSU 673

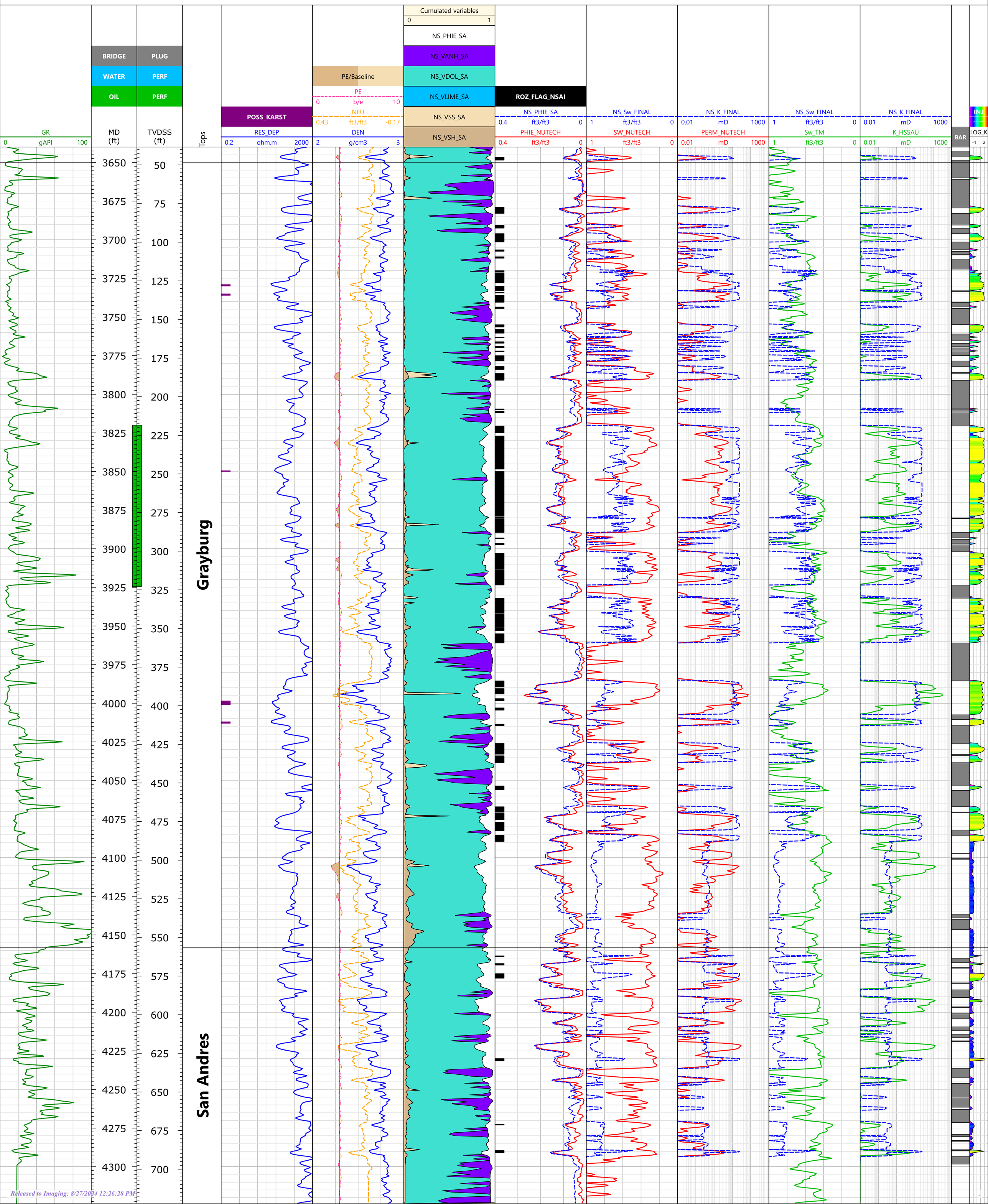
BRIDGE
PLUG
WATER
PERF
OIL
PERF
GR
0
gAPI
100
MD
(ft)
TVDSS
(ft)
Tops
Grayburg
San Andres
POSS_KARST
RES_DEP
0.2
ohm.m
2000
PE/Baseline
PE
0
b/e
10
NEU
0.43
ft3/ft3
-0.17
DEN
2
g/cm3
3
Cumulated variables
0
1
NS_PHIE_SA
NS_VANH_SA
NS_VDOL_SA
NS_VLIME_SA
NS_VSS_SA
NS_VSH_SA
ROZ_FLAG_NSAI
NS_PHIE_SA
0.4
ft3/ft3
0
PHIE_NUTECH
0.4
ft3/ft3
0
NS_Sw_FINAL
1
ft3/ft3
0
SW_NUTECH
1
ft3/ft3
0
NS_K_FINAL
0.01
mD
1000
PERM_NUTECH
0.01
mD
1000
NS_Sw_FINAL
1
ft3/ft3
0
Sw_TM
1
ft3/ft3
0
NS_K_FINAL
0.01
mD
1000
K_HSSAU
0.01
mD
1000
BAR
INJ
LOG_K
-1
2
3650
3675
3700
3725
3750
3775
3800
3825
3850
3875
3900
3925
3950
3975
4000
4025
4050
4075
4100
4125
4150
4175
4200
4225
4250
4275
4300
50
75
100
125
150
175
200
225
250
275
300
325
350
375
400
425
450
475
500
525
550
575
600
625
650
675
700

EMSU 679

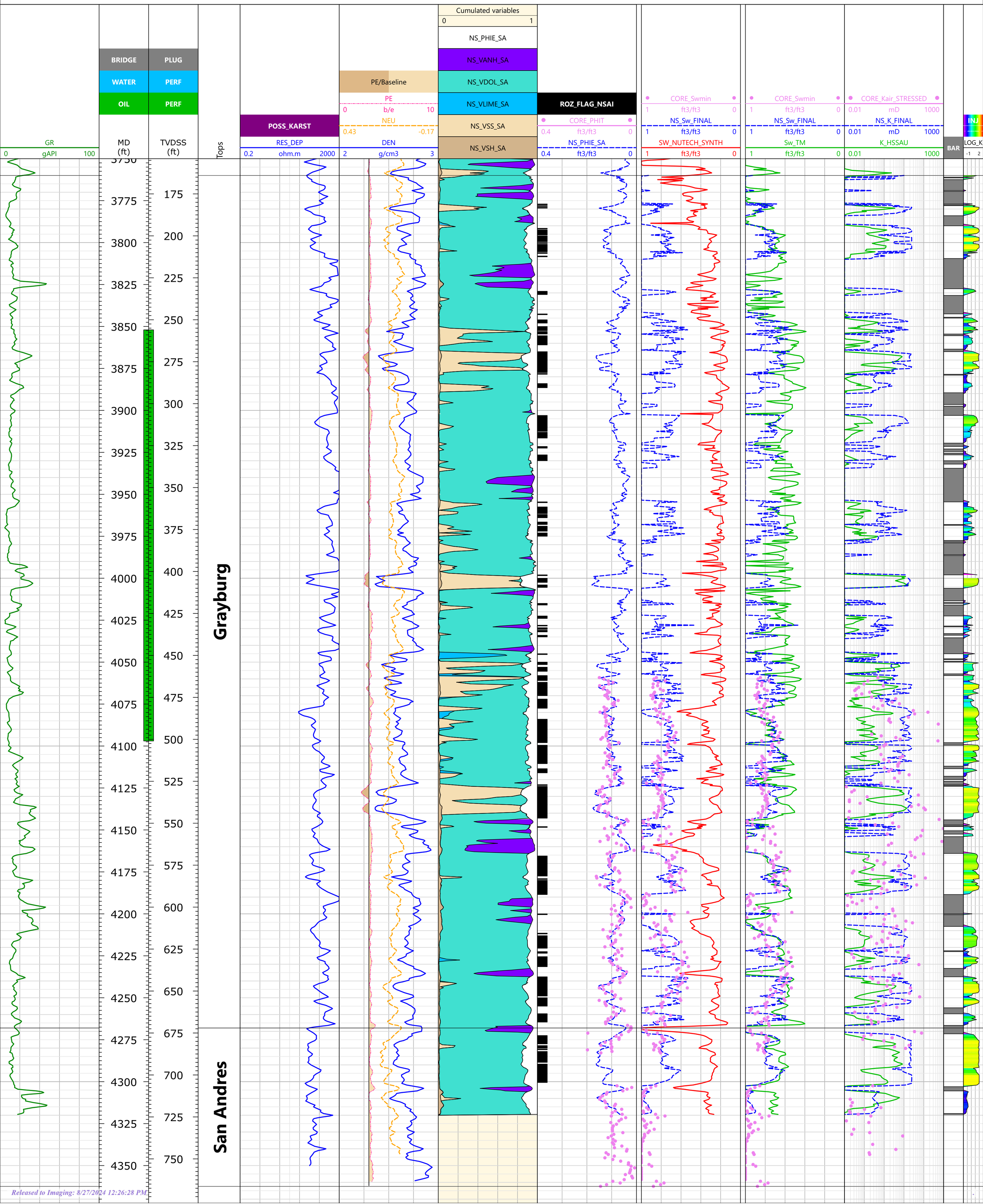
BRIDGE
PLUG
WATER
PERF
OIL
PERF
GR
0 gAPI 100
MD (ft)
TVDSS (ft)
Tops
POSS_KARST
RES_DEP
0.2 ohm.m 2000
PE/Baseline
PE
0 b/e 10
NEU
0.43 -0.17
DEN
2 g/cm3 3
Cumulated variables
0 1
NS_PHIE_SA
NS_VANH_SA
NS_VDOL_SA
NS_VLIME_SA
NS_VSS_SA
NS_VSH_SA
ROZ_FLAG_NSAI
CORE_PHIT
0.4 ft3/ft3 0
NS_PHIE_SA
0.4 ft3/ft3 0
CORE_Swmin
1 ft3/ft3 0
NS_Sw_FINAL
1 ft3/ft3 0
SW_NUTECH_SYNTH
1 ft3/ft3 0
CORE_Swmin
1 ft3/ft3 0
NS_Sw_FINAL
1 ft3/ft3 0
Sw_TM
1 ft3/ft3 0
CORE_Kair_STRESSED
0.01 mD 1000
NS_K_FINAL
0.01 mD 1000
K_HSSAU
0.01 1000
BAR
INJ
LOG_K
-1 2
3750
3775
3800
3825
3850
3875
3900
3925
3950
3975
4000
4025
4050
4075
4100
4125
4150
4175
4200
4225
4250
4275
4300
4325
4350
175
200
225
250
275
300
325
350
375
400
425
450
475
500
525
550
575
600
625
650
675
700
725
750
Grayburg
San Andres

EMSU 713

BRIDGE
WATER
OIL
PLUG
PERF
PERF

Cumulated variables
0 1
NS_PHIE_SA
NS_VANH_SA
NS_VDOL_SA
NS_VLIME_SA
NS_VSS_SA
NS_VSH_SA

PE/Baseline
PE
0 b/e 10
NEU
0.43 ft3/ft3 -0.17
DEN
2 g/cm3 3

POSS_KARST
RES_DEP
0.2 ohm.m 2000

ROZ_FLAG_NSAI
NS_PHIE_SA
0.4 ft3/ft3 0
PHIE_NUTECH
0.4 ft3/ft3 0

NS_Sw_FINAL
1 ft3/ft3 0
SW_NUTECH
1 ft3/ft3 0

NS_K_FINAL
0.01 mD 1000
PERM_NUTECH
0.01 mD 1000

NS_Sw_FINAL
1 ft3/ft3 0
Sw_TM
1 ft3/ft3 0

NS_K_FINAL
0.01 mD 1000
K_HSSAU
0.01 mD 1000

BAR

INJ
LOG_K
-1 2

GR
0 gAPI 100

MD (ft)
TVDSS (ft)

Tops
Grayburg

3775 175
3800 200
3825 225
3850 250
3875 275
3900 300
3925 325
3950 350
3975 375
4000 400
4025 425
4050 450
4075 475
4100 500
4125 525
4150 550
4175 575

EMSU 746

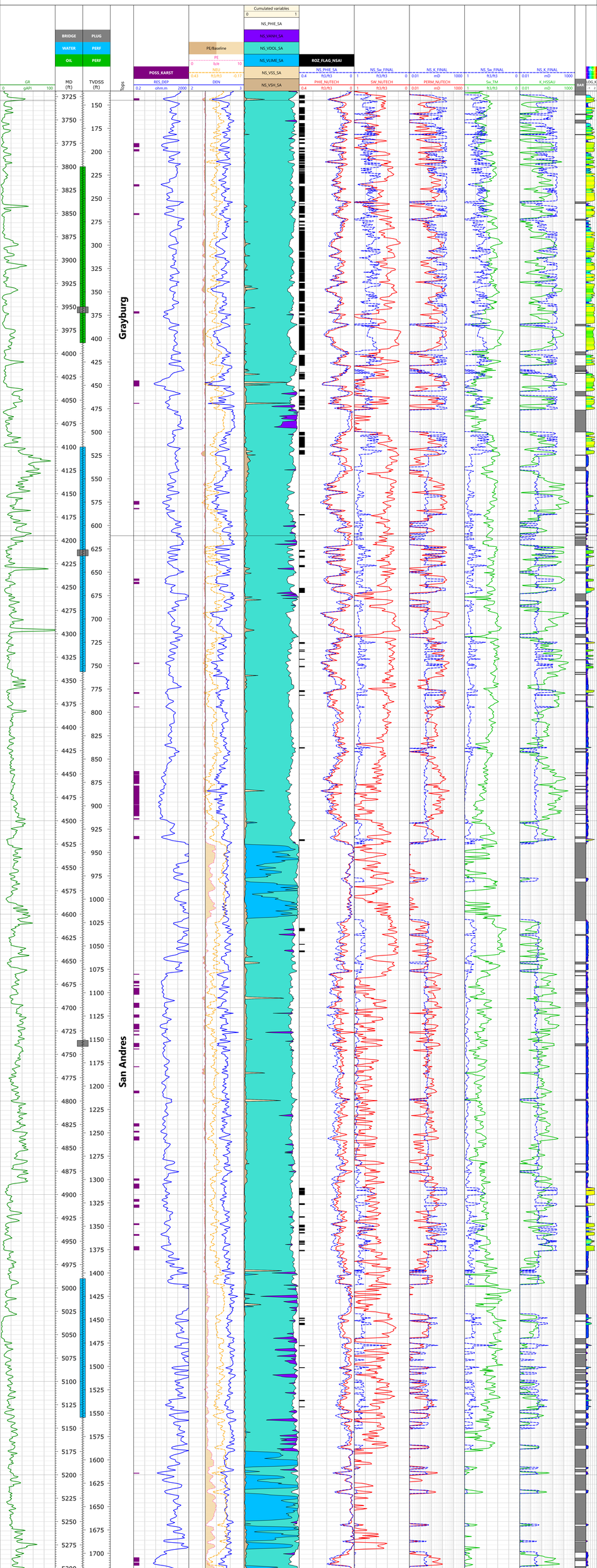
BRIDGE
PLUG
WATER
PERF
OIL
PERF
GR
gAPI
0
100
MD
(ft)
TVDSS
(ft)
Tops
POSS_KARST
RES_DEP
ohm.m
0.2
2000
PE/Baseline
PE
b/e
0
10
NEU
0.45
-0.15
DEN
2
3
Cumulated variables
0
1
NS_PHIE_SA
NS_VANH_SA
NS_VDOL_SA
NS_VLIME_SA
NS_VSS_SA
NS_VSH_SA
ROZ_FLAG_NSAI
NS_PHIE_SA
ft3/ft3
0.4
0
PHIE_NUTECH
NS_Sw_FINAL
ft3/ft3
1
0
SW_NUTECH
NS_K_FINAL
mD
0.01
1000
PERM_NUTECH
NS_Sw_FINAL
ft3/ft3
Sw_TM
NS_K_FINAL
mD
K_HSSAU
BAR
LOC_K
Grayburg
San Andres
3725
3750
3775
3800
3825
3850
3875
3900
3925
3950
3975
4000
4025
4050
4075
4100
4125
4150
4175
4200
4225
4250
4275
4300
4325
4350
4375
4400
4425
4450
4475
4500
4525
4550
4575
4600
4625
4650
4675
4700
4725
4750
4775
4800
4825
4850
4875
4900
4925
4950
4975
5000
5025
5050
5075
5100
5125
5150
5175
5200
5225
5250
5275
5300
150
175
200
225
250
275
300
325
350
375
400
425
450
475
500
525
550
575
600
625
650
675
700
725
750
775
800
825
850
875
900
925
950
975
1000
1025
1050
1075
1100
1125
1150
1175
1200
1225
1250
1275
1300
1325
1350
1375
1400
1425
1450
1475
1500
1525
1550
1575
1600
1625
1650
1675
1700
1725

Snyder SWD #1

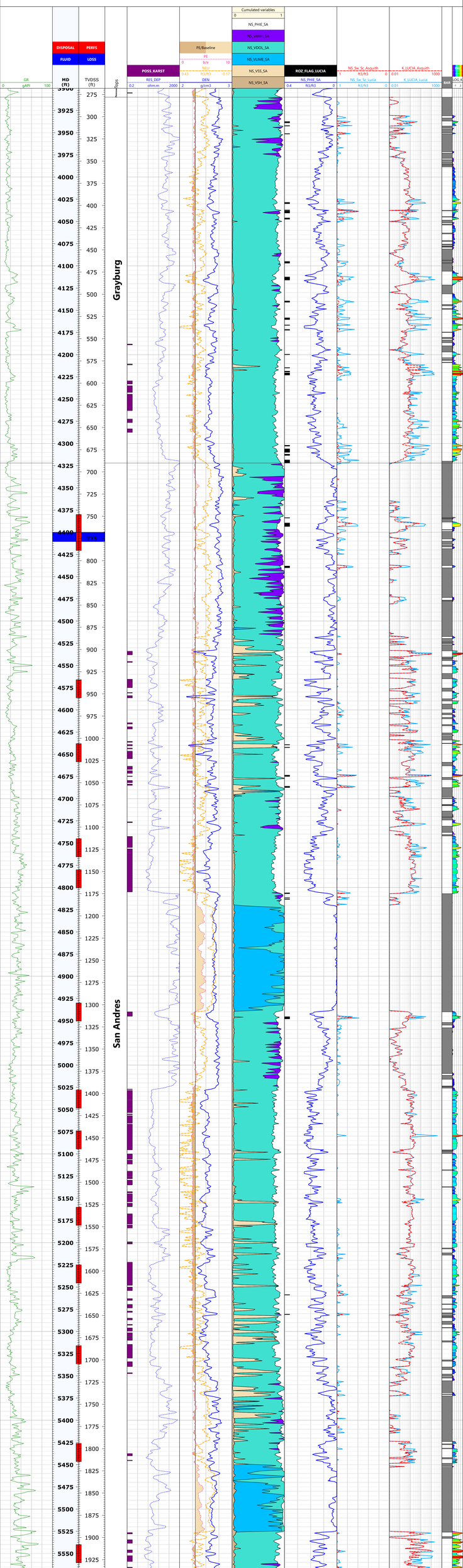
DISPOSAL
PERFS
FLUID
LOSS
GR
gAPI
MD (ft)
TVDSS (ft)
Tops
POSS_KARST
RES_DEP
ohm.m
PE/Baseline
PE
b/e
NEU
ft3/ft3
DEN
g/cm3
Cumulated variables
NS_PHIE_SA
NS_VANH_SA
NS_VDOL_SA
NS_VLIME_SA
NS_VSS_SA
NS_VSH_SA
ROZ_FLAG_LUCIA
NS_PHIE_SA
NS_Sw_Sc_Asquith
NS_Sw_Sc_Lucia
K_LUCIA_Asquith
K_LUCIA_Lucia
BARR
LOG_K
Grayburg
San Andres

APPENDIX C: INDIVIDUAL WELL COMMENTS

EMSU 660

1. Initially EMSU 660 was interpreted as a well which included sonic measurements. A Nutech interpretation was made available to NSAI which included a computed sonic porosity. NSAI backed out an estimate of the travel time curve. The travel time curve was used in our petrophysical model to compute vug porosity. The results were troubling because the interpreted vug volume and water saturation estimates differed considerably from the results obtained from all the other wells. In reviewing Empire's original exhibit from the testimony in September of 2023, numerous exhibits showed the Nutech log interpretation results from EMSU 660. Upon close inspection of the log header on the exhibits it was noted that the sonic porosity PSLS had a _SYN attached. This indicates that the sonic porosity displayed on the log display might have come from a synthetic sonic curve. Review of the Nutech interpretation provided to NSAI showed that the _SYN mnemonic was missing.

2. Subsequently it was confirmed that a sonic log was not available for EMSU 660 from New Mexico state records. The well was reinterpreted using the "no sonic" model. Results much more in line with the other wells interpreted by NSAI were obtained.

3. The "no sonic" model water saturation results are shown in separate tracks that include Nutech's interpretation and an interpretation using Trentham's screening model, respectively. Also included are comparisons of NSAI's permeability estimates with Nutech and the correlation developed from the Seminole San Andres Unit separately.

4. This well was initially completed in 2005. The first set of perforations completed the San Andres Formation and the perforated intervals are displayed on the interpreted log in the depth tracks. According to Empire's testimony in September 2023, the well produced 3 barrels of oil and 1057 barrels of water in an unspecified amount of time. This corresponds to a water cut of

99.7 percent. NSAI could find no documentation of this well test or production in the New Mexico state records. These perforations were subsequently plugged off and a shallower set of perforations were added to the Grayburg Formation. Early testing indicated that these perforations produced 11 barrels of oil and 158 barrels of water in a 24-hour test (about a 93.5 percent water cut).

5. NSAI also discovered that the Nutech interpretation in Empire's original testimony did not match what was provided to NSAI.

EMSU 746

6. In this well the San Andres formation was tested in its lower and upper sections individually and each produced 100% water. These perforations are displayed as blue flags on the interpreted log. The final producing perforations (in green) in the Grayburg formation produced at 96% water cut. Bridge plugs are also noted as large gray flags in the depth tracks. Nutech's interpretation indicates the presence of mobile oil (So > 40%) in both of the lower perforated intervals that produced 100% water. Their interpretation is also not consistent with the water cut in the producing interval.

EMSU 628

7. This well was initially perforated from 3812 – 4067 ft and produced 100% water. After the initial tests, the well was shut in for over a year and the perforations were squeezed and the well was recompleted and acidized in an interval from 3790 – 3817 ft. This interval produced oil at about a 25% initial water cut from the Grayburg.

EMSU 658

8. This well was initially perforated from 4126 – 4239 ft and plugged back to 4000 ft. The well was then recompleted in an interval from 3784 – 3912 and produced 11 barrels oil with 158 barrels of water in a 24-hour test. Initial production out of this interval was at a 99% water cut in the Grayburg.

EMSU 673

9. This well was completed over an interval from 3820 – 3924 ft in the Grayburg Formation. It produced with an initial water cut of 99%. This well looks to have been recompleted in late 2006; however, the state records are incomplete and do not state where this new completion was placed.

EMSU 679

10. This well was discussed in the testimony. A log display showing the full perforated interval is included. Oil saturations in the perforated portion of the Grayburg are consistent with the observed early time well water cuts (~94 percent). It is not clear whether log or core measurements were provided to Nutech for this well.

EMSU 713

11. In this well a deeper interval from 4042 – 4052 ft was perforated and then a bridge plug was placed above it at 4020 ft. The Grayburg was then perforated from 3885 – 3980 ft and initially produced with around a 94% water cut.

Ryno (previously Snyder)

12. This well experienced excessive fluid loss during drilling operations that appears to have affected the quality of the well logs. A majority of the Grayburg and San Andres intervals had density corrections greater than acceptable levels and the neutron readings were suspiciously high compared to the other wells evaluated. The deep resistivity measurements may have also been affected by the high levels of drilling fluid invasion.

13. The interpreted porosity, water saturation, and permeability estimates may not be representative of actual reservoir conditions as the result of uncertainties in the wireline log measurements.

NETHERLAND, SEWELL & ASSOCIATES, INC.

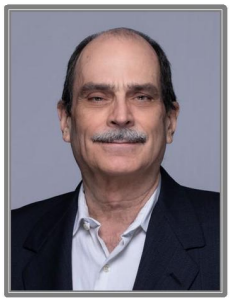

JAMES A. DAVIDSON

Vice President – Senior Technical Advisor

jdavidson@nsai-petro.com

+1 214-969-5401

Education: Ph.D., Petroleum Engineering, University of Texas at Austin; M.S., Petroleum Engineering, University of Texas at Austin; B.S., Petroleum Engineering, Texas Tech University.

Certifications/Associations: Member of the Society of Petroleum Engineers, Society of Professional Well Log Analysts, and Society of Core Analysts.

Jim has been a petroleum petrophysical consultant at NSAI since 1998. His work as a senior petrophysicist involves advanced petrophysical support for reserves evaluations, major field studies, and reservoir simulation studies; consulting services and technology transfer in the areas of well log analysis, core analysis, and reservoir description; and development of comprehensive logging and core analysis programs, including detailed laboratory procedures. Projects have included petrophysical parameter distributions for probabilistic reserves evaluations and multiple-model evaluations reflecting the uncertainties in net pay and hydrocarbon pore volume resulting from uncertainties in logging measurements, formation mineralogy, shale and clay distribution, and reservoir electrical conductivity. Jim has performed petrophysical evaluations for wells located in most of the major petroleum provinces of the world. Some of the major projects Jim has been involved with are listed below.

PROJECT EXPERIENCE

NORTH AMERICA

- Performed detailed petrophysical evaluation of the reservoirs within the Naval Petroleum Reserve No. 1 (Elk Hills Field), Kern County, California, for the final equity determination for the U.S. Department of Energy and Chevron U.S.A. Production Company.
- Developed a detailed petrophysical model for a fractured Monterey shale reservoir located offshore California and completed the corresponding resources assessment for Arguello Inc.
- Developed a comprehensive petrophysical model and reservoir description for a large carbonate reservoir complex operated by Pemex Exploración y Producción in the Gulf of Mexico.
- Developed a customized log analysis program for Wyoming tight gas reservoirs for Ultra Petroleum.
- Performed petrophysical evaluations for wells located in Alaska, the Gulf of Mexico, Texas and Louisiana Gulf Coasts, and California.
- Developed petrophysical training courses for Landmark Graphics Corporation.

SOUTH AMERICA

- Performed a detailed petrophysical evaluation and reservoir description for a recent reserves certification project for 3 fields located offshore Brazil for Petrobras.
- Evaluated well logs and core analysis data for wells located in Trinidad for Vintage Petroleum.
- Performed an independent petrophysical evaluation of 3 fields in Ecuador operated by Encana.
- Performed petrophysical evaluations of wells in Argentina, Colombia, Peru, and Venezuela for various operators.
- Conducted a detailed petrophysical evaluation for wells in the Ucayali Basin of Peru for the Ministry of Energy and Mines.

NETHERLAND, SEWELL & ASSOCIATES, INC.

JAMES A. DAVIDSON
(Continued)

- Performed a detailed petrophysical evaluation for several Ecuadorian oil fields located in Block 15 on behalf of Occidental Petroleum Corporation.
- Performed integrated petrophysical analyses for multiple onshore and offshore clastic and carbonate reservoir operated in Brazil by OGX.

EUROPE AND EURASIA

- Provided petrophysical support for the equity finalization for the Markham Field Unit, southern North Sea.
- Performed a petrophysical evaluation for a reserves certification for project financing of the ACG Field operated by BP in Azerbaijan.
- Performed petrophysical evaluations of several oil and gas fields in Spain, Russia, Georgia, and Kazakhstan.

ASIA PACIFIC

- Performed detailed petrophysical evaluations of large oil and gas fields in Papua New Guinea operated by Oil Search Limited and ExxonMobil.
- Evaluated well logs and core analysis data from Shell-operated Sakhalin Island wells for a reserves certification associated with project financing.
- Provided petrophysical support for the evaluation of the Maui gas field in New Zealand operated by Shell Todd.
- Provided petrophysical support for the reserves certification of several gas fields operated by ChevronTexaco and Woodside in Australia.
- Conducted log analysis studies for various fields in Indonesia, Malaysia, Vietnam, and offshore China.
- Prepared a detailed reservoir description for a dynamic model to support an LNG development in a carbonate reservoir in Indonesia.
- Prepared an integrated petrophysical analysis for a new carbonate discovery in Papua New Guinea that will be operated by Total.

AFRICA AND MIDDLE EAST

- Evaluated North Field in Qatar as part of gas reserves and deliverability certification studies for large international consortiums of lenders for the following LNG Projects: Ras Laffan LNG Trains 1&2, RasGas Expansion, Qatargas II, Qatargas 3, and Qatargas 4. Also conducted reserves certification for the Dolphin project.
- Conducted independent petrophysical evaluations for large oil fields operated by ExxonMobil in Chad, by Triton/Amerada Hess in Equatorial Guinea, and by Anadarko in Algeria.
- Independent petrophysical evaluation for Sonangol for fields located offshore Angola.
- Performed petrophysical evaluations for wells located in Nigeria, Egypt, Jordan, Iraq, Cameroon, and offshore Mauritania.
- Evaluated fractured carbonate reservoirs located offshore Yemen for Oil Search Limited.
- Conducted a detailed petrophysical evaluation for a contingent resources certification of Area 4 Block, offshore Mozambique.
- Conducted petrophysical evaluations associated with reserve certification for two large carbonate reservoirs located in Northern Iraq.

EXPERT WITNESS FOR ARBITRATIONS AND LAWSUITS

- Provided a written petrophysical evaluation and a videotaped deposition for a lawsuit involving Unocal and Agrium US Inc. for gas fields located in the Cook Inlet region of Alaska in July 2003.
- Provided the petrophysical analysis and written deposition for a lawsuit involving the Iona Gas Storage Field in Australia (Lochard Energy versus Energy Australia, July 2020).

NETHERLAND, SEWELL & ASSOCIATES, INC.

JAMES A. DAVIDSON
(Continued)

- Provided the petrophysical analysis and a written deposition for an arbitration decided by an international tribunal involving a dispute concerning the joint operating agreement for the Chemchemal oil field in Northern Iraq, March 2021.

PRIOR EXPERIENCE

Jim's prior work experience spans nearly 20 years and includes experience in engineering analysis and research, both internationally and in the domestic U.S. petroleum industry. This includes 5 years with ARCO Oil and Gas Company conducting reservoir performance evaluations and secondary recovery optimization programs; 5 years with Atlantic Richfield Indonesia Inc. providing reservoir petrophysical evaluations, improving logging procedures, and conducting special core analysis studies; 1 year at North Carolina State University conducting research in the areas of nuclear physics and radiation detection; 5 years with the University of Texas at Austin conducting research concerning the acoustic and electromagnetic properties of sandstones and shales, providing consulting services for the U.S. Environmental Protection Agency, and providing interpretation support for a petrophysical evaluation conducted by the University of Texas Bureau of Economic Geology; and 2 years with Landmark Graphics Corp. providing geoscience support for the development and testing of petrophysical and stratigraphic software.

PUBLICATIONS

Davidson, J.A., Morriss, S.L., and Podio, A.L., "Estimates of Formation Sound Speed from Ultrasonic Reflections", SPE Paper No. 24688, SPE Formation Evaluation, June, 1995, p. 72-78.

Truman, II, R.B., and Davidson, J.A., "SEC Defined Reserves Booking: What the Petrophysicist Needs to Know", SPE Paper No. 84388, presented at the SPE Annual Technical Conference, Denver, Colorado, October 5-8, 2003.

Reffell, O., Xie, Z.H., Davidson, J.A., and Markell, J., "Evaluation of Shale Oil and Gas Formation Reservoir Quality Using a Multidisciplinary Workflow of Crushed Rock Core Analysis", URTeC Paper No. 3724027, presented at the Unconventional Resources Technology Conference. Houston, Texas, June 20-22, 2022.

Markell, J., and Davidson, J.A., "Partitioning Fluids in NMR T1-T2 Measurements Using Gaussian Mixture Models and Surface Fitting", SPWLA Paper No. 2023-0109, presented at the SPWLA 64th Annual Logging Symposium, Lake Conroe, Texas, June 10-14, 2023.

REFERENCES

Dr. Augusto Podio – University of Texas at Austin, Austin, Texas
Stephen R. Kneller – Oil and Gas Exploration Consultant
Robert Lee – General Manager, Core Laboratories, Latin America

NETHERLAND, SEWELL & ASSOCIATES, INC.

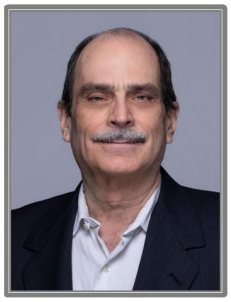

JAMES A. DAVIDSON

Vice President – Senior Technical Advisor

jdavidson@nsai-petro.com

+1 214-969-5401

Education: Ph.D., Petroleum Engineering, University of Texas at Austin; M.S., Petroleum Engineering, University of Texas at Austin; B.S., Petroleum Engineering, Texas Tech University.

Certifications/Associations: Member of the Society of Petroleum Engineers, Society of Professional Well Log Analysts, and Society of Core Analysts.

Jim has been a petroleum petrophysical consultant at NSAI since 1998. His work as a senior petrophysicist involves advanced petrophysical support for reserves evaluations, major field studies, and reservoir simulation studies; consulting services and technology transfer in the areas of well log analysis, core analysis, and reservoir description; and development of comprehensive logging and core analysis programs, including detailed laboratory procedures. Projects have included petrophysical parameter distributions for probabilistic reserves evaluations and multiple-model evaluations reflecting the uncertainties in net pay and hydrocarbon pore volume resulting from uncertainties in logging measurements, formation mineralogy, shale and clay distribution, and reservoir electrical conductivity. Jim has performed petrophysical evaluations for wells located in most of the major petroleum provinces of the world. Some of the major projects Jim has been involved with are listed below.

PROJECT EXPERIENCE

NORTH AMERICA

- Performed detailed petrophysical evaluation of the reservoirs within the Naval Petroleum Reserve No. 1 (Elk Hills Field), Kern County, California, for the final equity determination for the U.S. Department of Energy and Chevron U.S.A. Production Company.
- Developed a detailed petrophysical model for a fractured Monterey shale reservoir located offshore California and completed the corresponding resources assessment for Arguello Inc.
- Developed a comprehensive petrophysical model and reservoir description for a large carbonate reservoir complex operated by Pemex Exploración y Producción in the Gulf of Mexico.
- Developed a customized log analysis program for Wyoming tight gas reservoirs for Ultra Petroleum.
- Performed petrophysical evaluations for wells located in Alaska, the Gulf of Mexico, Texas and Louisiana Gulf Coasts, and California.
- Developed petrophysical training courses for Landmark Graphics Corporation.

SOUTH AMERICA

- Performed a detailed petrophysical evaluation and reservoir description for a recent reserves certification project for 3 fields located offshore Brazil for Petrobras.
- Evaluated well logs and core analysis data for wells located in Trinidad for Vintage Petroleum.
- Performed an independent petrophysical evaluation of 3 fields in Ecuador operated by Encana.
- Performed petrophysical evaluations of wells in Argentina, Colombia, Peru, and Venezuela for various operators.
- Conducted a detailed petrophysical evaluation for wells in the Ucayali Basin of Peru for the Ministry of Energy and Mines.

EXHIBIT - D-1

NETHERLAND, SEWELL & ASSOCIATES, INC.

JAMES A. DAVIDSON
(Continued)

- Performed a detailed petrophysical evaluation for several Ecuadorian oil fields located in Block 15 on behalf of Occidental Petroleum Corporation.
- Performed integrated petrophysical analyses for multiple onshore and offshore clastic and carbonate reservoir operated in Brazil by OGX.

EUROPE AND EURASIA

- Provided petrophysical support for the equity finalization for the Markham Field Unit, southern North Sea.
- Performed a petrophysical evaluation for a reserves certification for project financing of the ACG Field operated by BP in Azerbaijan.
- Performed petrophysical evaluations of several oil and gas fields in Spain, Russia, Georgia, and Kazakhstan.

ASIA PACIFIC

- Performed detailed petrophysical evaluations of large oil and gas fields in Papua New Guinea operated by Oil Search Limited and ExxonMobil.
- Evaluated well logs and core analysis data from Shell-operated Sakhalin Island wells for a reserves certification associated with project financing.
- Provided petrophysical support for the evaluation of the Maui gas field in New Zealand operated by Shell Todd.
- Provided petrophysical support for the reserves certification of several gas fields operated by ChevronTexaco and Woodside in Australia.
- Conducted log analysis studies for various fields in Indonesia, Malaysia, Vietnam, and offshore China.
- Prepared a detailed reservoir description for a dynamic model to support an LNG development in a carbonate reservoir in Indonesia.
- Prepared an integrated petrophysical analysis for a new carbonate discovery in Papua New Guinea that will be operated by Total.

AFRICA AND MIDDLE EAST

- Evaluated North Field in Qatar as part of gas reserves and deliverability certification studies for large international consortiums of lenders for the following LNG Projects: Ras Laffan LNG Trains 1&2, RasGas Expansion, Qatargas II, Qatargas 3, and Qatargas 4. Also conducted reserves certification for the Dolphin project.
- Conducted independent petrophysical evaluations for large oil fields operated by ExxonMobil in Chad, by Triton/Amerada Hess in Equatorial Guinea, and by Anadarko in Algeria.
- Independent petrophysical evaluation for Sonangol for fields located offshore Angola.
- Performed petrophysical evaluations for wells located in Nigeria, Egypt, Jordan, Iraq, Cameroon, and offshore Mauritania.
- Evaluated fractured carbonate reservoirs located offshore Yemen for Oil Search Limited.
- Conducted a detailed petrophysical evaluation for a contingent resources certification of Area 4 Block, offshore Mozambique.
- Conducted petrophysical evaluations associated with reserve certification for two large carbonate reservoirs located in Northern Iraq.

EXPERT WITNESS FOR ARBITRATIONS AND LAWSUITS

- Provided a written petrophysical evaluation and a videotaped deposition for a lawsuit involving Unocal and Agrium US Inc. for gas fields located in the Cook Inlet region of Alaska in July 2003.
- Provided the petrophysical analysis and written deposition for a lawsuit involving the Iona Gas Storage Field in Australia (Lochard Energy versus Energy Australia, July 2020).

NETHERLAND, SEWELL & ASSOCIATES, INC.

JAMES A. DAVIDSON
(Continued)

- Provided the petrophysical analysis and a written deposition for an arbitration decided by an international tribunal involving a dispute concerning the joint operating agreement for the Chemchemal oil field in Northern Iraq, March 2021.

PRIOR EXPERIENCE

Jim's prior work experience spans nearly 20 years and includes experience in engineering analysis and research, both internationally and in the domestic U.S. petroleum industry. This includes 5 years with ARCO Oil and Gas Company conducting reservoir performance evaluations and secondary recovery optimization programs; 5 years with Atlantic Richfield Indonesia Inc. providing reservoir petrophysical evaluations, improving logging procedures, and conducting special core analysis studies; 1 year at North Carolina State University conducting research in the areas of nuclear physics and radiation detection; 5 years with the University of Texas at Austin conducting research concerning the acoustic and electromagnetic properties of sandstones and shales, providing consulting services for the U.S. Environmental Protection Agency, and providing interpretation support for a petrophysical evaluation conducted by the University of Texas Bureau of Economic Geology; and 2 years with Landmark Graphics Corp. providing geoscience support for the development and testing of petrophysical and stratigraphic software.

PUBLICATIONS

Davidson, J.A., Morriss, S.L., and Podio, A.L., "Estimates of Formation Sound Speed from Ultrasonic Reflections", SPE Paper No. 24688, SPE Formation Evaluation, June, 1995, p. 72-78.

Truman, II, R.B., and Davidson, J.A., "SEC Defined Reserves Booking: What the Petrophysicist Needs to Know", SPE Paper No. 84388, presented at the SPE Annual Technical Conference, Denver, Colorado, October 5-8, 2003.

Reffell, O., Xie, Z.H., Davidson, J.A., and Markell, J., "Evaluation of Shale Oil and Gas Formation Reservoir Quality Using a Multidisciplinary Workflow of Crushed Rock Core Analysis", URTeC Paper No. 3724027, presented at the Unconventional Resources Technology Conference. Houston, Texas, June 20-22, 2022.

Markell, J., and Davidson, J.A., "Partitioning Fluids in NMR T1-T2 Measurements Using Gaussian Mixture Models and Surface Fitting", SPWLA Paper No. 2023-0109, presented at the SPWLA 64th Annual Logging Symposium, Lake Conroe, Texas, June 10-14, 2023.

REFERENCES

Dr. Augusto Podio – University of Texas at Austin, Austin, Texas
Stephen R. Kneller – Oil and Gas Exploration Consultant
Robert Lee – General Manager, Core Laboratories, Latin America